From the Clinic for Gastroenterology, Hepatology and Infectious Diseases at
Heinrich Heine University Düsseldorf

Mechanistic insights into feline lentiviral Vif interactions with feline APOBEC3 and Cullin family proteins

Dissertation

to obtain the academic title of Doctor of Philosophy (PhD) in Medical Sciences from the Faculty of Medicine at Heinrich Heine University Düsseldorf

submitted by

Zepei Li

2025

As an inaugural dissertation printed by permission of the Faculty of Medicine at Heinrich Heine University Düsseldorf

signed:

Dean:

First examiner:

Univ.-Prof. Dr. Carsten Münk

Clinic for Gastroenterology, Hepatology and Infectiology

Faculty of Medicine, Heinrich Heine University Düsseldorf

Second examiner:

Univ.-Prof. Dr. Philipp Lang

Institute of Molecular

Medicine II

Faculty of Medicine, Heinrich Heine University Düsseldorf

Zusammenfassung

Felines Immundefizienzvirus (FIV) und das Humane Immundefizienzvirus (HIV) gehören zur Gattung Lentivirus in der Familie Retroviridae und weisen strukturelle, genetische und Ähnlichkeiten in der Übertragung auf. FIV dient als wertvolles Modell zur Untersuchung der durch HIV induzierten AIDS-Pathogenese. Der Wirtsrestriktionsfaktor APOBEC3 (A3) hemmt sowohl HIV als auch FIV durch das Einfügen von Hypermutationen in virale Genome. Um A3 entgegenzuwirken, kodieren HIV und FIV den viralen Infektiositätsfaktor (Vif), der Cullin-RING-E3-Ubiquitin-Ligasen rekrutiert, um A3 in einem Proteasom abhängigen Mechanismus abzubauen. Ein besseres Verständnis der Vif-A3- und Vif-Cullin-Interaktionen birgt Potenzial für die Entwicklung neuer HIV-Therapeutika.

Diese Studie charakterisiert den durch FIV Vif-vermittelten Abbau von A3 und die restriktive Aktivität von felinem A3Z3 gegen FIV-Reporterviren. Es konnte festgestellt werden, dass das Vif-Protein des Puma-Lentivirus (PLV) Typ 1695 zwar feline A3Z2 und A3Z2Z3 abbauen kann, jedoch nicht A3Z3. Die Aminosäure 201 in Vif wurde als Schlüsselfaktor für die Interaktion mit A3Z3 identifiziert. Eine Mutation an dieser Position in PLV1695 Vif erklärt dessen Unfähigkeit A3Z3 zu antagonisieren. Das 201YRF203-Motiv in PLV Typ B (PLVB) Vif, welches auch in Vifs von FIV (Hauskatze), PLV Typ A (PLVA) und HIV-1 konserviert ist, erweist sich als entscheidend für die Interaktion für den Abbau von A3. Zusätzlich degradieren FIV und PLVA Vif A3Z3 über mittels Aminosäuren im N- und C-Terminus, während PLVB Vif ausschließlich auf seine C-terminale Bereiche angewiesen ist und die entsprechende N-terminalen Aminosäuren in der A3Z3-Degradation inaktiv bleiben.

Im Hinblick auf die Vif-Cullin-Interaktionen zeigt die Studie eine differenzielle Bindung feliner Vif-Proteine an CUL2 und CUL5. Ein konserviertes Interface, das die Bindung an CUL5 vermittelt, wurde sowohl in HIV-1- als auch in felinen Vifs identifiziert. Bemerkenswert ist, dass PLVB Vif sowohl CUL2- als auch CUL5-E3-Ligase-Komplexe rekrutiert, um A3Z3 abzubauen. Eine neuartige Interaktion zwischen HIV- und felinem Vif mit CUL1 wurde entdeckt, wobei die funktionelle

Relevanz dieser Interaktion noch weiterer Untersuchungen bedarf.

Zusammenfassend bietet diese Arbeit eine neuartige Perspektive auf die Interaktionen zwischen lentiviralen Vif-Proteinen und den Wirtsfaktoren A3 sowie CUL. Die Ergebnisse eröffnen neue Ansätze zur Aufklärung der komplexen Dynamik von Interaktionen zwischen viralen und Wirtsproteinen.

Summary

Feline immunodeficiency virus (FIV) and human immunodeficiency virus (HIV) are Lentivirus members within the Retroviridae family, sharing structural, genetic, and transmission similarities. FIV serves as a valuable model for studying HIV-induced AIDS. The host restriction factor APOBEC3 (A3) inhibits both HIV and FIV by introducing hypermutations into viral genomes. To counteract A3, HIV and FIV encode viral infectivity factor (Vif), which recruits Cullin-RING E3 ubiquitin ligases to degrade A3 through a proteasome dependent mechanism. Understanding Vif-A3 and Vif-Cullin interactions holds promise for HIV therapeutic development.

This study characterizes feline lentiviral Vif-mediated A3 degradation and the restriction activity of feline A3Z3 against FIV reporter viruses. Puma lentivirus (PLV) type 1695 Vif, identified as incapable of degrading feline A3Z3 but effective against A3Z2 and A3Z2Z3, highlights residue 201 as a key determinant for A3Z3 interaction. Mutation at this position in PLV1695 Vif explains its inability to counteract A3Z3. The 201YRF203 motif in PLV type B (PLVB) Vif, conserved across FIV domestic cat-, PLV type A (PLVA)-, and HIV-1 Vif, is essential for A3 interaction and degradation. Additionally, FIV and PLVA Vif degrade A3Z3 through both their N- and C-terminal regions, whereas PLVB Vif depends on its C-terminal, with the corresponding N-terminal inactive in A3Z3 degradation.

Regarding Vif-Cullin interactions, this study reveals differential binding of feline Vif proteins to CUL2 and CUL5. A conserved interface mediating CUL5 binding was identified in HIV-1 and feline Vifs. Notably, PLVB Vif recruits both CUL2 and CUL5 E3 ligase to degrade A3Z3. A novel interaction between HIV and feline Vif with CUL1 was discovered, although its functional relevance requires further investigation.

In summary, this work provides a novel perspective on the interactions between lentiviral Vif and host A3, as well as host Cullin proteins. These findings offer new avenues for uncovering the complex dynamics of lentiviral protein-host protein interactions.

List of abbreviations

AIDS	Acquired immunodeficiency syndrome
ALV	Avian leukosis virus
APOBEC3 (A3)	Apolipoprotein B mRNA-editing enzyme catalytic polypeptide-like 3
ART	Antiretroviral treatment
ATP	Adenosine triphosphate
β-TrCP	Beta-transducin repeat containing protein
BIV	Bovine immunodeficiency virus
BLV	Bovine leukemia virus
BST-2	Bone marrow stromal antigen 2, also known as Tetherin
CA	Capsid
CAEV	Caprine arthritis encephalitis virus
CBF-β	Core binding factor β
CD134	Tumor necrosis factor receptor superfamily member 4
CD4	Cluster of differentiation 4
CCR5	C-C chemokine receptor type 5
cDNA	Complementary DNA
CoIP	Co-immunoprecipitation assays
CRLs	Cullin-RING ubiquitin ligases
CUL	Cullin
CUL1	Cullin1
CUL2	Cullin2
CUL3	Cullin3
CUL4A	Cullin4A
CUL4B	Cullin4B
CUL5	Cullin5
CYPA	Cellular cyclophilin A

CXCR4	C-X-C chemokine receptor type 4
Δ	Deficient
DCAF1	DDB1 and CUL4 associated factor 1
DDB1	DNA damage-binding protein 1
DMEM	Dulbecco's high-glucose modified eagle's medium
DMSO	Dimethyl sulfoxide
DN	Dominant negative
DNA	Deoxyribonucleic acid
dNTP	Deoxynucleotide triphosphates
EIAV	Equine Infectious Anemia Virus
E1	Ubiquitin activating enzymes
E2	Ubiquitin conjugating enzymes
E3	Ubiquitin ligases
ELOB	Elongin B
ELOC	Elongin C
Env	Envelope
ERV	Endogenous retroviruses
FBS	Fetal bovine serum
Fca	Felis catus
FeLV	Feline leukemia virus
FFV	Feline foamy virus
FIV	Feline immunodeficiency virus
FIV-luc	FIV single-cycle luciferase viruses
FIVfca	FIV in Felis catus
FIVpco	FIV in puma
FIVple	FIV in lion
FLV	Feline leukemia virus
glycoGag	Glycosylated Gag
gRNA	Genomic RNA

HA	Hemagglutinin
HBV	Hepatitis B virus
HFV	Human foamy virus
HIV	Human immunodeficiency virus
HTLV	Human T-lymphotropic virus
IFN	Interferon
IN	Integrase
JDV	Jembrana disease virus
kDa	Kilodalton
LTR	Long terminal repeats
MA	Matrix
MG132	N-carbobenzoxy-L-leucyl-L-leucyl-L-leucinal, proteasome inhibitor
MLV	Murine leukemia virus
MMTV	Mouse mammary tumor virus
MUSCLE	Multiple sequence comparison by log-expectation
MVV	Maedi-visna virus
MX	Myxovirus resistance
NC	Nucleocapsid
Nef	Negative factor
OrfA	Open reading frame A
PBS	Phosphate buffered saline
PFV	Prototype foamy virus
PLV	Puma lentivirus
PLVA	Puma lentivirus type A
PLVB	Puma lentivirus type B
PLV1695	Puma lentivirus type 1695
PR	Protease
RELIK	Rabbit endogenous lentivirus K

Rev	Regulator of expression of virion proteins
RIPA	Radioimmunoprecipitation assay
RING	Really interesting new gene
RNA	Ribonucleic acid
RT	Reverse transcriptase
SAMHD	SAM and HD domain-containing protein
SERINC	Serine incorporator protein
SFV	Simian foamy virus
SDS	Sodium dodecyl sulfate
SIV	Simian immunodeficiency virus
SIVcpz	SIV of chimpanzees
SIVgor	SIV of gorilla
SKP1	S-phase Kinase-associated Protein 1
SIVsm	SIV of sooty mangabeys
SU	Surface
Tat	Transactivator (of HIV)
TM	Transmembrane
TRIM	Tripartite motif-containing protein
Ub	Ubiquitin
UNG2	Uracil-DNA glycosylase
Vif	Viral infectivity factor
VLPs	Viral-like particles
Vpr	Viral protein R
Vpu	Viral protein U
Vpx	Viral protein X
VSV-G	Envelope glycoprotein of vesicular stomatitis virus
WDSV	Walleye dermal sarcoma virus

Table of contents

1. Introduction

The worldwide impact of AIDS

Human immunodeficiency virus (HIV) belongs to the lentivirus subgroup of retroviruses. Acquired immunodeficiency syndrome (AIDS) is the clinical term used to describe the final stage of the disease resulting from HIV infection. From almost any criterion, HIV is considered one of the deadliest scourges in the world[1-3]. An end-of-year report from the United Nations' AIDS program estimated that the number of new HIV infections in 2022 was 1.3 million, bringing the total number of infected individuals worldwide to approximately 85.6 million; since the beginning of the epidemic, AIDS-related illnesses have claimed the lives of 40.4 million people[1]. Understanding HIV remains pivotal in global health efforts to combat this devastating virus and its implications for public health worldwide.

1.1 Retroviruses

1.1.1 Definition and importance

Retroviruses represent a large and diverse family of enveloped RNA viruses, characterized by shared taxonomic features including their structural organization, molecular composition, and replicative mechanisms[4]. Retroviruses are significant in human health due to their association with diseases such as acquired immunodeficiency syndrome (AIDS), caused by the human immunodeficiency virus (HIV), which depletes CD4+ T cells; and adult T-cell leukemia/lymphoma caused by human T-cell leukemia virus (HTLV)[5, 6]. In animals, retroviruses like avian leukosis virus (ALV), feline immunodeficiency virus (FIV) and feline leukemia virus (FeLV) cause diseases that impact agriculture and pet care[7, 8]. Additionally, retroviruses are valuable in scientific research, particularly in gene therapy where lentiviruses serve as vectors for long-term gene expression, and as model systems for studying gene regulation, cancer development, and immune responses[9, 10].

1.1.2 Classification of retroviruses

Retroviruses can be classified in several ways, one of which is based on genome organization, dividing them into simple and complex retroviruses. Simple retroviruses typically contain four essential genes: *gag*, *pro*, *pol*, and *env*. In contrast, complex retroviruses possess these four genes along with additional regulatory genes, which facilitate more sophisticated control of the viral replication cycle and interactions with the host's cellular machinery[4].

Additionally, retroviruses are further classified based on their evolutionary relationships into two subfamilies: Orthoretrovirinae and Spumaretrovirinae. The Orthoretrovirinae subfamily is subdivided into six genera, while the Spumaretrovirinae subfamily contains a single genus (Table 1.1)[11]. Among these groups, five consist of retroviruses with oncogenic potential, historically termed oncoviruses. The remaining two groups are lentiviruses and spumaviruses, which are distinguished by their unique biological characteristics and interactions with host organisms.

Subfamily	Genus	Example
Orthoretrovirinae	Alpharetrovirus	ALV
	Betaretrovirus	MMTV
	Gammaretrovirus	FLV
	Deltaretrovirus	HTLV
	Epsilonretrovirus	WDSV
	Lentivirus	BIV, FIV, HIV, SIV
Spumaretrovirinae	Spumavirus	FFV, PFV, SFV

Table 1.1 The classification of retroviruses. ALV: Avian leucosis virus, MMTV: Mouse mammary tumor virus, FLV: Feline leukemia virus, HTLV: Human T-lymphotropic virus, WDSV: Walleye dermal sarcoma virus, BIV: Bovine Immunodeficiency Virus, FIV: Feline immunodeficiency virus, HIV: Human immunodeficiency virus, SIV: Simian immunodeficiency virus, FFV: Feline foamy virus, PFV: Prototype foamy virus, SFV: Simian foamy virus.

1.1.3 Lentiviruses: A subfamily of retroviruses

Lentiviruses are a distinct genus within the family Retroviridae that cause immune deficiencies and disorders of the hematopoietic system, and can sometimes lead to arthritis and central nervous system disorders[12]. The equine infectious anemia lentivirus, identified as one of the earliest discovered viruses in 1904, causes episodic autoimmune hemolytic anemia in horses[12]. Lentiviruses have also been detected in sheep, goats, cats, cattle and primates.

Human immunodeficiency virus (HIV) is a lentivirus， acquired immunodeficiency syndrome (AIDS) is the term used to describe the final stage of the disease resulting from HIV infection. Simian immunodeficiency viruses (SIVs), lentiviruses identified in many African nonhuman primates, typically do not cause disease in their native hosts. However, laboratory infection of Asian macaques with viruses originating from African sooty mangabeys (SIVsm) results in AIDS and is widely used as an animal model for the human disease.

By analyzing the phylogenetic relationships of HIV and SIV, scientists determined that HIV-1 was transmitted from chimpanzees to humans in Kinshasa (Democratic Republic of Congo) around 1920[13]. Another HIV virus, HIV-2, emerged from the cross-species transmission of SIV from sooty mangabeys[14]. In 1986, researchers identified the feline immunodeficiency virus (FIV) in domestic cats[15]. FIV can cause AIDS-like syndromes in domestic cats, and its pathogenesis and genomic organization closely resemble those of HIV[16]. Therefore, FIV has been employed as an experimental model for HIV to study immune pathogenesis and to develop antiviral drugs[17].

All known lentiviruses are primarily exogenous and have been divided into five subgroups, each restricted to a single mammalian order or family[18]. Table 1.2 presents the classification of exogenous lentiviruses.

Subgroup	Host	Representative Viruses
Primate Subgroup	Primates	HIV-1, HIV-2, SIV
Bovine Subgroup	Cattle	BIV, Jembrana Disease Virus
Equine Subgroup	Horses	EIAV
Ovine/Caprine Subgroup	Sheep and Goats	Visna/Maedi Virus, CAEV
Feline Subgroup	Cats	FIV

Table 1.2 The classification of lentiviruses. HIV-1: Human Immunodeficiency Virus Type1, HIV-2: Human Immunodeficiency Virus Type2, SIV: Simian Immunodeficiency Virus, BIV: Bovine Immunodeficiency Virus, EIAV: Equine Infectious Anemia Virus, CAEV: Caprine Arthritis-Encephalitis Virus, FIV: Feline Immunodeficiency Virus.

In addition to exogenous lentiviruses, a few endogenous lentivirus lineages have now been identified. For example, rabbit endogenous lentivirus K (RELIK) insertions have been found at orthologous positions in the genomes of the rabbit (*Oryctolagus cuniculus*) and hare (*Lepus europaeus*)[19, 20]. Other examples include endogenous lentiviruses in lemurs (family Lemuridae)[21, 22]; mustelids (family Mustelidae)[23, 24]; and dermopterans (order Dermoptera, a group of arboreal gliding mammals, native to Southeast Asia)[25, 26].

1.1.4 The genome structure of retroviruses

Retroviruses are enveloped viruses with single-stranded, positive-sense RNA genomes. These viruses encode a reverse transcriptase enzyme that converts their RNA genome into DNA, and an integrase enzyme that facilitates the integration of this viral DNA into the host cell's genome. The viral genome, once integrated into the host cell's DNA, is termed a provirus. This proviral DNA is replicated in concert with the host's genome. The diameter of a retrovirus virion typically ranges from 80 to 120 nanometers, while the single-stranded RNA genome it contains is approximately 7 to 12 kilobases in length. All retroviruses

contain four essential genes: *gag*, *pro*, *pol*, and *env*. The *gag* gene encodes essential viral structural proteins, including matrix (MA), capsid (CA), and nucleocapsid (NC). The *pro* gene is responsible for producing a protease (PR), which cleaves and processes proteins synthesized from the *gag*, *pro*, *pol*, and *env* genes. The *pol* gene encodes key viral enzymes: reverse transcriptase (RT), integrase (IN), and RNase H. Notably, in some retroviruses, the *pro* gene is integrated within the *pol* gene. The *env* gene encodes viral envelope proteins, specifically the surface (SU) glycoprotein and the transmembrane (TM) protein. Moreover, certain retroviral genomes encode multiple regulatory genes such as *tat, rex*, *nef*, *rev, vpr*, *vif,* and *vpu*. These regulatory proteins are crucial for viral infection, replication, and pathogenicity. At the ends of viral genomes lie two long terminal repeats (5'-LTR and 3'-LTR). These LTRs are indispensable for viral transcription and integration processes (Fig.1.1) [4].

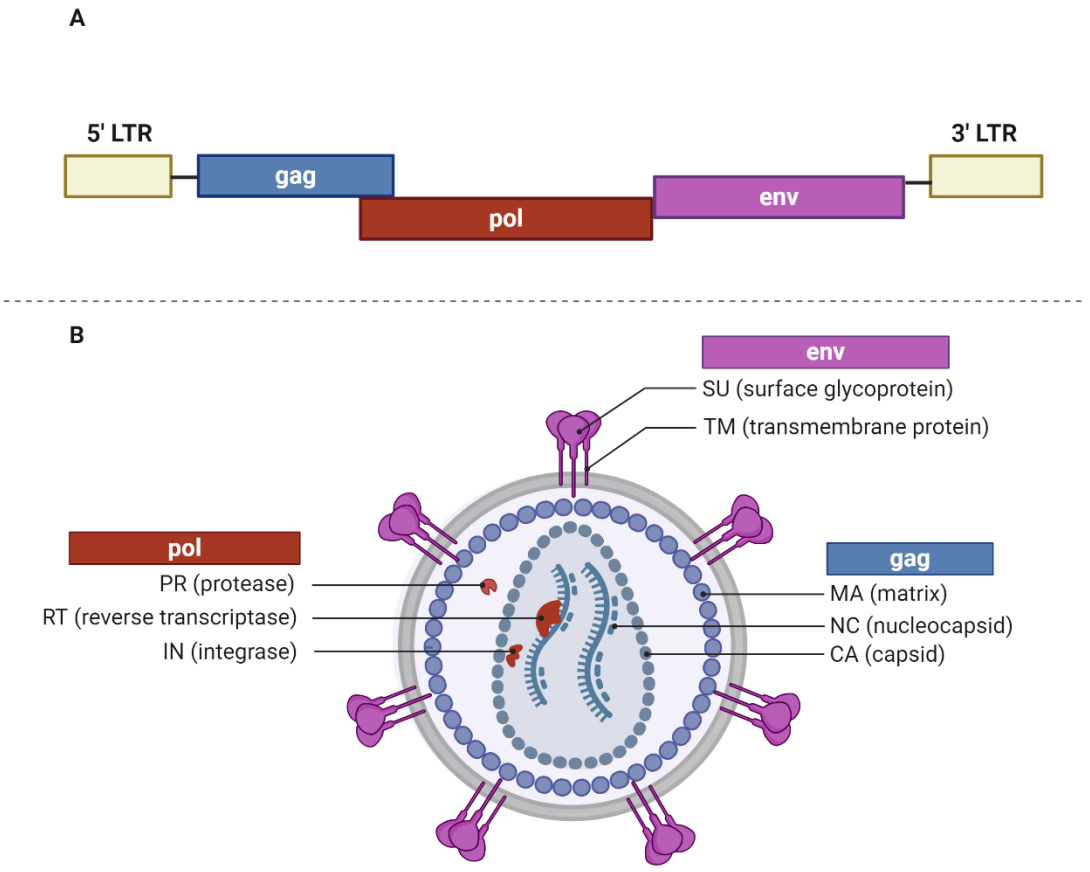

Fig. 1.1 A schematic representation of the retroviral genome and particles. (A) The primary genes of the retrovirus include gag, pol, and env. The viral genome contains long terminal repeats

(LTRs) at both the 5' and 3' ends. (B) The retroviral particle comprises RNA genomes and associated viral proteins. The *env* gene encodes the viral envelope proteins, including the surface (SU) glycoprotein and the transmembrane (TM) protein. The *gag* gene encodes the structural proteins of the virus: matrix (MA), capsid (CA), and nucleocapsid (NC). The *pol* gene encodes the viral enzymes: protease (PR) and integrase (IN). Created with BioRender.com.

1.1.5 Replication cycle of retroviruses

The replication cycle of retroviruses, illustrated here using HIV as a representative example, involves multiple key stages: 1) binding, 2) fusion, 3) reverse transcription initiation, 4) reverse transcription completion, 5) uncoating, 6) integration, 7) translation, 8) assembly and budding, 9) release maturation. Retroviral infection begins when the envelope glycoproteins bind to specific receptors on the host cell surface. HIV-1 binds to host cells through interactions with the CD4 receptor and the co-receptors CCR5 or CXCR4[27]. In contrast, FIV utilizes the receptors CD134 and CXCR4 for cellular attachment[28-30]. After the retrovirus attaches to the host cell, the virion envelope fuses with the host cell's plasma membrane, releasing the viral capsid into the cytoplasm. Inside the host cell, reverse transcriptase converts the viral single-stranded RNA into complementary DNA (cDNA). This cDNA then serves as a template for the synthesis of double-stranded viral DNA. For HIV-1, it has been demonstrated that both the process of reverse transcription and the uncoating of the viral core can occur within the nucleus[31]. After this process, the viral integrase integrates the double-stranded DNA into the host genome. Following integration, the 5'-LTR functions as a promoter that initiates viral transcription. In retroviruses, both unspliced and spliced RNAs need to be exported from the nucleus to the cytoplasm. This nuclear export is crucial because unspliced RNA is used for translating viral proteins and serving as genomic RNA for packaging into new virions. Retroviruses encode Gag-Pol or Gag-Pro-Pol proteins as precursor polyproteins, which are cleaved by the virally encoded protease to release the MA, CA, NC, PR, RT, and INT. Retroviral particle assembly begins with the Gag and

Gag-Pol precursors and necessitates the presence of genomic RNA (gRNA) to produce infectious virions. The Gag polyprotein forms the fundamental building blocks of retroviral particles, with each virion comprising approximately 2000–5000 Gag molecules[32]. The third assembly domain of the Gag protein, known as the late domain (L-domain), is crucial for the release of fully assembled immature virions from the plasma membrane[33]. Retroviruses must acquire envelope proteins and bud from the cell membrane to form infectious virions. Viral maturation is then triggered by the viral protease, which cleaves the Gag and Gag-Pol proteins, leading to the formation of mature, infectious virions (Fig.1.2).

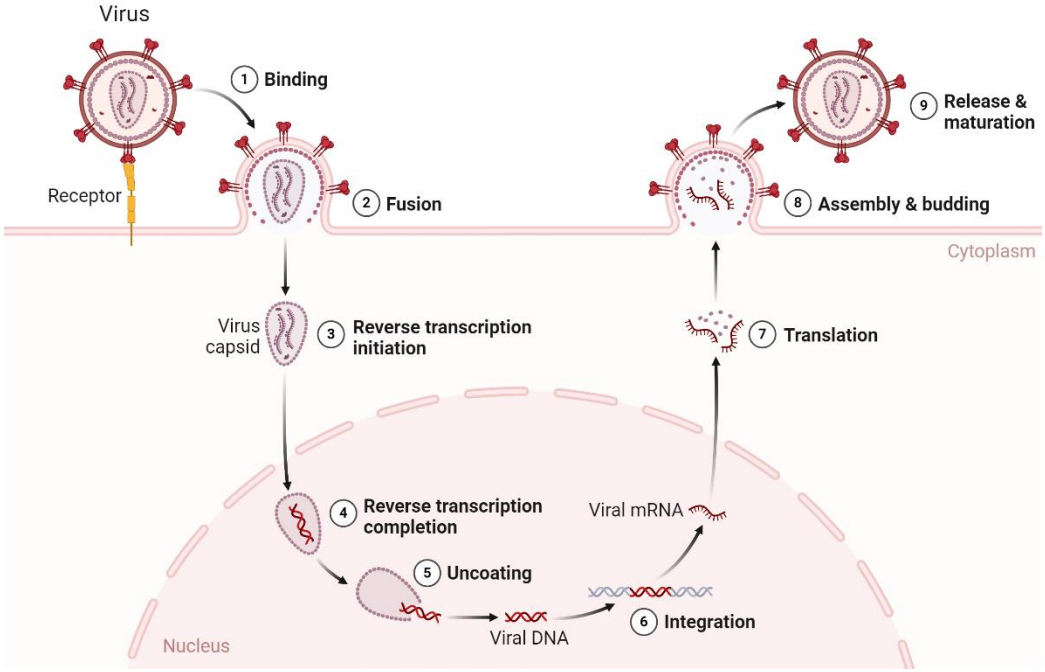

Fig. 1.2 The replication cycle of retroviruses (exemplified here by HIV). Nine main steps are included: 1) binding, 2) fusion, 3) reverse transcription initiation, 4) reverse transcription completion, 5) uncoating, 6) integration, 7) translation, 8) assembly and budding, 9) release maturation. Created with BioRender.com.

1.2 Human immunodeficiency virus

HIV is a lentivirus within the Retroviridae family. It primarily targets CD4+ T cells, macrophages, and dendritic cells, causing T cell depletion and cell dysfunction, and ultimately destroying the human immune system[34, 35]. Body fluids such as

semen, vaginal fluids, and blood from infected individuals contain both free-floating viruses and virus-infected CD4+ cells, which facilitate the transmission of HIV to new cells or hosts[36-38]. HIV is transmitted through several pathways, including vaginal and anal sexual intercourse, intravenous blood exposure from sharing needles, blood transfusions, and from mother to child during childbirth and breastfeeding[39, 40]. In the early stages of HIV infection, patients may not exhibit any symptoms. However, as the virus progresses, it gradually debilitates the immune system, eventually leading to acquired immune deficiency syndrome (AIDS). Without treatment, the immune system can sustain fatal damage within 5 - 10 years. Clinically, antiretroviral treatment (ART) suppresses HIV replication. Effective ART controls viral replication and protects the immune system. However, while combination ART manages HIV infection, it does not cure it due to the persistence of the virus in latent reservoirs[41]. Additionally, the growing prevalence of drug resistance necessitates ongoing research to develop new antiretroviral drugs[42]. These new therapeutic agents target different stages of the HIV lifecycle, such as inhibiting viral reverse transcription, preventing fusion of the virus with host cells, blocking viral integration into the host genome, and inhibiting the release of new HIV particles from infected cells.

HIV has two main strains, HIV-1 and HIV-2, which are similar but distinct viruses[13]. HIV-1 originated from the simian immunodeficiency virus (SIV) of chimpanzees (SIVcpz), while HIV-2 originated from the SIV of sooty mangabeys (SIVsm). Four transmissions from apes to humans led to the emergence of the four HIV-1 groups. Two separate transmissions from chimpanzees to humans gave rise to HIV-1 groups M and N. A single transmission event from chimpanzees to gorillas resulted in SIVgor lineages, which were then transmitted to humans on two occasions, leading to the HIV-1 groups O and P. In contrast, HIV-2 was transmitted from sooty mangabeys to humans on several independent occasions, resulting in ten HIV-2 groups that are almost indistinguishable in nucleotide sequence from SIVsm strains. HIV-1 is the most prevalent form of HIV, responsible for most infections

worldwide. Among the four groups of HIV-1, only group M has spread globally, accounting for 99% of HIV-1 infections. HIV-2 also leads to AIDS, but with slower progression and less severity. HIV-2 infections are mainly limited to specific regions in West Africa[12, 13].

The HIV-1 genome comprises LTR, *gag*, *pol*, *env*, and several accessory genes, including *vif*, *vpr*, *nef*, and *vpu*. In contrast, the HIV-2 genome contains LTR, *gag*, *pol*, *env,* and accessory genes such as *vif*, *vpr*, *nef*, and *vpx*. Notably, Vpu is unique to HIV-1, while Vpx is specific to HIV-2. These distinct accessory proteins play crucial roles in HIV replication and pathogenesis[43] (Fig.1.3).

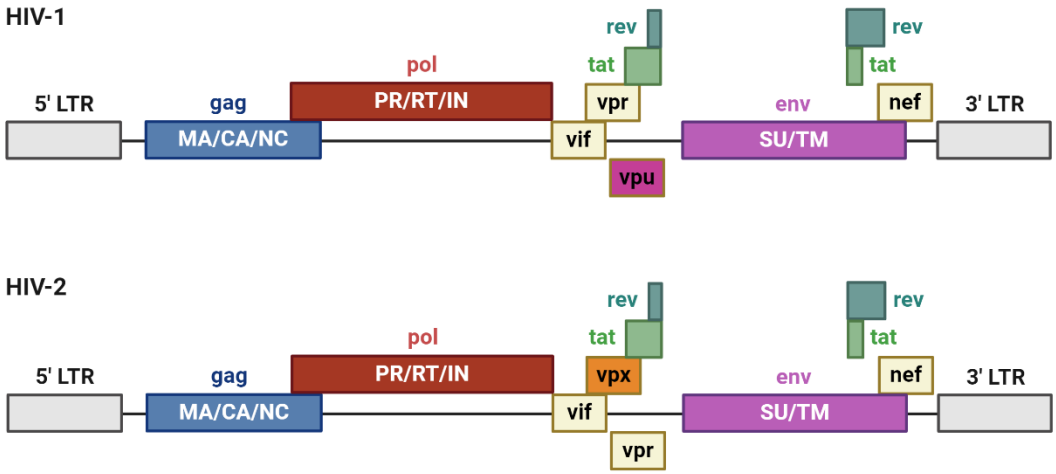

Fig. 1.3 The genome structure of HIV-1 and HIV-2. Both HIV-1 and HIV-2 genomes include two long terminal repeats (LTRs) and the genes gag, pol, env, vif, vpr, tat, rev, and nef. However, HIV-2 uniquely possesses the vpx gene, whereas HIV-1 contains the vpu gene. Created with BioRender.com.

1.3 Feline immunodeficiency virus

1.3.1 FIV infection

Feline immunodeficiency virus (FIV) is a lentivirus that shares a distant relationship with HIV and can be detected in various members of the Felidae family[44]. Approximately 2.5% to 4.4% of cats globally are infected with FIV[16]. FIV spreads among cats primarily through deep bite wounds. While it can be transmitted from infected mothers to their offspring, this mode of transmission is rare. FIV is

detectable in semen, but sexual transmission is uncommon. Infected cats may remain asymptomatic for several years due to the virus's slow progression. However, once the immune system is compromised, various secondary infections can occur. FIV-infected cats may show symptoms such as swollen lymph nodes, fever, anemia, weight loss, poor coat, reduced appetite, diarrhea, conjunctivitis, gingivitis, stomatitis, dental disease, skin issues, non-healing wounds, respiratory problems, frequent or difficult urination, and behavioral changes[16]. When a cat is diagnosed with FIV, its average survival time is approximately five years. Interestingly, only a small percentage of FIV infected domestic cats develop an immunodeficiency condition akin to AIDS caused by HIV-1[8]. However, under experimental conditions, highly pathogenic FIV isolates can result in mortality rates as high as 60%[45, 46]. Therefore, FIV-infected domestic cats have been employed as an experimental model for HIV-1 to study immune pathogenesis and to develop antiviral drugs[17].

1.3.2 FIV in Felidae family and cross-species transmission

Within the Felidae family, nine distinct lineages of FIV exhibit species-specific infectivity[47]. These FIVs can induce disease in both domestic cats and wild non-domestic Felidae species[48]. Phylogenetic analysis reveals that FIV in *Felis catus* (FIVfca) forms a monophyletic branch, which further diverges into three subtypes: A, B, and C[49]. Domestic cats are believed to have emerged relatively recently, approximately 10,000 years ago, originating from a subspecies of the wildcat *Felis silvestris* found in East Asia. This divergence marks a significant point in the evolutionary timeline of Felidae species. Genetic analysis reveals a lower genetic diversity of FIVfca compared to wild Felidae species. Furthermore, FIVfca exhibits higher evolutionary rates and increased mortality rates when compared to FIV in lion (FIVple) and FIV in puma (FIVpco)[50]. This observation suggests that the emergence of FIVfca is a relatively recent event. This is consistent with the notion that newly emerged viruses tend to exhibit higher evolutionary rates, as there is

limited co-adaptation between the virus and the new host species[49]. In addition to domestic cats, FIV also infects various wild felid species, including lion (FIVple), puma (FIVpco), bobcat (FIVlru), and others[48]. Some studies have referred to FIVpco as puma lentivirus (PLV)[51-56]. PLV encompasses subtypes A and B, designated as PLVA and PLVB, respectively. PLVB has been found to infect pumas across North and South America, while PLVA infects pumas and bobcats specifically in southern California and Florida[55].

The HIV pandemic originated from cross-species transmission events of SIVs to humans. Cross-species transmission of FIV among various Felidae species has been documented, paralleling the inter-species infections observed in primate lentiviruses[51]. For example, PLVA in pumas is believed to have originated from an ancestral transmission event of PLVA from bobcats. Moreover, the cross-species transmission of PLVA from bobcats to pumas is believed to be an ongoing process[54, 57]. Additionally, pumas are occasionally infected by the FIV of domestic cats, and FIV from lions has been shown to be transmissible to tigers and leopards[47, 53, 58, 59]. However, phylogenetic evidence suggests that FIV transmissions between wild cat species are exceedingly rare, likely due to host-specific restriction factors that act as barriers to the spread of FIV[51, 52, 60].

1.3.3 The genome structure of FIV

The FIV genome comprises the *gag*, *pol*, *env*, *vif*, *rev*, and *orfA* genes, which encode the Gag, Pol, and Envelope structural and enzymatic proteins, as well as the accessory proteins Vif and OrfA (Fig.1.4). FIV targets T cells, monocytes/macrophages, dendritic cells, and B lymphocytes. In contrast to HIV, which uses CD4, FIV employs CD134 as its receptor and CXCR4 as a co-receptor[28-30]. Despite this difference, the entry mechanisms of FIV and HIV are similar. During viral replication, the expression levels of Vif and OrfA are very low; however, both proteins play crucial roles in viral replication and infection. The Vif

protein counteracts the restriction imposed by feline APOBEC3 by promoting its degradation through E3 ubiquitination[61]. The OrfA protein downregulates the expression of the CD134 receptor on the cell surface and enhances viral release and replication in an ill-defined way[62, 63]. Additionally, OrfA modulates the expression of cellular splicing factors and proteins involved in the proteasome-ubiquitination pathway[64].

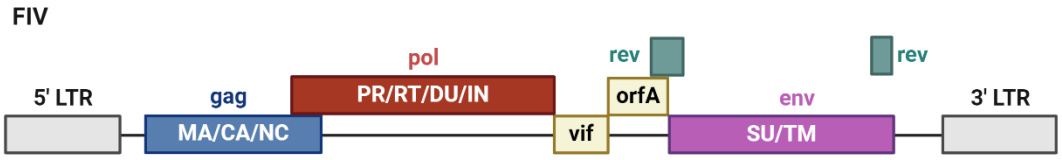

Fig. 1.4 The genome structure of FIV. FIV features two long terminal repeats (LTRs) located at its 5' and 3' termini. The viral genome includes structural genes: *gag*, *pol*, and *env*, regulatory genes: *vif*, *orfA*, and *rev*. The *gag* gene encodes viral structural proteins, including the matrix (MA) protein, capsid (CA) protein, and nucleocapsid (NC) protein. The *pol* gene encodes viral enzymes, namely protease (PR), reverse transcriptase (RT), integrase (IN), and dUTPase (DU). The *env* gene encodes envelope proteins, which are the surface (SU) glycoprotein and the transmembrane (TM) protein. Figure adapted from: Zhang ZL, Gu QY, Marino D, Lee KL, Kong IK, Häussinger D, et al. Feline APOBEC3s, Barriers to Cross-Species Transmission of FIV? Published in Viruses-Basel. 2018; 10(4)[65]. Published under the Creative Commons Attribution 4.0 International License (https://creativecommons.org/licenses/by/4.0/). Reproduced with BioRender.com.

1.4 Host restriction factors in felines

In mammals, including felids, the innate immune system serves as the first line of defense against pathogens. Among its components are a group of proteins known as restriction factors, which possess potent antiviral properties against many diverse viruses. These proteins are constitutively expressed in cells and can also be induced by type I interferon. Restriction factors can inhibit retrovirus replication by targeting specific steps in the viral life cycle through various mechanisms[66]. However, retroviruses have evolved specific counteracting mechanisms to escape inhibition by restriction factors, allowing them to survive and replicate in their

mammalian hosts. Numerous restriction factors have been identified that can inhibit the replication of HIV, SIV, and FIV. The most extensively studied examples include TRIM5α (tripartite motif-containing protein 5α), APOBEC3 (apolipoprotein B mRNA-editing enzyme, catalytic polypeptide-like 3), SAMHD1 (SAM and HD domain-containing protein 1), tetherin, MX2 (myxovirus resistance B, also known as MX2), and SERINC3/5 (serine incorporator proteins 3 and 5)[65] (Fig.1.5).

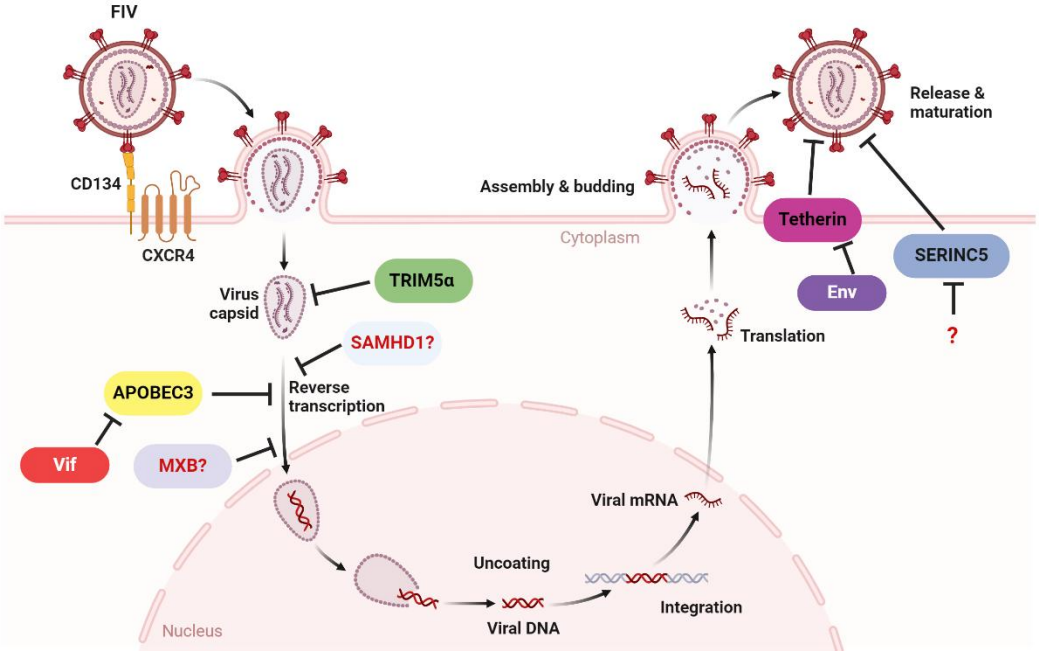

Fig. 1.5 Feline restriction factors targeting FIV. In the absence of viral antagonists, various cellular proteins known as restriction factors inhibit distinct stages of the viral replication cycle. For instance, monkey TRIM5α interacts with the FIV capsid, blocking an early step of infection. In contrast, felines express a truncated TRIM5 gene that lacks antiretroviral activity, although an engineered fusion protein combining feline TRIM5 with feline CypA has shown potential inhibitory effects against FIV. Feline APOBEC3 proteins induce hypermutations in FIVΔVif genomes through cytidine deamination. Feline tetherin impedes the release of FIV from the cell surface. Cats possess a mutation in the MXB gene, leading to a severely truncated transcript that does not produce a functional protein. Domestic cat SERINC5 inhibits FIV, but FIV does not exhibit a clear mechanism to counteract SERINC5 activity. However, these restriction factors are targeted by FIV-encoded proteins: FIV Vif binds to feline APOBEC3s, promoting their degradation via the proteasome pathway, while FIV Env antagonizes tetherin's restrictive effects. Created with BioRender.com.

1.4.1 TRIM5α

TRIM5α, a splice variant of tripartite motif (TRIM) family member 5, is a well-characterized restriction factor for HIV[67-69]. TRIM5α is expressed in cells of primates and most mammals and inhibits lentiviral infection by interacting with the lentiviral capsid, disturbing the uncoating process, inducing an innate signaling cascade, and potentially being involved in autophagy, thus providing an effective species-specific barrier to lentiviral infection[70, 71]. TRIM family proteins possess a functional motif at the N-terminus, comprising the RING (really interesting new gene), B-box, and coiled-coil domains[72]. TRIM5α, in addition, harbors a C-terminal PRYSPRY (B30.2) domain, which facilitates direct interaction with the capsid cores of HIV-1 and FIV, leading to its antiviral activity[70, 72-74]. The RING domain of TRIM5α exhibits E3 ubiquitin ligase activity, facilitating proteasome-dependent degradation of the HIV-1 core[73, 75]. In felines, a truncated TRIM5 gene is expressed, which lacks intrinsic antiretroviral activity[76]. Interestingly, a chimeric protein comprising feline TRIM5 and feline cyclophilin A (CYPA) demonstrates inhibitory potential against both FIV and HIV-1[77].

1.4.2 APOBEC3

The apolipoprotein B mRNA editing enzyme catalytic polypeptide-like 3 (APOBEC3; A3) proteins are anti-viral restriction factors found in placental mammals, characterized by the presence of one or two zinc (Z)-binding domains[61, 78, 79]. A3 proteins are selectively packaged into nascent lentiviral particles during the process of virus assembly and release, provided that the virus does not possess mechanisms to counteract these encapsidated A3 proteins. In subsequent rounds of infection, these incorporated A3 proteins play a crucial role in deaminating cytidines present in the negative-strand DNA formed during the process of reverse transcription. Consequently, this deamination process leads to the G-to-A hypermutations in the coding strand of the viral genome[80, 81] (Fig.1.6). The number and arrangement of A3 genes vary among different clades, cats possess four *A3*

genes: *A3Z2a*, *A3Z2b*, *A3Z2c*, and *A3Z3*[78, 82].

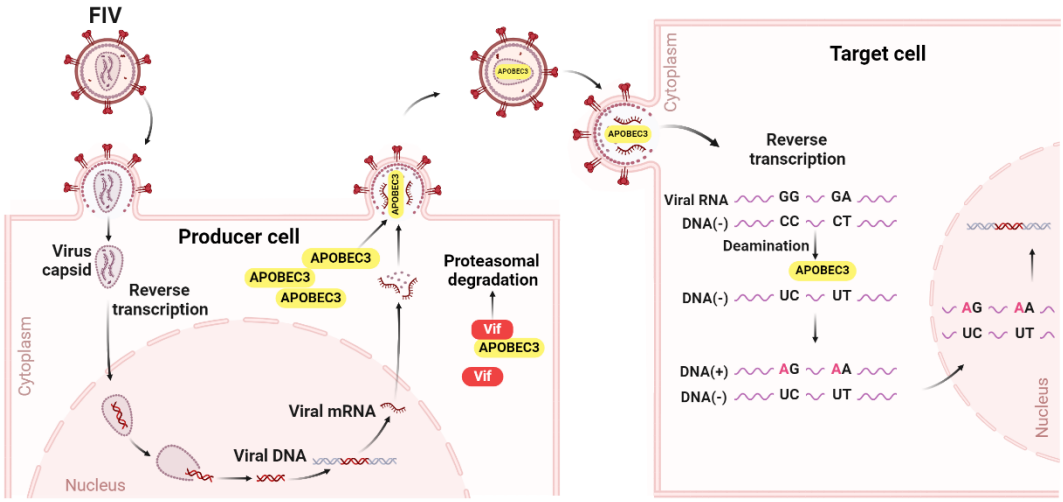

Fig. 1.6 Impact of feline A3 on FIV replication. In producer cells, A3 proteins can be incorporated into viral particles and transferred to target cells in the absence of Vif. During viral reverse transcription, A3s catalyze the deamination of cytidine to uridine in the viral cDNA. This process leads to the generation of numerous G-to-A hypermutations in the newly synthesized viral DNA strand. These heavily mutated viral genomes are subsequently degraded by cellular enzymes. However, FIV Vif counteracts this by directly interacting with feline A3 proteins, forming an A3-Vif-E3 ubiquitination complex that targets A3 for degradation via the proteasome pathway. Figure adapted from: Münk C, Jensen BE, Zielonka J, Häussinger D, Kamp C. Running loose or getting lost: how HIV-1 counters and capitalizes on APOBEC3-induced mutagenesis through its Vif protein. Published in Viruses-Basel 2012; 4(11):3132-3161[83]. Published under the Creative Commons Attribution 4.0 International License (https://creativecommons.org/licenses/by/4.0/). Reproduced with BioRender.com.

1.4.3 SAMHD1

Sterile α motif and histidine-aspartic acid domain-containing protein 1 (SAMHD1) is an enzyme that potently restricts HIV infection in non-cycling cells, including macrophages, dendritic cells, and resting CD4+ T cells[84-86]. SAMHD1 suppresses retroviral reverse transcription by hydrolyzing intracellular deoxynucleotide triphosphates (dNTPs), thereby depleting the dNTP pool essential for viral cDNA synthesis during the early stage of the replication cycle[87-89]. By reducing dNTP

availability, SAMHD1 effectively inhibits HIV replication in resting CD4+ T cells and monocytes. However, its antiviral activity can be counteracted by the viral accessory protein Vpx from HIV-2 and SIV, which targets SAMHD1 for proteasomal degradation[84, 85]. SAMHD1 also exhibits binding activity toward single-stranded DNA and RNA, suggesting a potential role in directly degrading HIV-1 genomic RNA to inhibit viral infection[90]. In addition to its activity against HIV-1, human SAMHD1 can also inhibit FIV replication[91]. Furthermore, feline SAMHD1 has been shown to restrict FIV replication in SAMHD1-knockout THP-1 cells[92]. Notably, a cytoplasmic variant of feline SAMHD1 demonstrates enhanced restriction of SIVmac239 and HIV-2 ROD compared to its wild-type counterpart, as it is less susceptible to Vpx-mediated degradation, a feature like cytoplasmic human SAMHD1[93].

1.4.4 Tetherin

Tetherin, also known as BST2, is a type I interferon (IFN-I)-inducible protein that forms homodimers and physically tethers newly formed HIV-1 particles to the plasma membrane via its transmembrane domain and C-terminal GPI anchor[94, 95]. This tethering function restricts viral particle release from infected cells, facilitating their internalization and degradation via endosomal/lysosomal pathways, while also triggering NF-κB-dependent proinflammatory signaling[96-98]. Certain viral proteins can counteract the inhibitory effects of tetherin. For instance, the Vpu protein of HIV-1 and the Nef proteins of SIVmus, SIVgsn, and SIVmon promote the internalization and subsequent downregulation of tetherin at the cell surface. Additionally, the Env proteins of HIV-2, SIVtan, FIV, EIAV, and Ebola virus can sequester tetherin within intracellular compartments[99-102]. Feline tetherin inhibits the release of both FIV and HIV-1; however, this restriction is antagonized by the FIV Env protein[103-105]. Recent research has identified the signal peptide of FIV Env as the tetherin antagonist, which, unlike primate lentiviral tetherin antagonists, prevents the incorporation of tetherin into viral particles without inducing its degradation or downregulation from the plasma membrane[106].

1.4.5 MX2

Myxovirus resistance (MX) proteins, encoded by the *MX* genes, are interferon-induced GTPases that function as viral restriction factors. Most mammals possess two *MX* genes: *MXA* (also known as *MX1*) and *MXB* (also known as *MX2*)[107]. The human MX1 protein is capable of restricting various viral pathogens, including influenza viruses[108]. MX2 protein functions as a capsid-interacting restriction factor that inhibits HIV replication after reverse transcription but before integration[109]. However, the precise mechanisms by which MX2 inhibits HIV, including how it recognizes and interacts with the HIV capsid, remain poorly understood. Beyond HIV, human MX2 also exhibits antiviral activity against herpesviruses and hepatitis C virus[110, 111]. Notably, human MX2 does not inhibit several non-primate retroviruses, such as FIV, EIAV, and MLV[109]. In contrast, one study reported that equine MX2 (eMX2) effectively restricts EIAV in vitro and additionally inhibits both HIV-1 and MLV, with moderate inhibition observed against FIV[112]. Interestingly, two studies have identified that cats carry a highly damaged and inactivated *MXB* gene[113, 114].

1.4.6 SERINC

The serine incorporator (SERINC) protein family comprises transmembrane proteins that are highly conserved across eukaryotes and include five distinct members (SERINC1–5)[115, 116]. Structurally, SERINC proteins are characterized by two domains formed by 10 transmembrane helices separated by a diagonal helix[117]. Functionally, SERINC proteins act as eukaryotic cell membrane transporters, incorporating serine into membrane lipids[115]. Among the SERINC family, human SERINC3 and SERINC5 have been identified as restriction factors against HIV[116, 118]. Their antiviral mechanism is thought to involve limiting the expansion of the viral fusion pore, thereby preventing the release of the viral core into the cytoplasm[116, 118, 119]. In addition to this membrane-level action, SERINC3

and SERINC5 also play intracellular roles, enhancing type I interferon production and activating NF-κB signaling[120]. However, the antiviral activity of SERINC3 and SERINC5 is counteracted by the Nef protein of HIV-1 and SIVs[116, 118, 121]. The Env protein of certain HIV-1 strains (AD8-1 and YU-2) and the glycoproteins of vesicular stomatitis virus (VSV) and Ebola virus can also inhibit the antiviral activity of SERINC5[122]. Interestingly, domestic cat SERINC5 has been shown to exhibit antiviral activity as well. A recent study reported that in the absence of Nef, HIV-1 is restricted by feline SERINC5, but this restriction is alleviated in the presence of Nef[123]. Both domestic cat and human SERINC5 inhibit FIV; however, FIV does not exhibit a clear mechanism to counteract SERINC5 activity[123].

1.5 Cullin-RING E3 ubiquitin ligase

Viruses extensively exploit the ubiquitin-proteasome system (UPS) to enhance their replication and counteract host defenses. Cullin-RING E3 ubiquitin ligases (CRLs), the largest family of eukaryotic ubiquitin ligases, are frequently targeted by a wide range of taxonomically diverse viruses to circumvent various host defense mechanisms[124]. The UPS is a principal mechanism for regulating protein activity by degrading various proteins. Its primary function is to remove dysfunctional or misfolded proteins through proteasomal degradation[125]. Ubiquitin (Ub) is a small, highly conserved regulatory protein present in most eukaryotic cells[126]. The human genome contains four ubiquitin genes: *UBB*, *UBC*, *UBA52*, and *RPS27A*[126]. Ubiquitination involves three main steps: activation, conjugation, and ligation, facilitated by three types of enzymes: ubiquitin-activating enzymes (E1s), ubiquitin-conjugating enzymes (E2s), and ubiquitin ligases (E3s). During the activation step, the E1 enzyme activates ubiquitin in the presence of ATP, forming the Ub-S-E1 complex. In the subsequent conjugation step, the E1 enzyme is replaced by the E2 enzyme, which interacts with the activated ubiquitin. Finally, during the ligation step, the E2 enzyme transfers ubiquitin to the E3 enzyme, which then facilitates the attachment of ubiquitin to specific substrate proteins[127]. In both humans and cats,

four families of E3 ubiquitin ligases have been identified: HECT, RING-finger, U-box, and RBR[127, 128] (Fig. 1.7). The RING-finger family, the largest of these, is commonly referred to as CRLs. CRLs comprise four components: cullins, RINGs, adaptor proteins, and substrate recognition receptors.

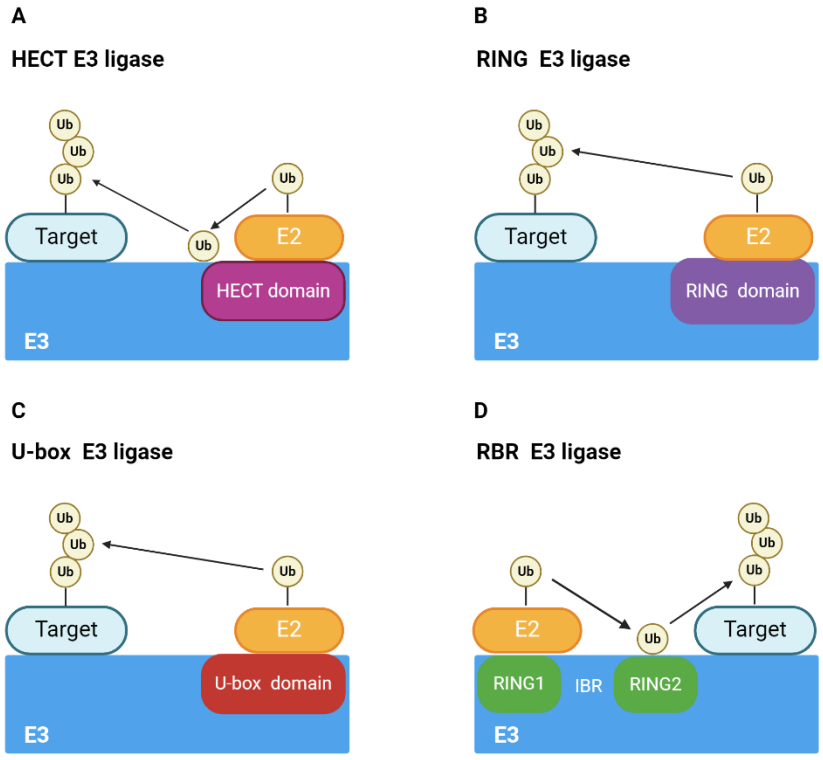

Fig. 1.7 Membership of E3 ubiquitin ligase. E3 ubiquitin ligases are categorized into four families: HECT, RING-finger, U-box, and RBR. The RING-finger E3 ligases, the largest of these families, are collectively known as cullin-RING ubiquitin ligases (CRLs). Typically, CRLs are composed of four components: cullins, RING proteins, adaptor proteins, and substrate recognition receptors. Figure adapted from "E3 ubiquitin ligases: styles, structures and functions" by Yang Q, Zhao J, Chen D, Wang Y, published in Molecular Biomedicine, 2021; 2(1):23[128], under the Creative Commons Attribution 4.0 International License (https://creativecommons.org/licenses/by/4.0/). Reproduced with BioRender.com.

The mammalian cullin protein family plays a crucial role in the post-translational modification of cellular proteins through ubiquitination. These proteins function as scaffolds that interact with RING proteins to form CRLs, facilitating the

ubiquitination process. The mammalian cullin protein family consists of eight members: CUL1, CUL2, CUL3, CUL4A, CUL4B, CUL5, CUL7, and CUL9 (also known as PARC). These proteins are distinguished by the presence of a cullin homology domain[129]. Each member of the cullin family associates with distinct RING proteins, adaptor proteins, and substrate recognition receptors (Fig. 1.8). Previous studies have demonstrated that HIV-1 Vif hijacks the CUL5 ubiquitin ligase complex to evade antiviral responses. CUL5 binds with the RING-box protein RBX2 to form CRL. In this CUL5-CRL complex, the adaptor proteins are Elongin B (ELOB) and Elongin C (ELOC), and the substrate recognition receptors are proteins containing SOCS-box motifs[130]. Vif, an accessory protein in certain lentiviruses, contains a SOCS-box domain and functions as a substrate receptor within the CUL5 ubiquitin ligase complex. This interaction facilitates the poly-ubiquitination and the proteasomal degradation of the APOBEC3 proteins [131, 132].

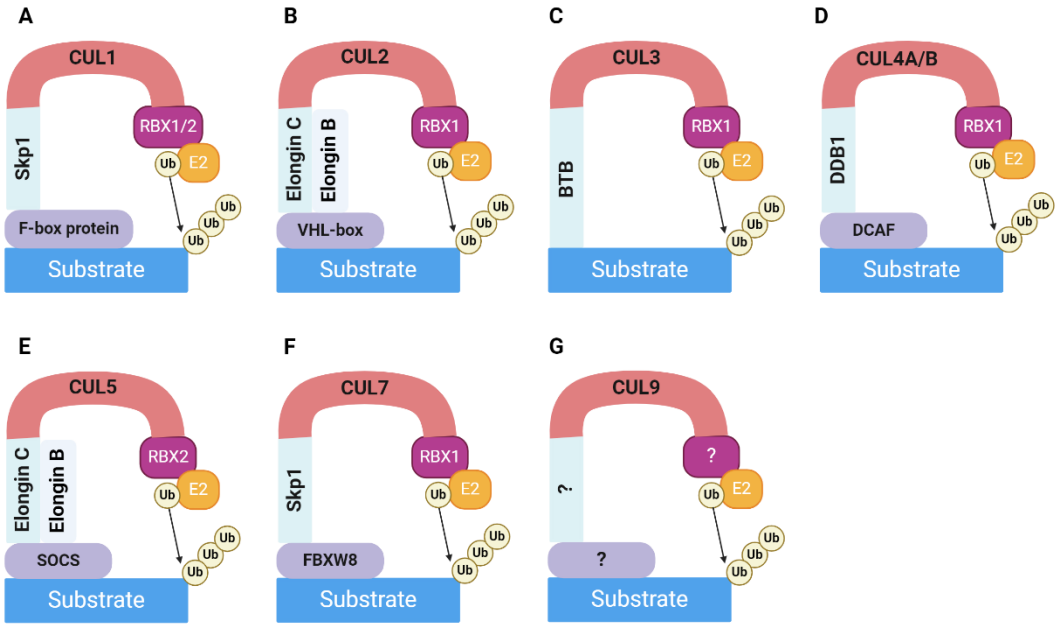

Fig. 1.8 Models of cullin-RING E3 ligase complexes. CUL1 and CUL7 proteins recruit SKP1 as an adaptor protein, whereas CUL2 and CUL5 proteins recruit Elongin B/C as adaptor proteins. CUL3 recruits BTB proteins as adaptor proteins, while CUL4A and CUL4B recruit DDB1 as an adaptor protein. The receptor proteins associated with CUL1, CUL2, CUL4A, CUL4B, CUL5, and CUL7 are F-box proteins, VHL-box proteins, DCAFs, SOCS proteins, and FBXW8 proteins, respectively. RING proteins (RBX1/2) interact with cullins to facilitate the transfer of ubiquitin from RBX1/RBX2-bound

E2 to substrates. The adaptor proteins, receptor proteins, and RING proteins associated with CUL9 remain unidentified. Figure adapted from: Chen, Z. Sui, J. Zhang, F. Zhang, C. (2015). Cullin family proteins and tumorigenesis: Genetic association and molecular mechanisms. Journal of Cancer, 6(3), 233–242[133]. Licensed under CC BY-NC 4.0 (https://creativecommons.org/licenses/by/4.0/). Reproduced with BioRender.com.

1.6 Feline APOBEC3 and FIV Vif

The domestic cat, as well as other members of the Felidae family, possesses four *A3* genes, these include three closely related *A3Z2* genes (*A3Z2a*, *A3Z2b*, *A3Z2c*) and one *A3Z3* gene. In addition to the four canonical A3 proteins, the cat genome has the capability to produce a fifth A3 protein through read-through transcription and alternative splicing, this protein is known as the double-domain A3Z2Z3[60, 61] (Fig.1.9). A3Z2Z3 proteins have also been identified in large cats (Pantherinae), suggesting evolutionary conservation in gene regulation[61, 134]. Feline A3s have been shown to inhibit FIVΔvif, similarly to how human A3s restrict HIV-1Δvif. Specifically, feline A3Z3 and A3Z2Z3 are effective against FIVΔvif, while A3Z2s are not. In contrast, A3Z2s strongly inhibit feline foamy virus (FFV) Δbet, whereas A3Z3 and A3Z2Z3 only slightly reduce FFV Δbet infectivity[61, 135]. In addition to their activity against feline retroviruses, feline A3s also function as restriction factors for HIV and SIV[136].

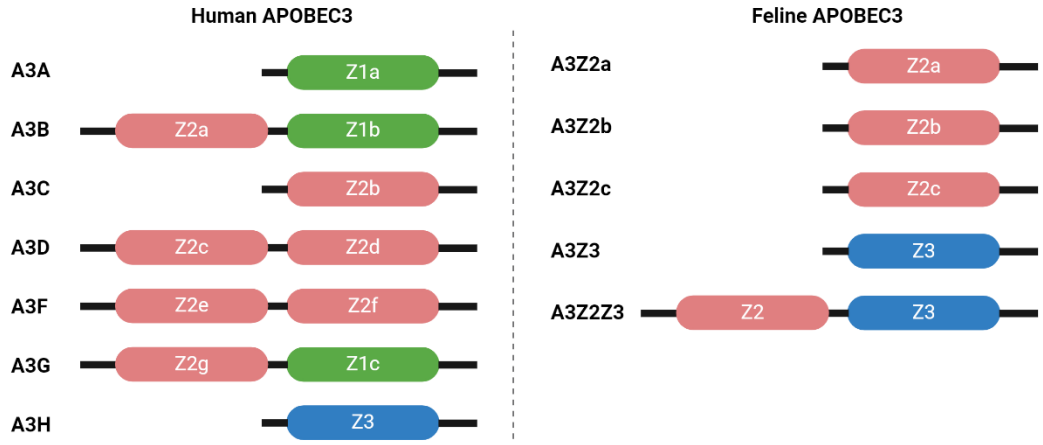

Fig. 1.9 Diagram of human and feline APOBEC3 proteins. Humans possess seven A3 proteins, each containing either one zinc-binding domain (A3A, A3C, and A3H) or two zinc-binding domains

(A3B, A3D, A3F, and A3G). In domestic cats, three single-domain A3Z2 proteins (A3Z2a, A3Z2b, and A3Z2c) and one A3Z3 protein are expressed. Additionally, double-domain A3Z2Z3 proteins are produced through read-through transcription and mRNA alternative splicing. Figure adapted from: Zielonka J, Münk C. Cellular Restriction Factors of Feline Immunodeficiency Virus. Viruses-Basel 2011; 3(10):1986-2005[60]. Published under the Creative Commons Attribution 4.0 International License(https://creativecommons.org/licenses/by/4.0/). Reproduced with BioRender.com.

Like HIV-1 Vif, FIV Vif assembles an E3 ubiquitin ligase complex that targets feline A3 proteins for degradation[137] (Fig. 1.10). However, HIV-1 Vif forms a Vif-E3 ligase complex with CUL 5, Elongin B/C, CBF-β, and RING box 2 proteins, where the cofactor CBF-β stabilizes the assembly[138]. In contrast, FIV Vif forms a Vif-E3 ligase complex with CUL 5, Elongin B/C, and RING box 2 proteins, but it does not require CBF-β for A3 degradation[139]. Similarly, Vifs from other non-primate lentiviruses, such as maedi-visna virus (MVV), caprine arthritis encephalitis virus (CAEV), and bovine immunodeficiency virus (BIV), do not require CBF-β to induce A3 degradation[139, 140]. Correspondingly, research indicates that MVV Vif utilizes cellular cyclophilin A (CYPA) as a cofactor to reconstitute the E3 ligase complex, while BIV Vif seems to function independently of any cofactors[139]. It remains unclear whether FIV Vif interacts with or recruits additional host proteins.

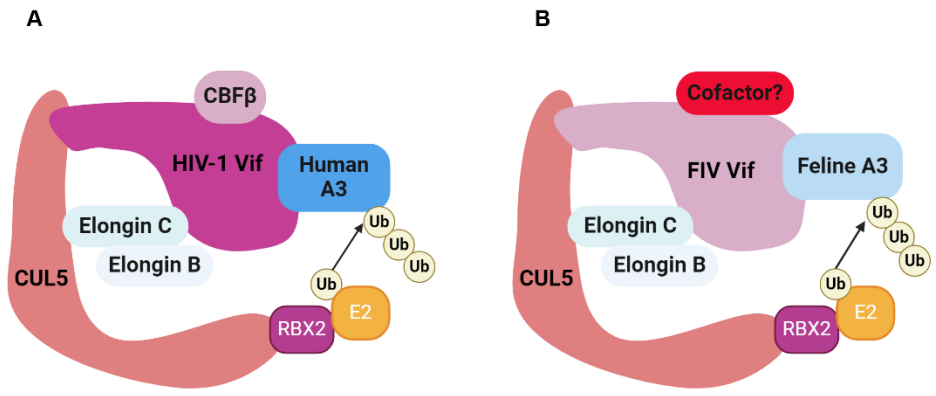

Fig. 1.10 Models of HIV-1/FIV Vif-E3 ligases. (A) HIV-1 Vif assembles an E3 ligase complex, known as Vif-E3 ligase, in association with CUL 5, Elongin B/C, CBF-β, and RING box 2 proteins. (B) FIV Vif forms a Vif-E3 ligase complex with CUL 5, Elongin B/C, and RING box 2 proteins. Human and

feline A3 proteins serve as the respective substrates for these Vif-E3 ligase complexes. Fig. 1.10A was adapted from: Collins DR, Collins KL. HIV-1 accessory proteins adapt cellular adaptors to facilitate immune evasion. PLoS Pathog 2014; 10(1): e1003851[141]. Licensed under CC BY 4.0 (https://creativecommons.org/licenses/by/4.0/). Reproduced with BioRender.com. Fig. 1.10B was created with BioRender.com.

1.7 The molecular interaction between Vif and APOBEC3

1.7.1 Vif interaction interface on A3 proteins

HIV-1 Vif directly binds to A3s and mediates their degradation via the proteasomal pathway[142]. Therefore, the molecular interaction between Vif and A3 is essential for the virus to overcome A3-mediated restriction. The hA3C and the C-terminal domain (CTD) of hA3F are conserved homologous Z2-type A3 proteins[78]. Ten equivalent residues in these Z2-type APOBEC3 proteins have been identified as crucial for interaction with HIV-1 Vif [143, 144]. However, it has been demonstrated that while E324 in hA3F is essential for HIV-1 Vif interaction, the equivalent residue E141 in hA3C is not [143, 145]. The 128DPDY131 motif in hA3G directly interacts with the 14YRHHY17 domain of HIV-1 Vif[142, 146]. Additionally, the E121 residue in hA3H hapII is crucial for its sensitivity to and binding with HIV-1 Vif derived from the NL4-3 strain[147]. These findings suggest that the Vif interaction interface may differ among A3 proteins (Fig. 1.11).

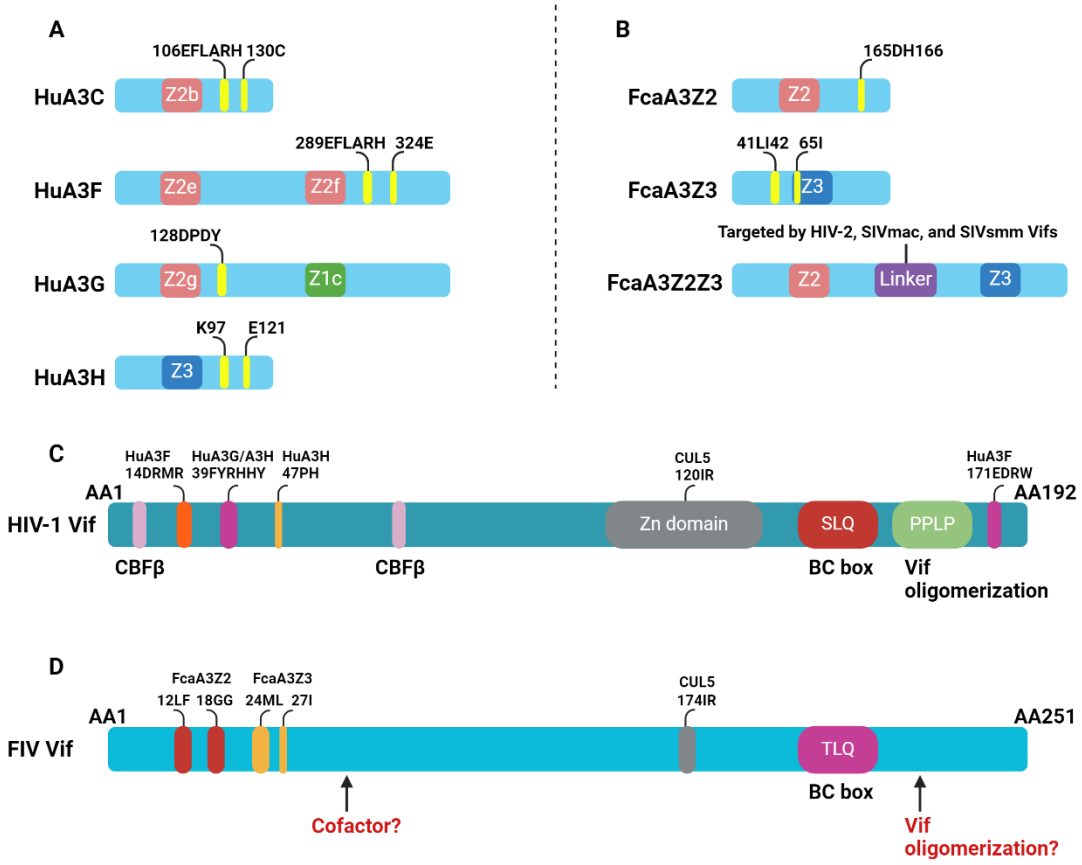

Fig. 1.11 Schematic representation of A3-Vif-CUL5 interaction sites. (A) HIV-1 Vif binding sites in hA3C, hA3F, hA3G, and hA3H. (B) FIV Vif binding sites in FcaA3Z2 and FcaA3Z3. (C) Binding sites for hA3F, hA3G, hA3H, CUL5, CBF-β, and Elongin B/C within HIV-1 Vif. (D) Binding sites for FcaA3Z2, FcaA3Z3, and CUL5 within FIV Vif. Figure adapted from: Zhang ZL, Gu QY, Marino D, Lee KL, Kong IK, Häussinger D, et al. Feline APOBEC3s, Barriers to Cross-Species Transmission of FIV? Viruses. 2018; 10(4)[65]. Published under the Creative Commons Attribution 4.0 International License (https://creativecommons.org/licenses/by/4.0/). Reproduced with BioRender.com.

1.7.2 A3 interaction interface on Vif proteins

The interaction sites of A3 proteins in HIV-1 Vif are crucial for their binding and subsequent degradation. The N-terminal region of HIV-1 Vif is particularly important for binding to human A3 proteins. A single study has identified that the residues D14, R15, and W79 in HIV-1 Vif are responsible for binding to A3C, A3D, and A3F[148]. The 40YRHHY44 motif is essential for the degradation of A3G, while the 14DRMR17 motif is critical for targeting A3F for degradation[149]. Additionally, A3H binds to a distinct site involving the residues F39, H48, and the 60GDAK63

motif[150, 151]. It has also been reported that the C-terminus of Vif binds to certain A3 proteins. For example, the 171EDRW174 motif binds to A3F, while the 161PPLP164 motif binds to A3G[152, 153].

Research on the interaction sites of feline A3 proteins in FIV Vif is relatively limited. One study reported that the N-terminal Vif motifs, specifically 12LF13 and 18GG19, interact with FcaA3Z2, while residues M24, L25, and I27 specifically interact with FcaA3Z3[154] (Fig. 1.11).

1.8 The molecular interaction between Vif and CUL5

1.8.1 Vif interaction interface on CUL5 proteins

CUL5 and CUL2 both utilize the evolutionarily conserved adaptor protein ELOC to assemble cullin-RING E3 ligase complexes[155]. However, HIV-1 Vif specifically prefers CUL5 over CUL2 as the scaffold protein for the degradation of A3G[132]. Structural analysis indicates that residues L52 and W53 in CUL5 play a crucial role in the selection of CUL5 by HIV-1 Vif. These HIV-1 Vif-interacting amino acids in CUL5 are highly variable compared to their counterparts in CUL2. Substituting these residues in CUL5 with their equivalents in CUL2 significantly impairs CUL5's ability to interact with the HIV-1 Vif-organized complex[156]. Feline CUL5 and human CUL5 differ by a single amino acid, and this mutation does not impact its interaction with FIV Vif[137]. One study reports that the 52LW53 region in CUL5 is also critical for binding to FIV Vif[157].

1.8.2 CUL5 interaction interface on Vif proteins

The HCCH motif in HIV-1 Vif (His108, Cys114, Cys133, and His139), which is a unique zinc finger motif, is crucial for binding to CUL5. This binding is essential for Vif-mediated degradation of A3G and overall HIV-1 infectivity[158]. In the structural complex of HIV-1 Vif and CUL5, the 120IR121 motif of Vif is essential for interaction with CUL5[156]. Like HIV-1 Vif, FIV Vif interacts with CUL5 to form an E3 ubiquitin ligase complex, leading to the degradation of feline A3 proteins[159]. However, unlike

HIV-1 Vif, FIV Vif does not require CBF-β to stabilize this complex[140]. One study identified a KCCC motif at the C-terminal region of FIV Vif, which is analogous to the HCCH motif found in HIV-1 Vif. Within this KCCC motif, a conserved hydrophobic region (174IR175) is crucial for the interaction with CUL5[157] (Fig. 1.11).

In summary, the interactions between lentiviral Vif proteins and host factors such as A3 proteins and CULs are not yet fully understood. Further research is necessary to address these gaps in our knowledge.

1.9 Objectives of the present study

Elucidation of the interaction between lentiviral Vif proteins, particularly those from feline lentivirus subgroups, and APOBEC3 proteins:

1. Mapping of key domains of Vif that interact specifically with feline APOBEC3 proteins. Identification of key residues responsible for the inability of PLV1695 Vif (a puma FIV subtype) to counteract A3Z3 restriction.
2. Determination of specific Cullin proteins that interact with lentiviral Vif proteins.
3. Characterize the interaction interface between Vif and CUL5.

2. Materials and Methods

2.1 Molecular biology

2.1.1 Plasmid construction

All A3s express a carboxy-terminal hemagglutinin (HA) tag. Previous studies have described A3s in both domestic cats and big cats (Pantherinae)[134]. FIV-34TF10 (codon-optimized), PLVA, PLVB, PLV1695, HIV-1, HIV-2, Vif genes, each containing a C-terminal V5 or Flag tag, were inserted into pcWPRE vector utilizing the EcoRI and NotI restriction sites.

Human CUL1 was inserted into the pcDNA3-myc vector using the BamHI and XhoI restriction sites. Human SKP1, containing an N-terminal Flag tag, was inserted into

the pcDNA3.1(+) vector utilizing the NheI and HindIII restriction sites. The constructs pcDNA3-DN-hCUL2-FLAG, pcDNA3-myc3-CUL2, pcDNA3-DN-hCUL5-FLAG, and pcDNA3-myc-CUL5 have been described in previous studies[157]. The plasmids pcDNA3-myc-CUL3 (19893), pcDNA3-myc-CUL4A (19951), pcDNA3-myc-CUL4B (19922), and pcDNA3-DN-hCUL1-FLAG (15818) were obtained from Addgene (Cambridge, USA).

The pFP93 plasmid (FIV GagPol construct) was kindly provided by Eric M. Poeschla[160]. For the construction of pFPLur15 (PLVA GagPol construct), the gag gene from PLVA was cloned into the construct vector due to the absence of suitable restriction sites in the PLVA sequence, with the pol gene sourced from pFP93. For the PLVB packaging construct, the gag-pol genes from PLVB were cloned into the construct vector, resulting in PLVB GagPol (pFP-X879).

PLVB and PLV1695 Vif chimeras were generated through overlap PCR (Fig. 2.1). Chimera 1 and Chimera 4 were designed to incorporate amino acids 1-72 and 1-25 from PLVB Vif, respectively, with the remaining portion derived from PLV1695 Vif. In contrast, Chimera 2, Chimera 3, Chimera 5, and Chimera 6 were engineered by integrating amino acids 1-72, 1-160, 1-192, and 1-207 from PLV1695 Vif, respectively, while the remaining segments were derived from PLVB Vif (Fig. 2.2). The 5' and 3' fragments of these chimeras were amplified separately using specific primer pairs (Table 2.2). These two fragments were then combined and further amplified using the external primers listed in Table 2.2. Additionally, FIV, PLVA, PLVB, PLV1695, HIV-1, and HIV-2 Vif mutants were generated through overlap PCR, with the primers used for these mutation constructs also listed in Table 2.2. All the plasmids used in this study are shown in Table 2.1.

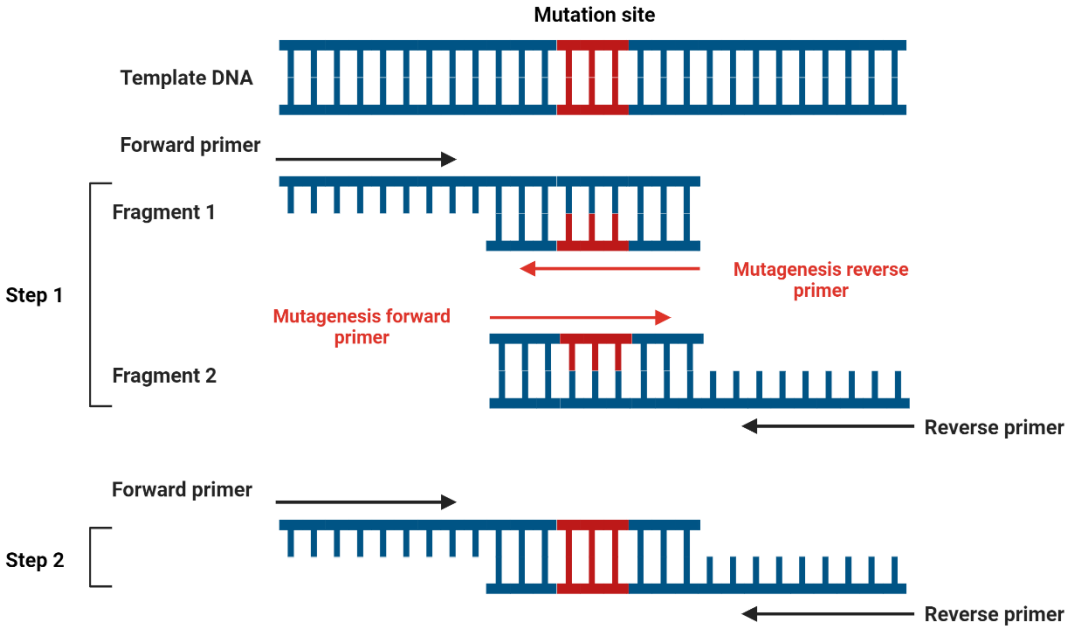

Fig. 2.1 Schematic illustration of overlap PCR. Overlap PCR involves two sequential amplification steps. In the first step, the primers used are either a forward primer paired with a mutagenesis reverse primer or a mutagenesis forward primer paired with a reverse primer. This initial amplification yields two distinct PCR fragments. These fragments, designated as Fragment 1 and Fragment 2, serve as templates in the second round of PCR, where amplification is carried out using the forward and reverse primers. Created with BioRender.com.

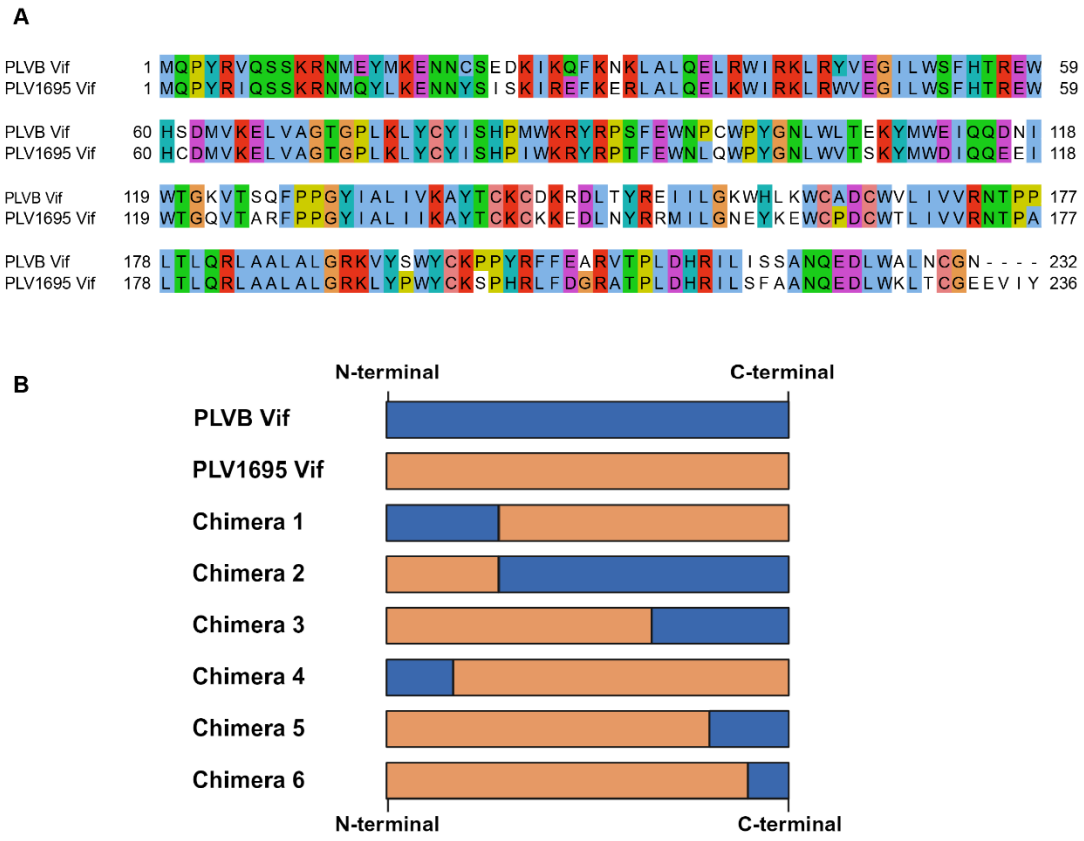

Fig. 2.2 Schematic representation of PLVB and PLV1695 Vif chimeras. (A) Sequence alignment of PLVB and PLV1695 Vif proteins. The alignment highlights conserved residues according to their physicochemical properties using the Clustal color scheme. For further details, refer to materials and methods section 2.3.4. (B) Schematic representation of the PLVB/PLV1695 Vif chimeras. Chimera 1 and Chimera 4 were designed to incorporate amino acids 1-72 and 1-25 from PLVB Vif, respectively, with the remaining portion derived from PLV1695 Vif. Chimera 2, Chimera 3, Chimera 5, and Chimera 6 were engineered by integrating amino acids 1-72, 1-160, 1-192, and 1-207 from PLV1695 Vif, respectively, while the remaining segments were derived from PLVB Vif. Fig. 2.2 B was created with BioRender.com.

Plasmids of this study:

Plasmid	Resistance gene	Tag
pcDNA3.1 empty	Ampicillin	No tag
pcWPRE empty	Ampicillin	No tag
pcCatA3Z2	Ampicillin	HA

pcCatA3Z3	Ampicillin	HA
pcCatA3Z2Z3	Ampicillin	HA
pcPumaA3Z2	Ampicillin	HA
pcPumaA3Z3	Ampicillin	HA
pcPumaA3Z2Z3	Ampicillin	HA
pcBobcatA3Z3A1	Ampicillin	HA
pcBobcatA3Z3A2	Ampicillin	HA
pcWPRE-FIV Vif	Ampicillin	V5
pcWPRE-FIV Vif	Ampicillin	Flag
pcWPRE-FIV Vif N221A	Ampicillin	V5
pcWPRE-FIV Vif Q222A	Ampicillin	V5
pcWPRE-FIV Vif R223A	Ampicillin	V5
pcWPRE-FIV Vif F224A	Ampicillin	V5
pcWPRE-PLVA Vif	Ampicillin	V5
pcWPRE-PLVA Vif	Ampicillin	Flag
pcWPRE-PLVA Vif Q231A	Ampicillin	V5
pcWPRE-PLVA Vif C232Y	Ampicillin	V5
pcWPRE-PLVA Vif T233A	Ampicillin	V5
pcWPRE-PLVA Vif F234A	Ampicillin	V5
pcWPRE-PLVA Vif Y24A	Ampicillin	V5
pcWPRE-PLVA Vif 184IR185-AA	Ampicillin	V5
pcWPRE-PLVB Vif	Ampicillin	V5
pcWPRE-PLVB Vif	Ampicillin	Flag
pcWPRE-PLVB Vif S194P	Ampicillin	V5
pcWPRE-PLVB Vif P199S	Ampicillin	V5
pcWPRE-PLVB Vif Y201H	Ampicillin	V5
pcWPRE-PLVB Vif Y201H	Ampicillin	Flag
pcWPRE- PLVB Vif F203L	Ampicillin	V5
pcWPRE-PLVB Vif E205D	Ampicillin	V5

pcWPRE-PLVB Vif A206G	Ampicillin	V5
pcWPRE-PLVB Vif Y15A	Ampicillin	V5
pcWPRE-PLVB Vif M16A	Ampicillin	V5
pcWPRE-PLVB Vif E18A	Ampicillin	V5
pcWPRE-PLVB Vif N20A	Ampicillin	V5
pcWPRE-PLVB Vif C21A	Ampicillin	V5
pcWPRE-PLVB Vif E23A	Ampicillin	V5
pcWPRE-PLVB Vif K198A	Ampicillin	V5
pcWPRE-PLVB Vif P199A	Ampicillin	V5
pcWPRE-PLVB Vif P200A	Ampicillin	V5
pcWPRE-PLVB Vif P200A	Ampicillin	Flag
pcWPRE-PLVB Vif R202A	Ampicillin	V5
pcWPRE-PLVB Vif R202A	Ampicillin	Flag
pcWPRE-PLVB Vif Y201R202-AA	Ampicillin	V5
pcWPRE-PLVB Vif F203A	Ampicillin	V5
pcWPRE-PLVB Vif F203A	Ampicillin	Flag
pcWPRE-PLVB Vif F204A	Ampicillin	V5
pcWPRE-PLVB Vif 154IL155-AA	Ampicillin	V5
pcWPRE-PLVB Vif 154IL155-AA	Ampicillin	Flag
pcWPRE-PLV1695 Vif	Ampicillin	V5
pcWPRE-PLV1695 Vif	Ampicillin	Flag
pcWPRE-PLV1695 Vif H201Y	Ampicillin	V5
pcWPRE-PLV1695 Vif H201Y	Ampicillin	Flag
pFP93 (FIV GagPol)	kanamycin	No tag
pFPLur15 (PLVA GagPol)	kanamycin	No tag
pFP-X879 (PLVB GagPol)	kanamycin	No tag
pLinSin (the FIV luciferase transfer vector)	Ampicillin	No tag
pMD.G (VSVG)	Ampicillin	No tag

pcWPRE-PLVB-PLV1695 Vif Chimera 1	Ampicillin	V5
pcWPRE-PLVB-PLV1695 Vif Chimera 2	Ampicillin	V5
pcWPRE-PLVB-PLV1695 Vif Chimera 3	Ampicillin	V5
pcWPRE-PLVB-PLV1695 Vif Chimera 4	Ampicillin	V5
pcWPRE-PLVB-PLV1695 Vif Chimera 5	Ampicillin	V5
pcWPRE-PLVB-PLV1695 Vif Chimera 6	Ampicillin	V5
pcHuA3C	Ampicillin	HA
pcHuA3G	Ampicillin	HA
pcWPRE-HIV-1 Vif	Ampicillin	V5
pCRV1-HIV-1 Vif	Ampicillin	Flag
pcWPRE-HIV-1 Vif E171A	Ampicillin	V5
pcWPRE-HIV-1 Vif D172A	Ampicillin	V5
pcWPRE-HIV-1 Vif R173A	Ampicillin	V5
pcWPRE-HIV-1 Vif W174A	Ampicillin	V5
pcWPRE-HIV-2 Vif	Ampicillin	V5
pcWPRE-HIV-2 Vif	Ampicillin	Flag
pcWPRE-HIV-2 Vif R174A	Ampicillin	V5
pcWPRE-HIV-2 Vif D175H	Ampicillin	V5
pcWPRE-HIV-2 Vif Y176A	Ampicillin	V5
pcWPRE-HIV-2 Vif R177A	Ampicillin	V5
pcCUL1	Ampicillin	Myc
pcCUL2	Ampicillin	Myc
pcCUL3	Ampicillin	Myc

pcCUL4A	Ampicillin	Myc
pcCUL4B	Ampicillin	Myc
pcCUL5	Ampicillin	Myc
pcDN-CUL1	Ampicillin	Flag
pcDN-CUL2	Ampicillin	Flag
pcDN-CUL5	Ampicillin	Flag
pCRV1-NL4-3 Vif	Ampicillin	No tag
pCRV1-LAI Vif	Ampicillin	No tag
pCRV1-F-1 Vif	Ampicillin	No tag
pCRV1-N-116 Vif	Ampicillin	No tag
pcSKP1	Ampicillin	Flag

Table 2.1 Plasmids used in this study.

Primer	**Forward (5' to 3')**	**Reverse (5' to 3')**
Human A3G-HA	AGGGAATTCGCCACCATGAAGC CTCACTTCAGAAACACA	CCTGCGGCCGCTCAAGCGTA ATCTGGAACATCGTATGGATAG TTTTCCTGATTCTGGAGAATG GCCCGC
PumaA3Z2-HA	GGAGAATTCGCCACCATGGAGC CCTGGCGCCCCAGCCCA	GAGGCGGCCGCTCAAGCGTA ATCTGGAACATCGTATGGA
PumaA3Z2Z3-HA	GGAGAATTCGCCACCATGGAGC CCTGGCGCCCCAGCCCA	GAGGCGGCCGCTCAAGCGTA ATCTGGAACATCGTATGGA
PLVB Vif-V5	GTGGAATTCGCCACCATGCAGC CCTACAGAGTGCAGAGC	CGAGCGGCCGCTTAGGTGCT GTCGAGGCCCAGCAGAGGA
PLVB Vif-Flag	GTGGAATTCGCCACCATGCAGC CCTACAGAGTGCAGAGC	CGAGCGGCCGCTTACTTGTCA TCGTCGTCCTTGTAATCGTTG CCGCAATTCAGGGCCCACAG GTCC
PLV1695 Vif-V5	GTGGAATTCGCCACCATGCAGC	CGAGCGGCCGCTTAGGTGCT

	CCTACAGAATCCAGAGC	GTCGAGGCCCAGCAGAGGA
PLV1695 Vif-Flag	GTGGAATTCGCCACCATGCAGC CCTACAGAATCCAGAGC	CGAGCGGCCGCTTACTTGTCA TCGTCGTCCTTGTAATCGTAG ATCACTTCCTCGCCGCAGGTC AGC
PLVB-PLV1695 Vif Chimera 1	CTGGTGGCCGGCACAGGCCCTC TGAAGCTGTACTGC	GCAGTACAGCTTCAGAGGGC CTGTGCCGGCCACCAG
PLVB-PLV1695 Vif Chimera 2	CTGGTGGCCGGCACAGGCCCTC TGAAGCTGTACTGC	GCAGTACAGCTTCAGAGGGC CTGTGCCGGCCACCAG
PLVB-PLV1695 Vif Chimera 3	CTGGGCAACGAGTACAAAAAGT GGTGCGCTGATTGC	GCAATCAGCGCACCACTTTTT GTACTCGTTGCCCAG
PLVB-PLV1695 Vif Chimera 4	AACTGCAGCGAGGACAAGATCC GCGAGTTCAAAGAG	CTCTTTGAACTCGCGGATCTT GTCCTCGCTGCAGTT
PLVB-PLV1695 Vif Chimera 5	GCCCTGGGAAGAAAGCTGTACA GCTGGTACTGCAAG	CTTGCAGTACCAGCTGTACAG CTTTCTTCCCAGGGC
PLVB-PLV1695 Vif Chimera 6	AGACTGTTCGACGGCAGAGTGA CCCCTCTGGACCAC	GTGGTCCAGAGGGGTCACTC TGCCGTCGAACAGTC
PLVB Vif S194P	GGAAGAAAGGTGTACCCCTGGT ACTGCAAGCCT	AGGCTTGCAGTACCAGGGGTA CACCTTTCTTCC
PLVB Vif P199S	AGCTGGTACTGCAAGTCTCCTTA CCGGTTCTTC	GAAGAACCGGTAAGGAGACTT GCAGTACCAGCT
PLVB Vif Y201H	TACTGCAAGCCTCCTCACCGGTT CTTCGAGGCC	GGCCTCGAAGAACCGGTGAG GAGGCTTGCAGTA
PLVB Vif F203L	AAGCCTCCTTACCGGCTCTTCGA GGCCAGAGTG	CACTCTGGCCTCGAAGAGCC GGTAAGGAGGCTT
PLVB Vif E205D	CCTTACCGGTTCTTCGACGCCAG AGTGACCCCT	AGGGGTCACTCTGGCGTCGA AGAACCGGTAAGG
PLVB Vif A206G	TACCGGTTCTTCGAGGGCAGAG TGACCCCTCTG	CAGAGGGGTCACTCTGCCCT CGAAGAACCGGTA

PLV1695 Vif H201Y	TACTGCAAGTCCCCTTACAGACT GTTCGACGGC	GCCGTCGAACAGTCTGTAAGG GGACTTGCAGTA
PLVB Vif Y15A	AAGCGGAACATGGAGGCCATGA AGGAAAACAAC	GTTGTTTTCCTTCATGGCCTC CATGTTCCGCTT
PLVB Vif M16A	CGGAACATGGAGTACGCGAAGG AAAACAACTGC	GCAGTTGTTTTCCTTCGCGTA CTCCATGTTCCG
PLVB Vif E18A	ATGGAGTACATGAAGGCAAACAA CTGCAGCGAG	CTCGCTGCAGTTGTTTGCCTT CATGTACTCCAT
PLVB Vif N20A	AAGGAAAACGCCTGCAGCGAG	CTCGCTGCAGGCGTTTTCCTT
PLVB Vif C21A	GAAAACAACGCCAGCGAGGAC	GTCCTCGCTGGCGTTGTTTTC
PLVB Vif E23A	AACTGCAGCGCGGACAAGATC	GATCTTGTCCGCGCTGCAGTT
PLVB Vif K198A	AGCTGGTACTGCGCGCCTCCTTA CCGG	CCGGTAAGGAGGCGCGCAGT ACCAGCT
PLVB Vif P199A	TGGTACTGCAAGGCTCCTTACCG GTTC	GAACCGGTAAGGAGCCTTGC AGTACCA
PLVB Vif P200A	TACTGCAAGCCTGCTTACCGGTT CTTC	GAAGAACCGGTAAGCAGGCTT GCAGTA
PLVB Vif R202A	AAGCCTCCTTACGCGTTCTTCGA GGCC	GGCCTCGAAGAACGCGTAAG GAGGCTT
PLVB Vif Y201R202-AA	TGCAAGCCTCCTGCCGCGTTCTT CGAG	CTCGAAGAACGCGGCAGGAG GCTTGCA
PLVB Vif F203A	CCTCCTTACCGGGCCTTCGAGG CCAGA	TCTGGCCTCGAAGGCCCGGT AAGGAGG
PLVB Vif F204A	CCTTACCGGTTCGCCGAGGCCA GAGTG	CACTCTGGCCTCGGCGAACC GGTAAGG
PLVB Vif 154IL155-AA	ACCTACAGAGAGATCGCCGCCG GCAAGTGGCAC	GTGCCACTTGCCGGCGGCGA TCTCTCTGTAGGT
FIV Vif-V5	AGCGAATTCGCCACCATGAGCG AAGAGGACTGGCAGGTG	CGAGCGGCCGCTCAGGTGCT GTCCAGGCCCAGCAGGGGG

FIV Vif-Flag	AGCGAATTCGCCACCATGAGCG AAGAGGACTGGCAGGTG	CGAGCGGCCGCTCACTTGTC ATCGTCGTCCTTGTAATCCAG CTCGCCGCTCCACAGCAGATT CCA
FIV Vif N221A	TGGCGGGGCTGCTGCGCCCAG CGGTTCGTGAGC	GGGGCTCACGAACCGCTGGG CGCAGCAGCCCCG
FIV Vif Q222A	GCTGCTGCAACGCTCGGTTCGT GAG	CTCACGAACCGAGCGTTGCA GCAGC
FIV Vif R223A	TGCTGCAACCAGGCGTTCGTGA GCCCC	GGGGCTCACGAACGCCTGGT TGCAGCA
FIV Vif F224A	TGCTGCAACCAGCGGGCCGTGA GCCCCTACCGG	CCGGTAGGGGCTCACGGCCC GCTGGTTGCAGCA
PLVA Vif-V5	GTGGAATTCGCCACCATGCCCA GCCGGGAAGAGAACCAG	CGAGCGGCCGCTCACGTAGA ATCCAGTCCCAAGAGCGGG
PLVA Vif-Flag	GTGGAATTCGCCACCATGCCCA GCCGGGAAGAGAACCAG	CGAGCGGCCGCTCACTTGTC ATCGTCGTCCTTGTAATCGAA GCTCATGGTCAGGTCCATGGC CACC
PLVA Vif Q231A	TGGAAGTGCAACAGCGCGTGCA CCTTCCTGGAC	GTCCAGGAAGGTGCACGCGC TGTTGCACTTCCA
PLVA Vif C232Y	AAGTGCAACAGCCAGTACACCTT CCTGGACTGG	CCAGTCCAGGAAGGTGTACTG GCTGTTGCACTT
PLVA Vif T233A	TGCAACAGCCAGTGCGCCTTCC TGGACTGGCGG	CCGCCAGTCCAGGAAGGCGC ACTGGCTGTTGCA
PLVA Vif F234A	AACAGCCAGTGCACCGCCCTGG ACTGGCGGAGA	TCTCCGCCAGTCCAGGGCGG TGCACTGGCTGTT
PLVA Vif Y24A	CGGCTGCAGGACGAGGCCTGG CACCTGAACCAG	CTGGTTCAGGTGCCAGGCCT CGTCCTGCAGCCG

PLVA Vif 184IR185-AA	ACCCCCATGGACGTGGCCGCGG GCGAAGTGGACCCC	GGGGTCCACTTCGCCCGCGG CCACGTCCATGGGGGT
HIV-1 Vif-V5	ACCGAATTCGCCACCATGGAAAA CAGATGGCAGGTGATG	CGAGCGGCCGCTCACGTAGA ATCCAGTCCCAAGAGCGGG
HIV-1 Vif E171A	GTTAGGAAACTGACAGCGGACA GATGGAACAAG	CTTGTTCCATCTGTCCGCTGT CAGTTTCCTAAC
HIV-1 Vif D172A	AAACTGACAGAGGCCAGATGGA ACAAG	CTTGTTCCATCTGGCCTCTGT CAGTTT
HIV-1 Vif R173A	AAACTGACAGAGGACGCATGGA ACAAGCCCCAG	CTGGGGCTTGTTCCATGCGTC CTCTGTCAGTTT
HIV-1 Vif W174A	CTGACAGAGGACAGAGCGAACA AGCCCCAGAAG	CTTCTGGGGCTTGTTCGCTCT GTCCTCTGTCAG
HIV-2 Vif-V5	GTGGAATTCGCCACCATGGAAGA GGACAAGCGGTGGATCGTG	CGAGCGGCCGCTCAGGTGCT GTCGAGGCCCAGCAGAGGAT TAGGAATGGGCTTGCCGGCC AGAATTTCCAGCACCTCGG
HIV-2 R174A	CGGAAGCAGCGGCGGGCAGATT ACAGAAGAGGA	TCCTCTTCTGTAATCTGCCCG CCGCTGCTTCCG
HIV-2 D175H	AAGCAGCGGCGGAGACATTACA GAAGAGGACTG	CAGTCCTCTTCTGTAATGTCTC CGCCGCTGCTT
HIV-2 Y176A	CAGCGGCGGAGAGATGCCAGAA GAGGACTGAGA	TCTCAGTCCTCTTCTGGCATC TCTCCGCCGCTG
HIV-2 R177A	CGGCGGAGAGATTACGCAAGAG GACTGAGACTG	CAGTCTCAGTCCTCTTGCGTA ATCTCTCCGCCG
Human Cullin1-Myc	TCAGGATCCCCGCCACCATGTC GTCAACCCGGAGCCAGAACCCC C	ATGCTCGAGAGCGACATTAAG CCAAGTAACTGTAGGTGTCCT TTT

SKP1-Flag	ACCGCTAGCGCCACCATGGATTA CAAGGACGACGATGACAAGCCT TCAATTAAGTTGCAGAGT	CGAAAGCTTTCACTTCTCTTC ACACCACTGGTTCTC

Table 2.2 List of primers used for plasmid generation in this study.

2.1.2 Polymerase chain reaction (PCR)

PCR was employed to synthesize new DNA fragments for various applications, including cloning DNA sequences into an expression vector. DNA amplification was performed using Q5® High-Fidelity DNA Polymerase (New England Biolabs, Ipswich, USA), following the manufacturer's protocol. The 50-microliter (µl) reaction mixture comprised nuclease-free water, 10 µl of 5X Q5 reaction buffer, 10 micromolar (µM) forward primer, 10 µM reverse primer, 0.5 µl of Q5 High-Fidelity DNA Polymerase, 10 millimolar (mM) deoxynucleoside triphosphates (dNTPs) (New England Biolabs, Ipswich, USA), and 10 nanograms (ng) of plasmid or genomic DNA template. The reaction mixture was gently mixed and then placed in a PCR machine (Bioer GeneTouch™ Thermal Cycler, Hangzhou, China) with the following cycling conditions: (i) initial denaturation at 98°C for 30 seconds (s); (ii) 30 cycles of denaturation at 95°C for 45 s, annealing at 60-70°C for 60 s, and extension at 72°C for 1 kilobase per minute (min/kb); and (iii) a final extension at 72°C for 10 minutes.

2.1.3 Agarose gel electrophoresis and DNA fragment extraction

DNA fragments were separated by agarose gel electrophoresis based on their size. Following PCR, the PCR products were mixed with DNA gel loading buffer and loaded into the wells of an agarose gel. A 1 kilobase plus DNA ladder (Thermo Fisher Scientific, Waltham, USA) was also loaded into a separate well. Electrophoresis was carried out at a constant voltage of 160 V for 25 minutes. The DNA fragments were visualized using a camera, and the desired fragments were excised from the gel based on the DNA ladder. The DNA-containing agarose gel

slices were purified using a modified protocol of the QIAquick Gel Extraction Kit (QIAGEN, Venlo, Netherlands). To each tube, 500-700 microliters (µl) of QG buffer were added, and the tubes were incubated in a shaker at 700 revolutions per minute (rpm) for 10 minutes at 50°C. The solution was then transferred to a QIAquick spin column and centrifuged at maximum speed for 1 minute. The column was washed with 700 µl of PE buffer, followed by centrifugation at full speed for 1 minute; this step was repeated once. Finally, 20 µl of EB buffer was added to the column, and the DNA was eluted by centrifugation at full speed for 1 minute. The DNA concentration was measured photometrically at 260 nanometers (nm).

2.1.4 Double-enzyme restriction digest

One microgram (µg) each of the purified insert and donor plasmid backbone were digested using two restriction enzymes, following the manufacturer's instructions. The 20 µl reaction mixture consisted of 1 µg of either the purified insert or donor plasmid backbone, 1X or 2X enzyme-specific buffer as recommended by the double digest calculator, 1-2 µl of each restriction enzyme, and nuclease-free water added to bring the total volume to 20 µl. The components were gently mixed by pipetting and incubated at 37°C for 2 hours. Following incubation, the digested DNA was assessed by gel electrophoresis and subsequently purified by gel extraction.

2.1.5 Ligation of vector and insert

The ligation reaction was carried out using T4 DNA ligase following the manufacturer's protocol. The 20 µl ligation mixture was prepared by combining 2 µl of 10X T4 DNA ligase buffer, 1 µl of T4 ligase, the purified sticky-end insert and vector at a 1:3 molar ratio, and nuclease-free water in a 1.5 ml microcentrifuge tube. The components were thoroughly mixed, briefly spun down, and incubated at room temperature (RT) for 2 hours. A 10 µl portion of the ligation mixture was then used to transform an aliquot of competent cells.

2.1.6 *E. coli* transformation

The ligated DNA constructs were introduced into Top10 or Stbl2 chemically competent *E. coli* cells (Thermo Fisher Scientific, Waltham, USA) according to the manufacturer's instructions. An aliquot of competent cells was thawed on ice. To the thawed competent cells, 10 µl of the ligated DNA constructs were added and mixed by pipetting. The mixture was incubated on ice for 10 minutes for Top10 cells or 30 minutes for Stbl2 cells. Following incubation, a heat shock was applied at 42°C for 1 minute, after which the cells were placed on ice for 5 minutes for Top10 cells or 10 minutes for Stbl2 cells. Subsequently, 500 µl of fresh Luria-Bertani (LB) liquid medium was added to the DNA-cell mixture, which was then cultured in a shaker at 550 rpm for 1 hour at 37°C for Top10 cells or 30°C for Stbl2 cells. The transformed cells were spread on LB agar plates containing 100 µg/ml ampicillin or 100 µg/ml kanamycin and incubated overnight at 37°C for Top10 cells or 30°C for Stbl2 cells. Single colonies were subsequently inoculated into 4 ml of LB medium with the appropriate antibiotic (ampicillin or kanamycin) and cultured with vigorous shaking at 160 rpm overnight at 37°C for Top10 cells or 30°C for Stbl2 cells.

2.1.7 Plasmid extraction

Plasmid extraction from bacterial cells was performed using a modified protocol based on the ZR Plasmid Miniprep-Classic kit (Zymo Research, Irvine, USA). A 2 ml bacterial culture was harvested by centrifugation at maximum speed for 20 seconds. The resulting pellet was resuspended in 200 µl of P1 buffer. Subsequently, 200 µl of P2 buffer was added, and the mixture was inverted 2-4 times before incubation for 2 minutes. Following this, 400 µl of P3 buffer was added, mixed gently but thoroughly, and the solution was incubated at room temperature (RT) for 2 minutes. The mixture was then centrifuged at maximum speed for 3 minutes. The supernatant was transferred to a Zymo-Spin™ IIN column and centrifuged at

maximum speed for 1 minute. After discarding the effluent in the collection tube, 200 µl of endo-wash buffer was added to the column, followed by centrifugation at maximum speed for 1 minute. Next, 400 µl of plasmid wash buffer was added, and the column was centrifuged at maximum speed for 1 minute. Finally, the column was eluted with 30 µl of nuclease-free water, and the plasmids were collected into a 1.5 ml microcentrifuge tube by centrifugation at maximum speed for 1 minute. The concentration of plasmids was measured photometrically at 260 nm. For large-scale plasmid purification, the PureYield™ Plasmid Maxiprep System (Promega, Madison, USA) was utilized according to the manufacturer's instructions.

2.1.8 Plasmid verification

Following plasmid extraction, 300 ng of plasmid DNA was subjected to verification through double restriction enzyme digestion. A 10 µl reaction mixture was prepared, containing 300 ng of plasmid DNA, 1X or 2X enzyme-specific buffer as recommended by the double digest calculator, 0.25 µl of each restriction enzyme, and nuclease-free water. The components were mixed by pipetting, briefly centrifuged, and incubated at 37°C for 1 hour. The digested plasmids were analyzed by gel electrophoresis to confirm their size. Subsequently, plasmid identity was verified by Sanger sequencing performed by Eurofins (Eurofins, Luxembourg), and pairwise sequence alignment was conducted using SnapGene software (www.snapgene.com).

2.2 Cell culture and virological methods

2.2.1 Cells

HEK293T (293T) and HEK293A (293A) cells were procured from the American Type Culture Collection (ATCC) and cultured in Dulbecco’s Modified Eagle Medium (DMEM) (PAN-Biotech, Aidenbach, Germany), supplemented with 10% fetal bovine serum (FBS) (PAN-Biotech, Aidenbach, Germany), 2 mM L-glutamine (PAN-Biotech, Aidenbach, Germany), and 100 units per milliliter (U/ml) penicillin-

streptomycin (PAN-Biotech, Aidenbach, Germany). The cells were maintained at 37°C in a 5% CO_2 incubator under sterile conditions. For serial passaging, cells were washed with Dulbecco's phosphate-buffered saline (DPBS) and subsequently treated with 0.05% trypsin (PAN-Biotech, Aidenbach, Germany) for 1-2 minutes at 37°C. For long-term storage, cells were centrifuged at 500 relative centrifugal force (rcf) for 5 minutes, resuspended in 1 ml of 10% dimethyl sulfoxide (DMSO) (PanReac AppliChem, Chicago, IL, USA) in FBS, and aliquoted into cryovials. The vials were placed in a Nalgene Mr. Frosty freezing container with 100% isopropyl alcohol at -80°C for 48 hours before being transferred to liquid nitrogen.

2.2.2 Plasmid transfection

293T or 293A cells were plated into 6-well or 12-well plates (Sigma-Aldrich, Carlsbad, USA) and allowed to reach approximately 80% confluence before transfection. Transfections were performed using PolyJet™ *in vitro* DNA transfection reagent (SignaGen Laboratories, Frederick, USA) following the manufacturer's protocol. For each well of a 6-well or 12-well plate, 2000-3000 ng or 600-1200 ng of plasmid DNA was diluted in 200 µl or 100 µl of DMEM and gently vortexed. Subsequently, 4 µl or 2 µl of PolyJet™ reagent was added to the DNA solution and vortexed gently. The mixture was then incubated at room temperature (RT) for 10-15 minutes. Following incubation, the PolyJet™/plasmid DNA complexes were introduced into the cells.

The A3 degradation experiments were conducted using 12-well plates. A total of 3 × 10^5 293T cells were seeded 24 hours before the transfection, after 24 hours, these 293T cells were transfected with 500 ng A3 expression plasmids along with 500 ng each of PLVA, PLVB, PLV1695, HIV-1, and HIV-2 Vif expression plasmids or 100 ng of a codon-optimized FIV Vif expression plasmid, to reach a total plasmid amount of 1000 ng, pcDNA3.1 (+) vector (Life Technologies) was utilized.

For the Vif-A3 binding assay:

Method 1:

A total of 6 × 10^5 293T cells were seeded in 6-well plates 24 hours prior to transfection. After 24 hours, the 293T cells were transfected with 1000 ng of A3 expression plasmids along with 1000 ng each of PLVA, PLVB, PLV1695, HIV-1, and HIV-2 Vif/Vif mutant expression plasmids, 500 ng of a codon-optimized FIV Vif/Vif mutant expression plasmids, or an empty pcDNA3.1 vector. 8 hours post-transfection, the cells were treated with 10 μM MG132 (474790, Calbiochem). After 24 hours of treatment, the cells were harvested for downstream applications (immunoprecipitation).

Method 2:

A total of 6 × 10^5 293T cells were seeded in 6-well plates 24 hours prior to transfection. After 24 hours, the 293T cells were transfected with 1600 ng of DN-CUL5 and 1000 ng of A3 expression plasmids along with 1000 ng each of PLVA, PLVB, PLV1695, HIV-1, and HIV-2 Vif/Vif mutant expression plasmids, 500 ng of a codon-optimized FIV Vif/Vif mutant expression plasmids, or an empty pcDNA3.1 vector. 32 hours post-transfection, the cells were harvested for downstream applications (immunoprecipitation).

To determine Vif and CULs binding:

A total of 6 × 10^5 293T cells were seeded in 6-well plates 24 hours prior to transfection. After 24 hours, the 293T cells were transfected with 1000 ng each of PLVA, PLVB, PLV1695, HIV-1, and HIV-2 Vif/Vif mutant expression plasmids, 500 ng of a codon-optimized FIV Vif expression plasmid, along with 1000 ng of CULs expression plasmids or a pcDNA3.1 vector. 32 hours post-transfection, the cells were harvested for downstream applications (immunoprecipitation).

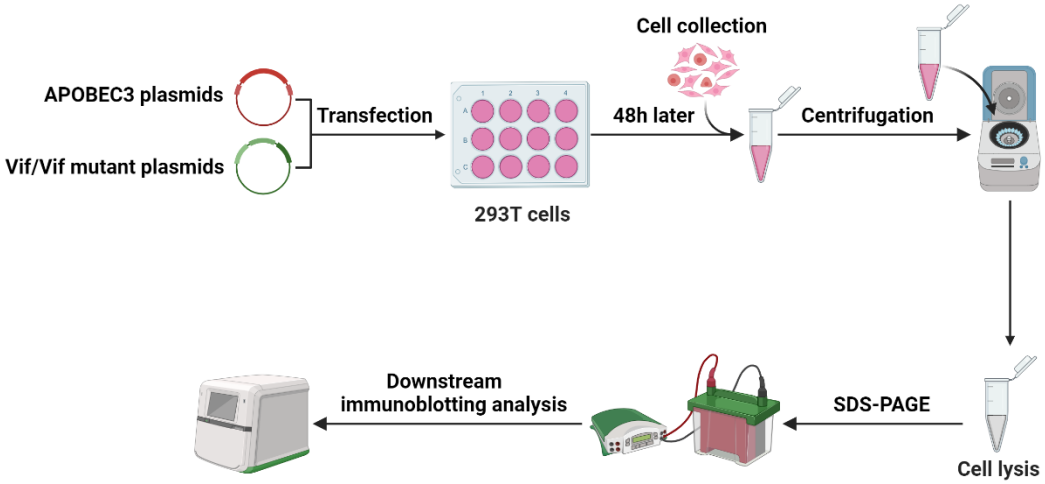

Fig. 2.3 Schematic representation of the A3 degradation assay. The A3 degradation experiments were conducted using 12-well plates. A total of 3 × 10^5 293T cells were seeded 24 hours before transfection. After 24 hours, the cells were transfected with A3 expression plasmids along with Vif expression plasmids. 48 hours post-transfection, the cells were collected for downstream applications (Western blot). Created with BioRender.com.

2.2.3 Viral production and single-round infection assay

Replication-deficient luciferase pseudo-viruses were generated in 12-well plates. To produce FIV, PLVA, and PLVB single-cycle luciferase pseudo-viruses, 3 × 10^5 293T cells were seeded 24 hours prior to transfection. The 293T cells were then co-transfected with 400 ng of the replication-deficient packaging construct pFP93 (FIV, kindly provided by Eric M. Poeschla[160]), pFPLur15 (PLVA), or pFP-X879 (PLVB), these constructs express only the Gag, Pol, and Rev proteins (Fig. 2.4); 400 ng of the FIV luciferase vector pLinSin; 100 ng of the VSV-G; 250 ng of the A3 expression plasmid; and 100 ng each of the PLVA, PLVB, and PLV1695 Vif expression plasmids, or 50 ng of a codon-optimized FIV Vif expression plasmid. In certain cases, pcDNA3.1(+) (Life Technologies) was substituted for the Vif or A3 expression plasmids. 48 hours after transfection, the supernatant was collected. Subsequently, to ensure consistency, the reverse transcriptase (RT) activity of the viruses was quantified using a SYBR Green I-based product-enhanced reverse transcriptase assay[161].

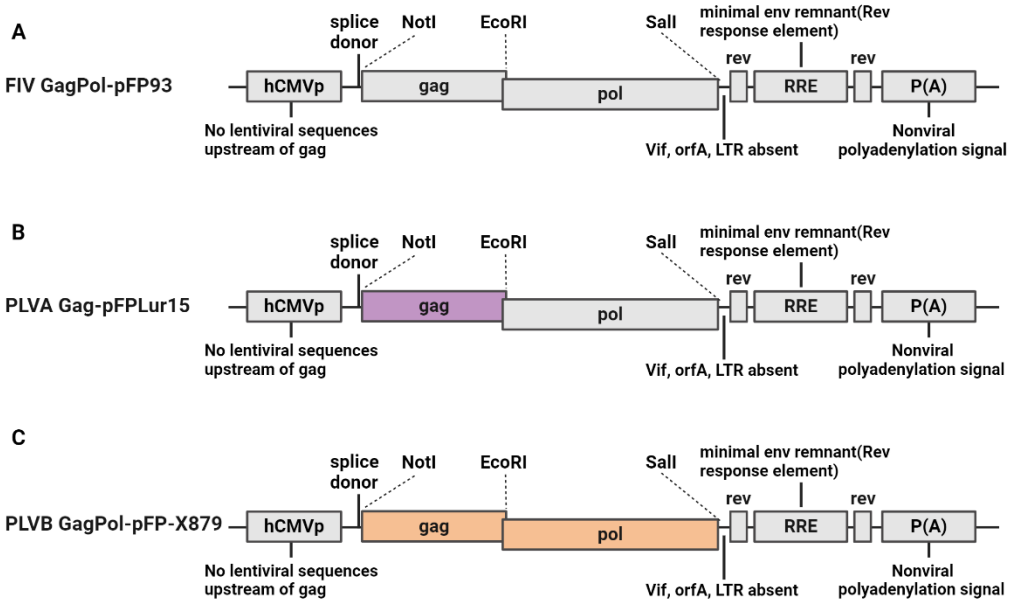

Fig. 2.4 Schematic representation of the genome structure of single-round infection FIV, PLVA, and PLVB reporter viruses. (A) The FIV GagPol construct (pFP93) was kindly provided by Eric M. Poeschla[160]. For the construction of pFPLur15 (PLVA GagPol construct), the gag gene from PLVA was cloned into the construct vector due to the absence of suitable restriction sites in the PLVA sequence, with the pol gene sourced from pFP93. For the PLVB packaging construct, the gag-pol genes from PLVB were cloned into the construct vector, resulting in PLVB GagPol (pFP-X879). The restriction sites utilized for the generation of these single-round infection reporter viruses are indicated. These constructs express only the Gag, Pol, and Rev proteins. Fig. 2.4A: Adapted from Saenz DT, Barraza R, Loewen N, Teo W, Poeschla EM. Feline Immunodeficiency Virus-Based Lentiviral Vectors. Cold Spring Harb Protoc. 2012;2012(1):71-76[162]. Published by Cold Spring Harbor Laboratory Press. Reproduced with permission and created with BioRender.com. Fig. 2.4B, C: Created with BioRender.com.

For reporter virus infection, 293T cells were seeded in a 96-well plate one day prior to transduction. Equal viral loads were then added to the 293T cells to initiate the infection process. 48 hours after transduction, firefly luciferase activity was measured using the Steadylite HTS reporter gene assay system (PerkinElmer, Cologne, Germany) according to the manufacturer's instructions. Measurements were performed on a MicroLumat Plus luminometer (Berthold Detection Systems,

Pforzheim, Germany). The procedure for viral production and the single-round infection assay is illustrated in Fig. 2.5. Each transduction was conducted in triplicate, with three independent replicates analyzed. The data are presented with error bars to illustrate the variability within each triplicate measurement.

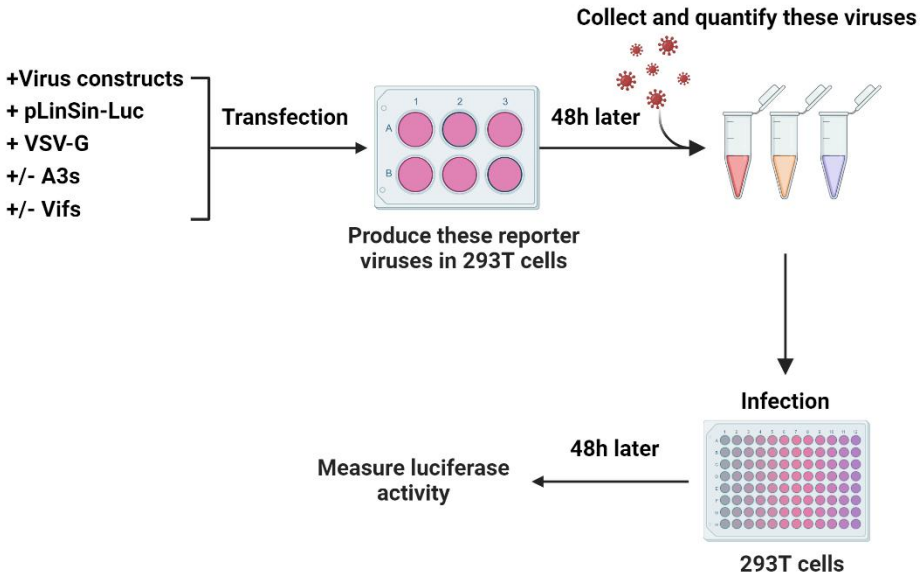

Fig. 2.5 Schematic representation of the single-round infection assay using feline luciferase reporter viruses. Feline A3 and Vif expression plasmids, along with a viral-based three-plasmid system, were co-transfected into 293T cells. After 48 hours, the viruses were collected and quantified. These viruses were then used to infect 293T cells. 48 hours post-infection, viral infectivity was assessed by measuring luciferase activity. Created with BioRender.com.

2.3 Protein biochemistry

2.3.1 Cell lysis and microvolume protein concentration determination

The cells of interest were collected, washed with cold DPBS, and then lysed on ice for 20 minutes using 100-200 µl of cold mild lysis buffer. This buffer consisted of 50 mM Tris-HCl (pH 8), 150 mM sodium chloride (Carl Roth, Karlsruhe, Germany), 0.8% NP-40 (PanReac AppliChem, Chicago IL, USA), 10% glycerol (PanReac AppliChem, Chicago IL, USA), 1 mM phenylmethylsulfonyl fluoride, a protease inhibitor cocktail III tablet (Sigma-Aldrich, Carlsbad, USA), and 1% phosphatase inhibitor cocktail I (MedChemExpress, South Brunswick Township, USA). After lysis,

the samples were clarified by centrifugation at 14,000 rpm for 20 minutes at 4°C. Protein concentrations were then measured using the A280 method on a NanoDrop 1000 spectrophotometer (Thermo Fisher Scientific, Waltham, USA). A blank measurement was taken using water, and 2 µl of the sample was used for protein concentration assessment.

2.3.2 Western blot assay

Polyacrylamide gels were prepared according to the protocol outlined in Table 2.3. For sodium dodecyl sulfate-polyacrylamide gel electrophoresis (SDS-PAGE), equal amounts of protein were mixed with ROTI®Load 1, a reducing loading buffer (Carl Roth, Karlsruhe, Germany), and then heated at 95°C for 5 minutes. The prepared samples, along with a prestained protein molecular weight marker (Thermo Fisher Scientific, Waltham, USA), were then loaded into the gel wells. Protein separation was conducted at a constant voltage of 130 V using a 1X SDS running buffer.

After electrophoresis, proteins were transferred from the gels onto a polyvinylidene fluoride (PVDF) membrane (Sigma-Aldrich, Carlsbad, USA) using a Bio-Rad semi-dry transfer cell (Bio-Rad, Hercules, USA) at a constant 20 V for 45 minutes. The semi-dry transfer setup included the following layers: SDS-containing transfer buffer prewetted filter paper (Bio-Rad, Hercules, USA), a methanol-prewetted PVDF membrane, the SDS gel, and another layer of SDS-containing transfer buffer prewetted filter paper.

The membranes were then blocked with 5% nonfat milk (PanReac AppliChem, Chicago IL, USA) for 1 hour at room temperature. After blocking, membranes were incubated overnight at 4°C with the primary antibody solution under gentle agitation. The following day, membranes were washed three times with TBST buffer, each wash lasting 10 minutes. The membranes were then incubated with an HRP-conjugated secondary antibody for 2 hours at room temperature with gentle agitation. Following secondary antibody incubation, the membranes were washed

three times for 10 minutes each with TBST.

For detection, membranes were treated with the Amersham™ ECL Prime Western Blot detection reagent (GE Healthcare, Chicago, USA) according to the manufacturer's instructions. Signal detection was performed using the ChemiDoc MP imaging system (Bio-Rad, Hercules, USA). The antibodies utilized in this study are listed in Table 2.4.

	Stacking gel 10%	Running gel 10%
Rotiphorese® Gel 30 (37.5:1) (Carl Roth, Karlsruhe, Germany)	840 µl	5 ml
1.5 mole (M) Tris-HCl pH 8.6 (PanReac AppliChem, Chicago IL, USA)	/	3.75 ml
1 M Tris-HCl pH 6.8 (PanReac AppliChem, Chicago IL, USA)	630 µl	/
10% SDS (PanReac AppliChem, Chicago IL, USA)	50 µl	150 µl
20% Ammonium persulphate solution (APS) (Sigma-Aldrich, Carlsbad, USA)	25 µl	75 µl
N, N, N′, N′- Tetramethylethylenediamine (TEMED) (VWR, Radnor, PA/USA)	5 µl	15 µl
H_2O	3.5 ml	6.1 ml

Table 2.3 Pipetting scheme for SDS-PAGE gels.

Antibody	**Source & Identifier& Supplier**	**Host**	**Dilution**
Anti-HA	66006-2-Ig (Proteintech, Rosemont, USA)	mouse	1:7,500
Anti-HA	51064-2-AP (Proteintech, Rosemont, USA)	rabbit	1:7,500
Anti-V5	V8012 (Sigma-Aldrich, Carlsbad, USA)	mouse	1:4,000
Anti-V5	V8137 (Sigma-Aldrich, Carlsbad, USA)	rabbit	1:3,000

Anti-Tubulin	T5168 (Sigma-Aldrich, Carlsbad, USA)	mouse	1:7,500
Anti-Flag	F3165 (Sigma-Aldrich, Carlsbad, USA)	mouse	1:1,000
Anti-Flag	F7425 (Sigma-Aldrich, Carlsbad, USA)	rabbit	1:2,000
Anti-Myc	60003-2-Ig (Proteintech, Rosemont, USA)	mouse	1:2,000
Anti-HIV-1 Vif	MAb319 (NIH AIDS Research and Reference Reagent Program[163, 164])	mouse	1:1,000
Anti-CUL1	66978-1-Ig (Proteintech, Rosemont, USA)	mouse	1:4,000
HRP-conjugated sheep anti-mouse IgG	NA931V (GE Healthcare, Chicago, USA)	sheep	1:10,000
HRP-conjugated donkey anti-rabbit IgG	NA9340V (GE Healthcare, Chicago, USA)	donkey	1:10,000

Table 2.4 Antibodies used for Western blotting in this study.

2.3.3 Immunoprecipitation

To determine Vif and A3 binding:

Method 1: HEK293T cells were transfected with A3 expression plasmids along with Vif/Vif mutant expression plasmids or an empty pcDNA3.1 vector. 8 hours post-transfection, the cells were treated with 10 μM MG132 (474790, Calbiochem). After 24 hours of treatment, the cells were harvested.

Method 2: HEK293T cells were transfected with DN-CUL5 and A3 expression plasmids, along with Vif/Vif mutant expression plasmids or an empty pcDNA3.1 vector. 32 hours post-transfection, the cells were harvested.

To determine Vif and CULs binding:

HEK293T cells were transfected with Vif/Vif mutant expression plasmids along with CULs expression plasmids or an empty pcDNA3.1 vector. 32 hours post-transfection, the cells were harvested.

The harvested cells were lysed in 400 µl of IP lysis buffer (50 mM Tris-HCl [pH 8], 10% glycerol, 0.8% NP-40, 150 mM NaCl) containing a protease inhibitor cocktail set III (Calbiochem, Darmstadt, Germany) on ice for 20 minutes. The lysates were clarified by centrifugation at 14,000 rpm for 20 minutes at 4°C. Subsequently, 360 µl of the whole-cell lysates were incubated overnight at 4°C with 10 µl of Anti-Flag Magnetic Beads (HY-K0207, MedChemExpress) or Anti-c-Myc Magnetic Beads (HY-K0206, MedChemExpress) with gentle rotation. The beads were washed five times with 1 ml of IP lysis buffer. Affinity-tagged proteins were eluted by boiling the beads for 5 minutes at 95°C in a reducing loading buffer. The remaining lysates were mixed with a reducing loading buffer and heated at 95°C for 5 minutes. Both the immunoprecipitates and the remaining cell lysates were subjected to immunoblotting analysis.

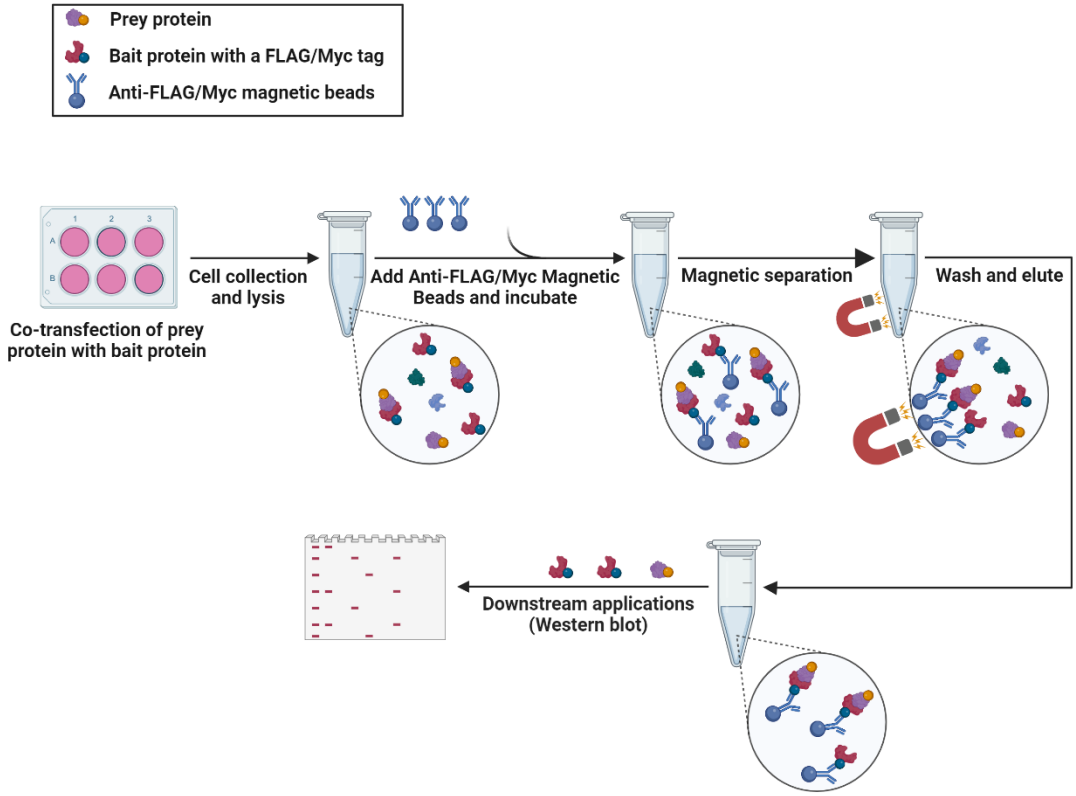

Fig. 2.6 Schematic representation of the immunoprecipitation procedure. HEK293T cells were transfected with prey protein expression plasmids along with bait protein expression plasmids or an empty pcDNA3.1 vector. Thirty-two hours post-transfection, the cells were harvested and lysed. After clarification of the lysates, the cell lysates were incubated with Anti-Flag magnetic beads or Anti-c-

Myc magnetic beads with gentle rotation. The beads were then washed and eluted, and the samples were subjected to immunoblotting analysis. Created with BioRender.com.

2.3.4 Amino acid sequence alignment

Amino acid sequences were aligned using the multiple sequence comparison by log-expectation (MUSCLE) algorithm, which is designed for high accuracy in multiple sequence alignments[165]. Conserved residues were identified and visualized based on their physicochemical properties using the Clustal color scheme. In this scheme, colors are assigned to residues in the alignment based on their amino acid profile at each position, provided they meet specific criteria associated with the residue type (Table 2.5)[166].

Category	Color	Residue at position	(Threshold, Residue group)
Hydrophobic	Blue	A, C, I, L, M, F, W, V	(>60%, WLVIMAFCYHP)
		C	(>60%, WLVIMAFCYHP)
Positive charge	Red	K, R	(>60%, KR), (>85%, K, R, Q)
Negative charge	Magenta	E	(>60%, KR), (>50%, QE), (>50%, ED), (>85%, E, Q, D)
		D	(>60%, KR), (>85%, D, E, N), (>50%, ED)
Polar	Green	N	(>50%, N), (>85%, N, D)
		Q	(>60%, KR), (>50%, QE), (>85%, Q, T, K, R)
		S, T	(>60%, WLVIMAFCYHP), (>50%, TS), (>85%, S, T)
Cysteines	Pink	C	(>85%, C)
Glycines	Orange	G	(>0%, G)
Prolines	Yellow	P	(>0%, P)
Aromatic	Cyan	H, Y	(>60%, WLVIMAFCYHP), (>85%, W, Y, A, C, P, Q, F, H, I, L, M, V)
Unconserved	White	any / gap	If none of the above criteria are met

Table 2.5 The Clustal color scheme criteria. The criteria are expressed as thresholds: (>X%, xx, y), where X represents the minimum percentage of a residue type (xx or y) required at a given position for it to be assigned a specific color. For instance, residues are assigned a red color when

a column contains more than 60% of lysine (K) and arginine (R) combined, or when either K, R, or glutamine (Q) individually exceeds 80%.

2.4 Homology modeling

The structures of the feline lentiviral Vif-feline A3Z3 complexes were predicted using the AlphaFold server (https://alphafoldserver.com/). To generate the models, the amino acid sequences of feline lentiviral Vif and feline A3Z3 were input simultaneously into the AlphaFold server interface.

The resulting models were analyzed using PyMOL to visualize the structures and identify key interaction residues. Hydrogen bonding and other potential interaction types, such as hydrophobic or electrostatic interactions, were examined to characterize the binding interface between Vif and A3Z3. Confidence scores (pLDDT) provided by AlphaFold were also evaluated to ensure the reliability of the predicted structures, with particular attention paid to the interface regions.

2.5 Nucleotide Sequence Accession Numbers

The GenBank accession numbers for feline lentiviral Vif and A3 sequences are as follows: FIV Vif (EF989123), PLVA Vif (KF906143), PLVB Vif (KF906194.1), PLV1695 Vif (DQ192583.1), CatA3Z2 (AY971954), CatA3Z3 (EU109281), CatA3Z2Z3 (EU109281), PumaA3Z2 (EU007545), PumaA3Z3 (LC376042), PumaA3Z2Z3 (GU097659), BobcatA3Z3A1 (LC376041), and BobcatA3Z3A2 (LC376040).

2.6 Statistical analysis

The data are presented as the mean with standard deviation (SD) in all bar diagrams. Statistical analysis for significant differences between two groups was conducted using the unpaired Student's t-test, performed with GraphPad Prism version 8 (GraphPad Software, San Diego, CA, USA). A P-value of ≤0.05 was deemed statistically significant; a P-value of ≤0.001 was regarded as extremely

significant, a P-value ranging from 0.001 to 0.01 was considered very significant, and a P-value ranging from 0.01 to 0.05 was considered significant. Conversely, a P-value of ≥0.05 was considered not statistically significant.

3. Results

3.1 Investigation of the interaction between feline Vif and feline A3 proteins

3.1.1 Test of the degradation effect of feline Vif on feline A3 proteins

To investigate the molecular interaction between feline Vif and feline A3 proteins, I tested Vif proteins from FIV of domestic cats (*Felis catus*, Fca), puma lentivirus (PLV) types A, B, and 1695, hereafter referred to as FIV, PLVA, PLVB, and PLV1695 Vif, respectively. Co-transfection experiments involving feline A3 and feline Vif expression plasmids were conducted in 293T cells. All A3 constructs were expressed with a C-terminal HA-tag, while Vif was expressed as a C-terminal V5-tag fusion protein. Immunoblotting results demonstrated that FIV Vif completely degraded all the feline A3Z2, A3Z3, and A3Z2Z3 proteins tested, while PLVA and PLVB Vif largely or partially degraded these feline A3 proteins (Fig. 3.1B, C, D).

3.1.2 Identification of a Vif protein specifically unable to degrade feline A3Z3

In this study, I identified a strain of PLVB Vif, named PLV1695 Vif, which is unable to degrade feline A3Z3 proteins but can degrade feline A3Z2 and A3Z2Z3 proteins (Fig. 3.1B, C, D). This finding aligns with a previous study that demonstrated the inability of PLV1695 Vif to counteract puma A3Z3[167]. PLV1695 is a prototypic infectious molecular clone of PLVB, which resulted from several passages in domestic cat[168]. Theoretically, Vif binds to A3, leading to its degradation via the proteasome pathway. The specific inability of PLV1695 Vif to degrade feline A3Z3 suggests that Vif interacts with different A3 proteins at distinct binding sites. This finding implies that certain subtypes of the PLVB virus, such as PLV1695, may have acquired mutations or modifications that affect their ability to target and

degrade feline A3Z3.

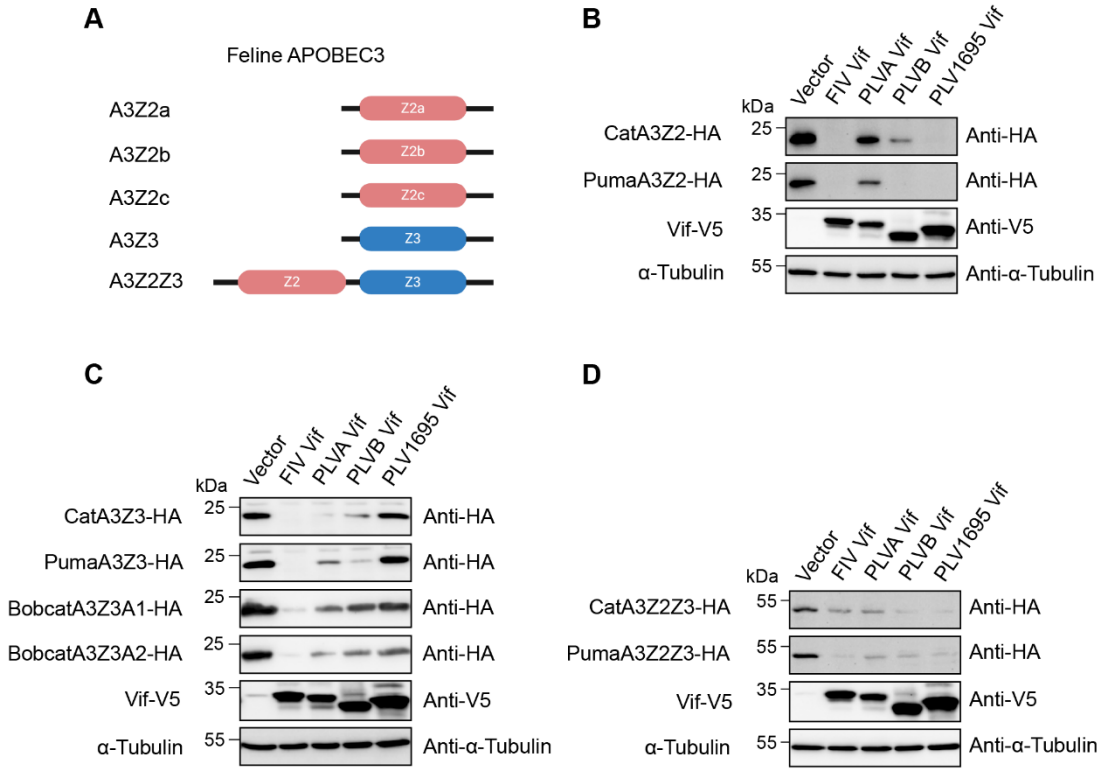

Fig 3.1 The degradation effect of feline Vif on feline A3 proteins. (A) Diagram of feline APOBEC3 Proteins. (B), (C), (D) 293T cells were transfected with expression plasmids for feline A3Z2-HA, A3Z3-HA, or A3Z2Z3-HA, along with expression plasmids for FIV Vif-V5, PLVA Vif-V5, PLVB Vif-V5, or PLV1695 Vif-V5. pcDNA3.1(+) was used as a vector control. Forty-eight hours post-transfection, cell lysates were analyzed by immunoblotting using anti-HA and anti-V5 antibodies, respectively. Tubulin was used as a loading control. Fig. 3.1A was adapted from: Zielonka J, Münk C. Cellular Restriction Factors of Feline Immunodeficiency Virus. Viruses-Basel 2011; 3(10):1986-2005[60]. Published under the Creative Commons Attribution 4.0 International License(https://creativecommons.org/licenses/by/4.0/). Reproduced with BioRender.com.

3.1.3 Characterization of luciferase reporter viruses for PLV

Previous research has reported single round reporter viruses only for FIV of domestic cats, using, *e.g.,* the Gag-Pol packaging construct pFP93[160]. To develop the PLVA packaging construct, the *gag* gene from PLVA was cloned into an expression vector, with the *pol* gene sourced from pFP93, resulting in PLVA GagPol (pFPLur15). For the PLVB packaging construct, the gag-pol genes from PLVB were

cloned into an expression vector, named PLVB GagPol (pFP-X879). To generate luciferase reporter viruses, the packaging constructs were cotransfected with a FIV-based luciferase transfer vector pLinSin and a VSV-G expression plasmid. The luciferase activity of these viral vectors demonstrated that the constructs are suitable for subsequent experimental studies (Fig. 3.2). PLVB and FIV vectors had a similar infectivity, while PLVA vectors displayed much lower infectivity. The reason for these differences is unknown.

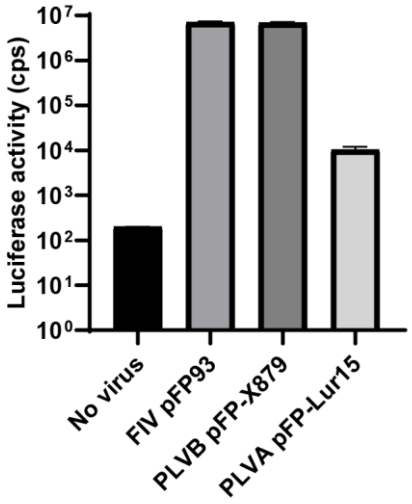

Fig 3.2 Single-round infection assay of PLV reporter viruses. Luciferase reporter viruses were produced in 293T cells using the FIV luciferase vector pLinSin and the VSV-G expression plasmid. Virions with 20 pg of reverse transcription activity were used to infect 293T cells. Viral infectivity was assessed by quantifying luciferase activity in the lysates of infected cells, measured in counts per second (cps). “No virus” represents uninfected cells.

3.1.4 Feline A3Z3 proteins exhibit antiviral activity against PLVs and are counteracted by feline Vif proteins

Previous research has confirmed that feline A3Z2 proteins exhibit no antiviral activity against either ΔVif FIV or wild-type (wt) FIV[134]. However, limited research has explored the interaction between A3 proteins and Vif proteins in large felids. To address this gap, further studies were conducted to investigate the interaction between feline A3Z3 proteins and PLV Vif proteins. Results from infection assays

indicated that Cat A3Z3, Puma A3Z3, Bobcat A3Z3A1, and Bobcat A3Z3A2 proteins effectively inhibited ΔVif FIV (Fig. 3.3A), ΔVif PLVA (Fig. 3.3C), and ΔVif PLVB viruses (Fig. 3.3E). While FIV and PLVB Vif showed broad activity in counteracting the restriction mediated by Cat A3Z3, Puma A3Z3, Bobcat A3Z3A1, and Bobcat A3Z3A2 (Fig. 3.3B, F), PLVA Vif demonstrated comparatively weaker activity against Cat A3Z3, Puma A3Z3, Bobcat A3Z3A1, and Bobcat A3Z3A2 (Fig. 3.3D).

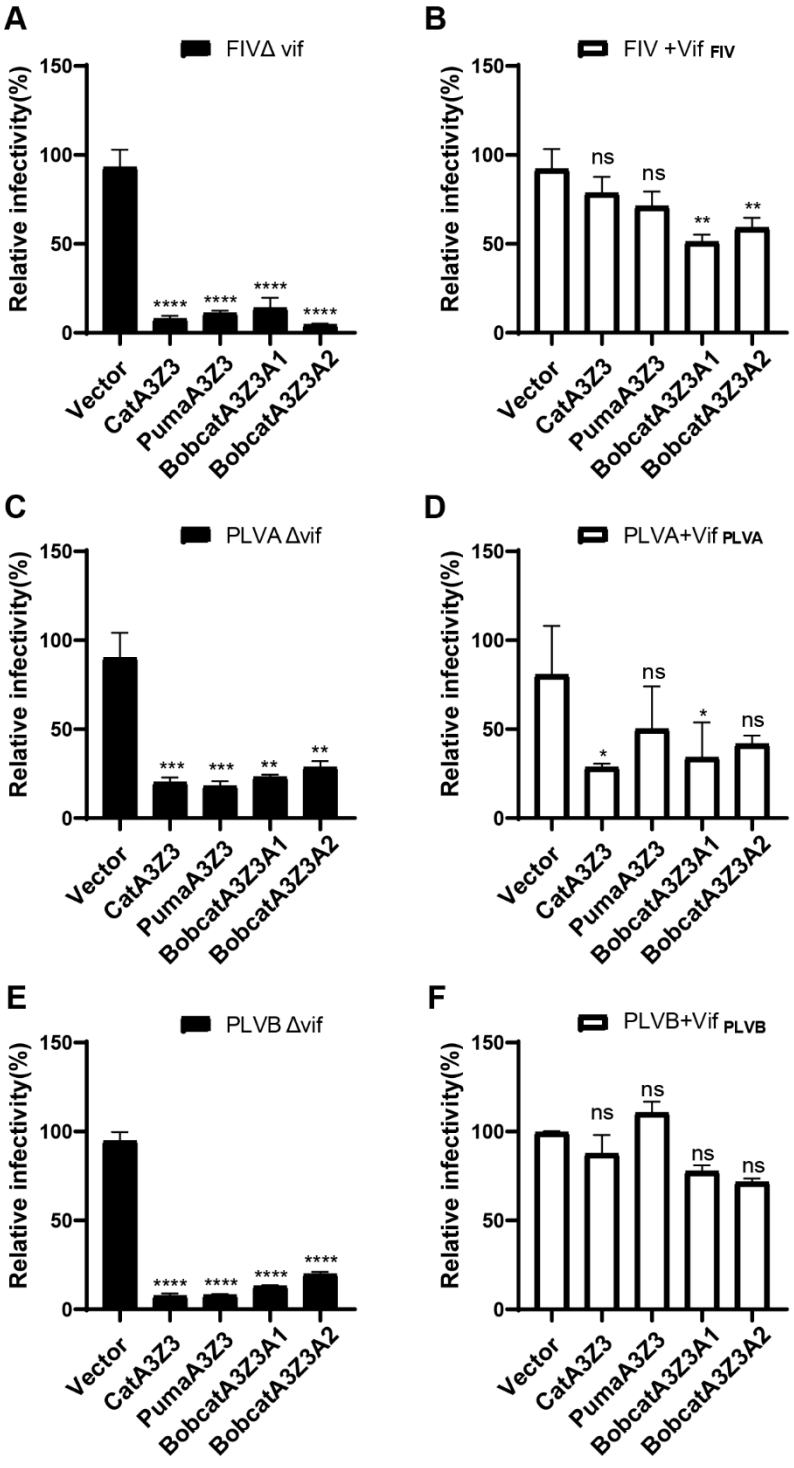

Fig 3.3 Feline A3Z3 proteins inhibit ΔVif PLVs and are antagonized by feline Vif proteins. (A-F) Reporter viruses for FIV, PLVA, and PLVB ΔVif, as well as FIV, PLVA, and PLVB ΔVif with their respective Vif proteins, were generated in 293T cells in the presence or absence of Cat A3Z3, Puma A3Z3, Bobcat A3Z3A1, or Bobcat A3Z3A2 proteins. “vector”: pcDNA3.1(+) was used as a control vector for A3Z3 expression. Two days post-transfection, normalized viral quantities were used to infect 293T cells, and firefly luciferase activity (relative light units, RLU) was measured 48 hours

post-infection. Values represent the means and standard deviations (error bars) from a representative experiment conducted in triplicate. Statistically significant differences are indicated by asterisks: P value < 0.0001 extremely significant (****), P value < 0.001 highly significant (***), 0.001 to 0.01 very significant (**), 0.01 to 0.05 significant (*), P value >0.05 not significant (ns).

3.1.5 PLV1695 Vif is specifically incapable of counteracting feline A3Z3 restriction

Co-transfected 293T cells were used to test for Vif-induced A3 depletions, short "A3 degradation assay", which confirmed that PLV1695 Vif is specifically unable to degrade feline A3Z3 (Fig. 3.1B, C, D). Subsequently, I assessed the functionality of PLV1695 Vif using a PLVB virus infection assay. The results demonstrated that PLVB Vif was able to overcome the restriction imposed by Cat A3Z3, Puma A3Z3, Bobcat A3Z3A1, and Bobcat A3Z3A2. In contrast, PLV1695 Vif failed to counteract the restriction mediated by these A3Z3 proteins (Fig. 3.4). Taken together, these findings indicate that PLV1695 Vif cannot overcome feline A3Z3-mediated restriction.

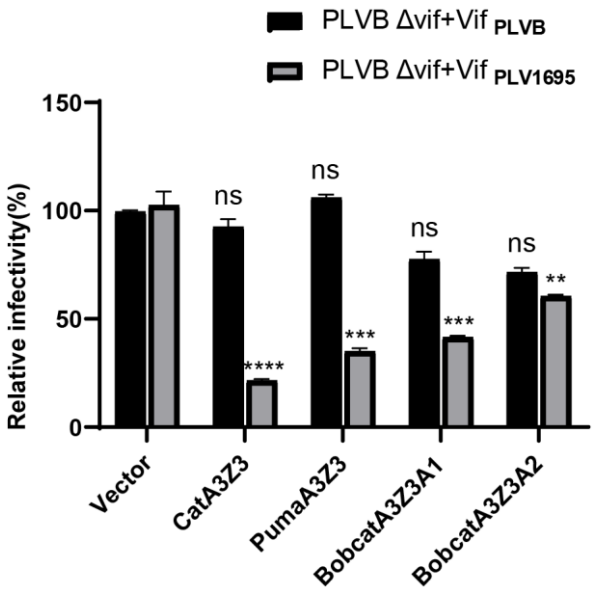

Fig 3.4 PLV1695 Vif is unable to overcome feline A3Z3 restriction. PLVB ΔVif + PLVB Vif or PLVB ΔVif + PLV1695 Vif reporter viruses were generated in 293T cells in the presence or absence of Cat A3Z3, Puma A3Z3, Bobcat A3Z3A1, or Bobcat A3Z3A2 proteins, with pcDNA3.1(+) serving as a control vector for A3Z3. Statistically significant differences are indicated by asterisks: P value <

0.0001 extremely significant (****), P value < 0.001 highly significant (***), 0.001 to 0.01 very significant (**), 0.01 to 0.05 significant (*), P value >0.05 not significant (ns).

3.1.6 PLV1695 Vif is unable to counteract A3Z3 restriction because it cannot bind to A3Z3

To counteract A3 restriction, Vif proteins bind directly to A3 proteins and recruit them to an E3 ubiquitin ligase complex, leading to the polyubiquitination and subsequent proteasomal degradation of A3 proteins[132, 169]. Given that PLV1695 Vif is specifically incapable of degrading feline A3Z3 while retaining its ability to degrade both feline A3Z2 and A3Z2Z3, I hypothesized that PLV1695 Vif may have lost its ability to bind feline A3Z3. Therefore, my next objective was to investigate the interaction between PLVB Vif and PLV1695 Vif with PumaA3Z3. To do this, I co-immunoprecipitated PumaA3Z3 and Vif from lysates of 293T cells transfected with expression plasmids for PumaA3Z3-HA, PLVB Vif-flag, or PLV1695 Vif-flag. As anticipated, PumaA3Z3 was detected in the PLVB Vif immunoprecipitated complex, whereas no PumaA3Z3 was observed in the PLV1695 Vif immunoprecipitation (Fig. 3.5A).

Next, to further validate the findings obtained from Fig. 3.5A, I utilized dominant-negative CUL5 (DN-CUL5) (Fig. 3.5C) as a bait protein to investigate the Vif-A3 binding complex. DN-CUL5 contains a C-terminal deletion that prevents its binding to RBX2, thus inhibiting ubiquitination and proteasomal degradation of substrates. However, it retains the capacity to bind Vif, making it suitable as a bait protein to investigate the Vif-A3 binding complex without the need for proteasome inhibitors to block Vif-mediated degradation of A3. I co-transfected DN-CUL5 and PumaA3Z3 with either PLVB Vif or PLV1695 Vif. Co-IP results indicated that DN-CUL5 binds to both PLVB Vif and PLV1695 Vif. PumaA3Z3 was detected in the DN-CUL5-PLVB Vif immunoprecipitated complex, whereas no PumaA3Z3 was observed in the DN-CUL5-PLV1695 Vif immunoprecipitation (Fig. 3.5D). These results are consistent with those in Fig. 3.5A. Collectively, these findings confirm that the inability of

PLV1695 Vif to counteract A3Z3 restriction is due to its failure to bind A3Z3.

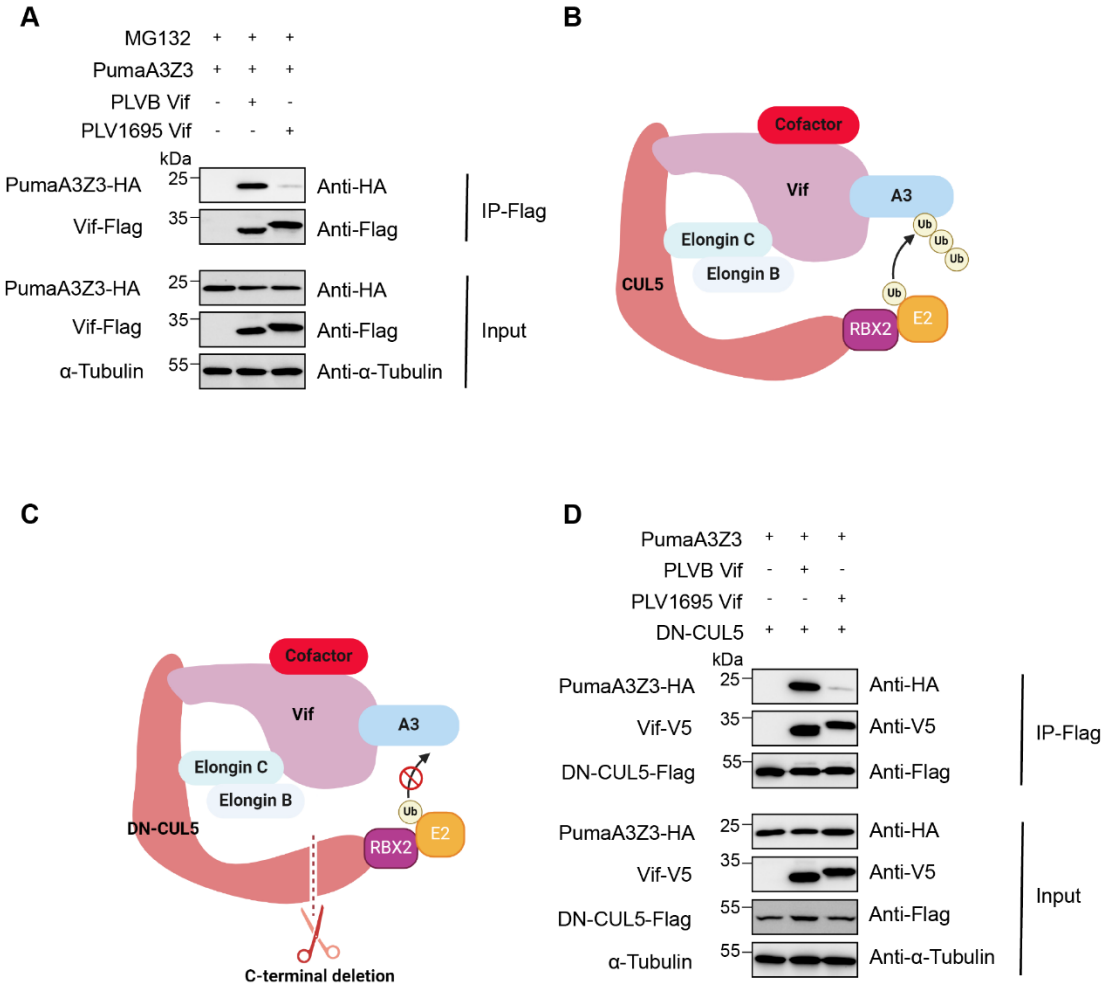

Fig 3.5 PLV1695 Vif cannot interact with A3Z3. (A) PLVB Vif-Flag or PLV1695 Vif-Flag expression plasmids were co-transfected with PumaA3Z3-HA expression plasmid, and MG132 was added to inhibit the proteasomal degradation of PumaA3Z3. Cell lysates were immunoprecipitated using anti-Flag magnetic beads and analyzed by immunoblotting with anti-Flag antibody to detect Vifs, and anti-HA antibody to detect PumaA3Z3. Tubulin was used as a loading control for the input samples. (B) Schematic representation of the CUL5–Vif–A3 binding complex. (C) Schematic representation of the DN-CUL5–Vif–A3 binding complex. (D) DN-CUL5-Flag and PumaA3Z3-HA were co-transfected with either PLVB Vif-V5 or PLV1695 Vif-V5. Cell lysates were immunoprecipitated using anti-Flag magnetic beads and analyzed by immunoblotting with anti-Flag antibody to detect DN-CUL5, anti-V5 antibody to detect Vifs, and anti-HA antibody to detect PumaA3Z3. Tubulin was used as a loading control for the input samples. Fig 3.5 B, C were created with BioRender.com.

3.1.7 Identification of Vif residues that determine the differential antagonism of PLVB and PLV1695 Vif against A3Z3

PLVB Vif can induce the degradation of PumaA3Z3, whereas PLV1695 Vif is unable to degrade PumaA3Z3 (Fig. 3.1C). The rational design of chimeric Vif proteins, combining elements from PLVB and PLV1695, provides a promising strategy for identifying specific residues within the Vif protein that contribute to these functional differences. To explore this, I generated six distinct PLVB/PLV1695 Vif chimeras.

Vif chimera 1 (Vif C1) and Vif C4 were designed to incorporate amino acids 1-72 and 1-25 from PLVB Vif, respectively, while the remaining portion was derived from PLV1695 Vif. Vif C2, Vif C3, Vif C5, and Vif C6 were engineered by integrating amino acids 1-72, 1-160, 1-192, and 1-207 from PLV1695 Vif, respectively, with the remaining segment derived from PLVB Vif (Fig. 3.6A, B).

A3 degradation assays showed that, among the six Vif chimeras tested, Vif C2, Vif C3, and Vif C5 efficiently degraded PumaA3Z3, whereas Vif C1, Vif C4, and Vif C6 failed to degrade PumaA3Z3 (Fig. 3.6C).

These findings suggest that the C-terminal residues derived from PLVB Vif, specifically those shared by the Vif C5 region (positions 193-207) (Fig. 3.6A, B), are crucial for the degradation of PumaA3Z3.

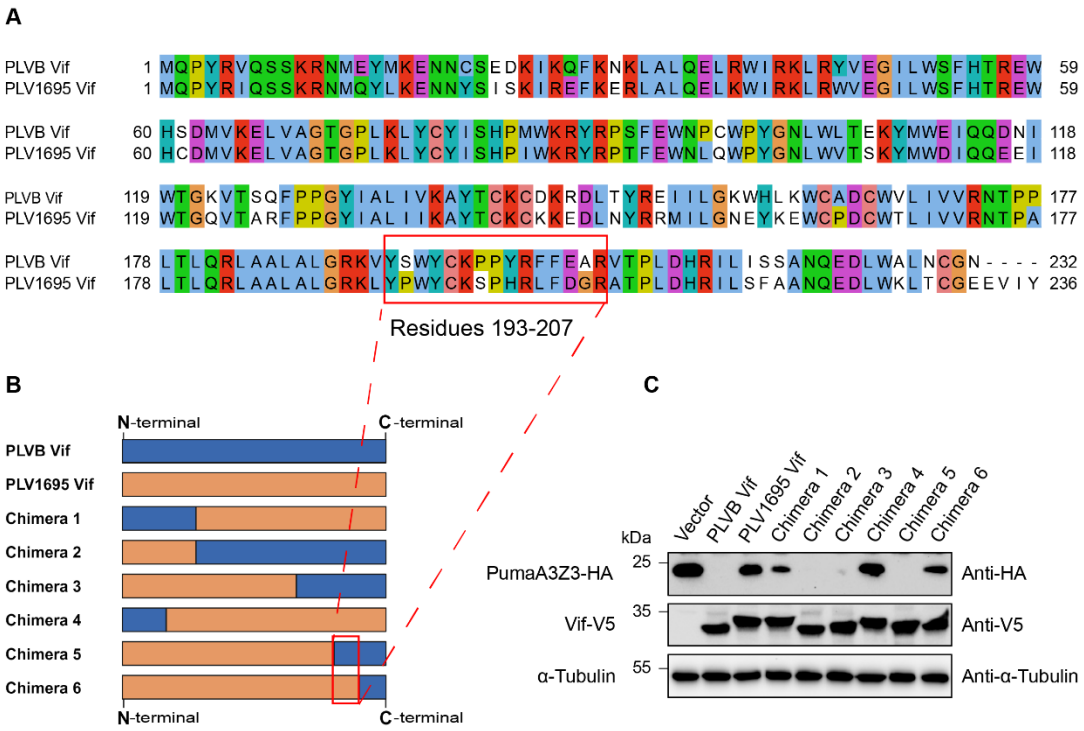

Figure 3.6 Residues 193-207 in PLVB Vif are critical for the degradation of PumaA3Z3. (A) Sequence alignment of PLVB and PLV1695 Vif proteins. The alignment highlights conserved residues according to their physicochemical properties using the Clustal color scheme. For further details, refer to materials and methods section 2.3.4. Notably, the 193–207 residue region is specifically emphasized. (B)Schematic representation of the PLVB/PLV1695 Vif chimeras (C1, C2, C3, C4, C5, C6). Notably, the 193–207 residue region in Chimera5 and Chimera6 models is specifically emphasized. (C) 293T cells were transfected with expression plasmids for PumaA3Z3-HA, along with expression plasmids for PLVB Vif-V5 or PLV1695 Vif-V5, or one of the chimeras (C1-C6). pcDNA3.1(+) was used as a vector control. 48 hours post-transfection, cell lysates were analyzed by immunoblotting with anti-HA and anti-V5 antibodies. Tubulin served as a loading control. Fig 3.6 B was created with BioRender.com.

3.1.8 Identification of specific residues in Vif that determine differential antagonism of PLVB and PLV1695 Vif against PumaA3Z3

The Vif region spanning positions 193–207 exhibits six amino acid differences between PLVB Vif and PLV1695 Vif (Fig. 3.7A). To investigate the significance of these differences, I initially generated six PLVB Vif mutants, each containing a

single amino acid substitution corresponding to the respective positions in the PLV1695 Vif sequence. Under my experimental conditions, I observed that only the PLVB Vif Y201H mutant lost its ability to degrade PumaA3Z3 (Fig. 3.7B).

Subsequently, I generated a PLV1695 Vif mutant where residue 201 was substituted with the corresponding residue from PLVB Vif. The A3 degradation assays demonstrated that the PLV1695 Vif H201Y mutant regained the ability to degrade PumaA3Z3 effectively (Fig. 3.7C). Notably, both the PLVB Vif Y201H and PLV1695 Vif H201Y mutants degraded PumaA3Z2 and PumaA3Z2Z3 as effectively as their respective wild-type Vifs (Fig. 3.7D). These findings indicate that residue 201 in Vif plays a specific role in the degradation of PumaA3Z3.

I further assessed the anti-PLVB viral activity of PumaA3Z3 in the presence of wild-type and mutant Vifs from PLVB and PLV1695. Luciferase activity assays revealed that, compared to their wild-type counterparts, the PLVB Vif Y201H mutant lost its ability to counteract PumaA3Z3, while the PLV1695 Vif H201Y mutant gained the capacity to overcome PumaA3Z3 restriction (Fig. 3.7E). These results are consistent with those obtained from the A3 degradation assays (Fig. 3.7C).

Taken together, these findings demonstrate that residue 201 in Vif determines differential antagonism of PLVB and PLV1695 Vif against PumaA3Z3.

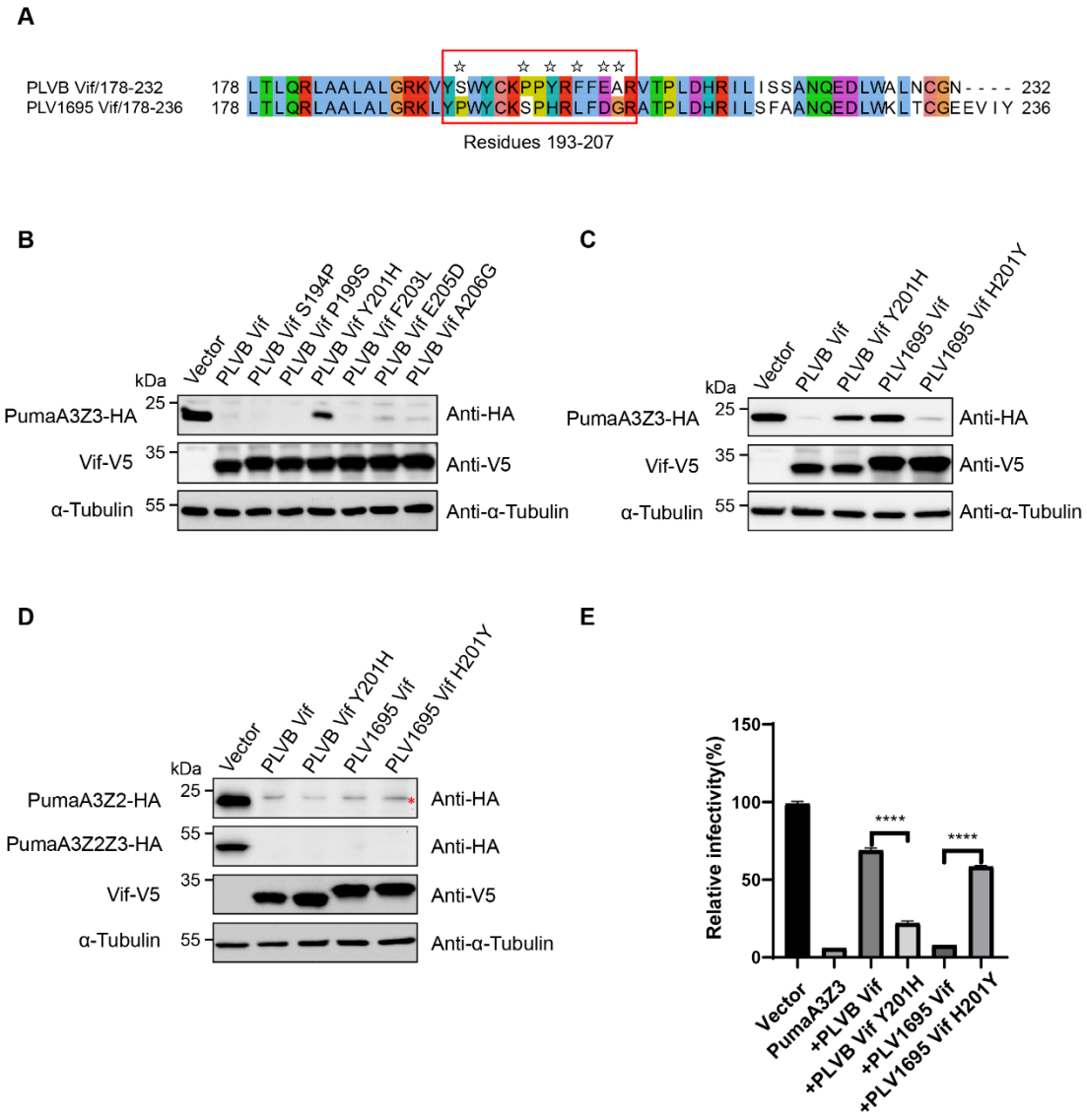

Fig 3.7 Residue 201 in Vif determines the differential antagonism of PLVB and PLV1695 Vif against PumaA3Z3. (A) Sequence alignment of PLVB and PLV1695 Vif proteins. The alignment depicts the C-terminal regions of PLVB and PLV1695 Vif proteins, with conserved residues highlighted according to their physicochemical properties using the Clustal color scheme. For further details, refer to materials and methods section 2.3.4. Notably, six amino acid differences between PLVB Vif and PLV1695 Vif within the 193–207 residue region are specifically emphasized. (B), (C), (D) 293T cells were transfected with expression plasmids for PumaA3Z3-HA, PumaA3Z2-HA, or PumaA3Z2Z3-HA, along with plasmids expressing wild-type or mutant PLVB Vif-V5 and PLV1695 Vif-V5. pcDNA3.1(+) was used as a vector control. Forty-eight hours post-transfection, cell lysates were analyzed by immunoblotting using anti-HA and anti-V5 antibodies. Tubulin was used as a loading control. *Denotes non-specific bands. (E) PLVB ΔVif reporter viruses were generated in 293T

cells in the presence of PLVB Vif, PLV1695 Vif, PLVB Vif Y201H, PLV1695 Vif H201Y, or pcDNA3.1(+) as a control vector. Statistically significant differences are indicated by asterisks: P < 0.0001 (****).

3.1.9 Residue 201 in PLVB and PLV1695 Vifs is responsible for feline A3Z3 degradation

It has been established that residue 201 in the PLVB and PLV1695 Vif proteins is responsible for the degradation of Puma A3Z3. Subsequently, it became important to investigate whether residue 201 is also critical for the degradation of other feline A3Z3 proteins. To address this, I co-transfected PLVB, PLV1695 Vif, and their respective Vif mutants with Cat and Bobcat A3Z3. The degradation experiments revealed that, in comparison to the wild types, PLVB Vif Y201H lost its ability to degrade Cat and Bobcat A3Z3, whereas PLV1695 Vif H201Y gained the ability to degrade both Cat and Bobcat A3Z3 (Fig. 3.8A, B). Taken together, these results demonstrate that residue 201 in the PLVB and PLV1695 Vif proteins is responsible for Feline A3Z3 degradation.

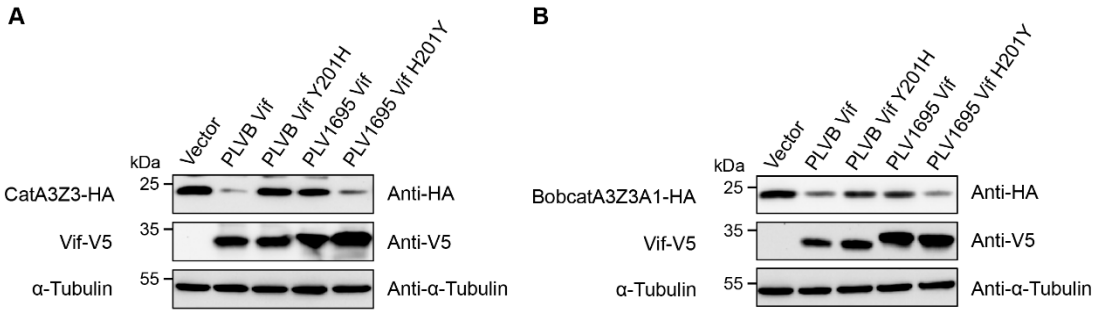

Fig 3.8 Residue 201 in PLVB and PLV1695 Vifs is responsible for feline A3Z3 degradation. (A), (B) 293T cells were transfected with expression plasmids for CatA3Z3-HA or BobcatA3Z3A1-HA, along with plasmids expressing PLVB Vif-V5, PLV1695 Vif-V5, PLVB Vif Y201H-V5, or PLV1695 Vif H201Y-V5. pcDNA3.1(+) was used as a vector control. 48 hours post-transfection, cell lysates were analyzed by immunoblotting with anti-HA and anti-V5 antibodies. Tubulin was used as a loading control.

3.1.10 Residue 201 in PLVB and PLV1695 Vifs is the PumaA3Z3 interaction site

To further investigate the function of residue 201 in the PLVB and PLV1695 Vif proteins, I focused on its role in interaction PumaA3Z3, which is likely a direct binding. Previous experiments confirmed that PLVB Vif complexes with PumaA3Z3, while PLV1695 Vif does not (Fig. 3.5A, B), suggesting that residue 201 may be responsible for this difference.

To test this hypothesis, I conducted co-transfections with expression plasmids for PumaA3Z3-HA along with plasmids expressing PLVB Vif-FLAG, PLVB Vif Y201H-FLAG, PLV1695 Vif-FLAG, or PLV1695 Vif H201Y-FLAG. Results from the FLAG-IP assay demonstrated that PLVB Vif formed a complex with PumaA3Z3, while PLVB Vif Y201H lost such ability. In contrast, PLV1695 Vif showed no interaction with PumaA3Z3, but PLV1695 Vif H201Y acquired the ability to precipitate PumaA3Z3 (Fig. 3.9A).

Next, I used DN-CUL5 as the bait protein to further investigate the Vif-A3 complex interaction. I co-transfected DN-CUL5 and PumaA3Z3 with either PLVB Vif, PLVB Vif Y201H, PLV1695 Vif, or PLV1695 Vif H201Y. Co-IP results indicated that DN-CUL5 forms a complex with both the wild-type and mutant forms of PLVB and PLV1695 Vif. However, compared to the wild type proteins, PLVB Vif Y201H lost its ability to complex PumaA3Z3, whereas PLV1695 Vif H201Y gained this ability (Fig. 3.9B). These results are consistent with those shown in Fig. 3.9A.

Subsequently, the PLVB Vif-PumaA3Z3 and PLV1695 Vif-PumaA3Z3 complexes were predicted using the AlphaFold server. The resulting models were analyzed in PyMOL to visualize the structures and identify key interaction residues. The analysis revealed that PLVB Vif residue Y201 interacts with R202, which subsequently binds to PumaA3Z3 residues K175 and D182 (Fig. 3.9C). In contrast, the H201 in PLV1695 Vif altered the protein conformation, causing R202 to shift away from PumaA3Z3 residues K175 and D182, thereby disrupting their interaction (Fig. 3.9D). These findings further support the Co-IP results shown in Fig. 3.9A and 3.9B.

In summary, these findings conclusively demonstrate that residue 201 in PLVB and

PLV1695 Vifs is the critical interaction site for PumaA3Z3.

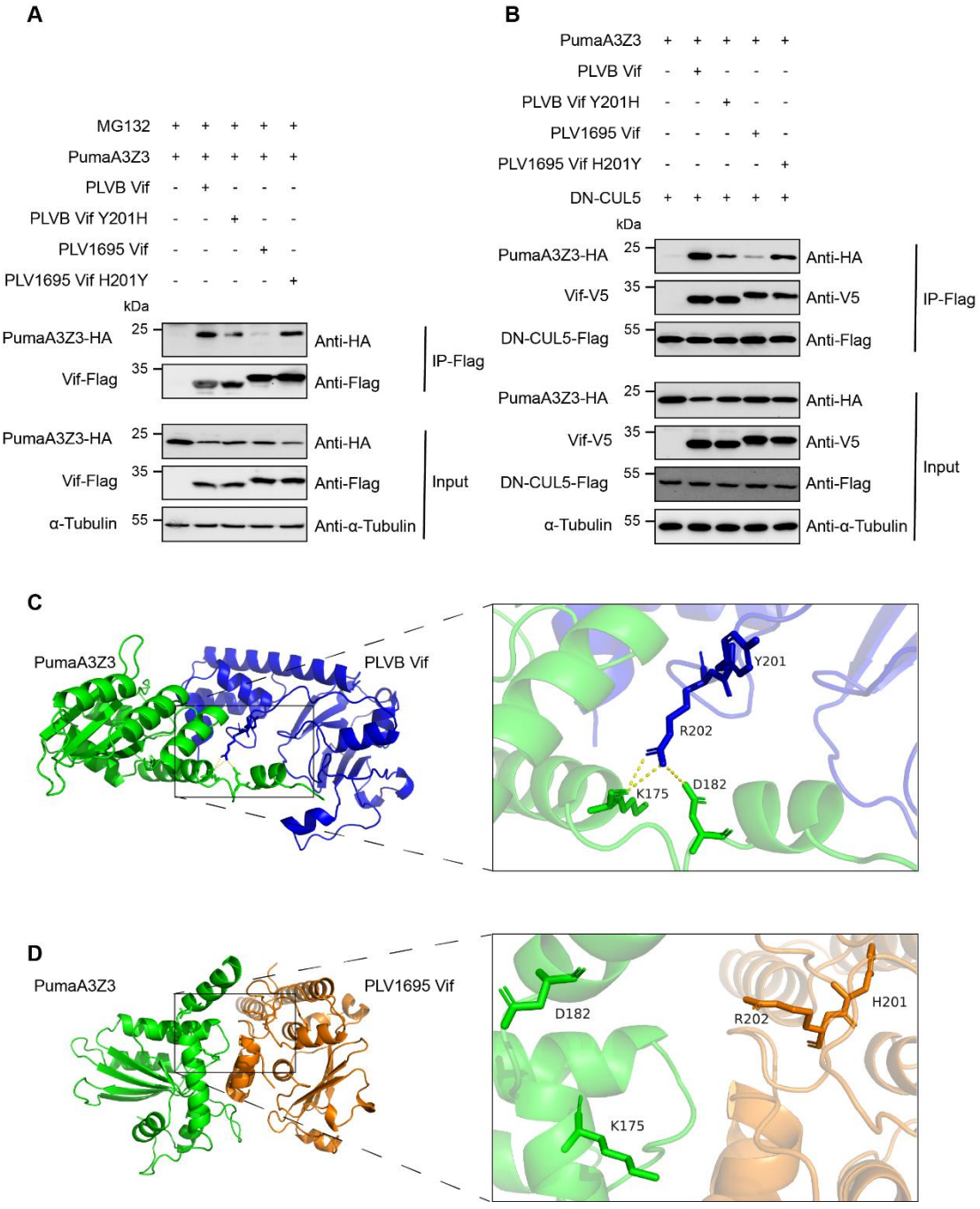

Fig 3.9 Residue 201 in PLVB and PLV1695 Vifs is the PumaA3Z3 interaction site. (A) PLVB Vif-FLAG, PLVB Vif Y201H-FLAG, PLV1695 Vif-FLAG, or PLV1695 Vif H201Y-FLAG expression plasmids were co-transfected with PumaA3Z3-HA expression plasmid, and MG132 was added to inhibit the proteasomal degradation of PumaA3Z3. Cell lysates were immunoprecipitated using anti-Flag magnetic beads and analyzed by immunoblotting with anti-Flag antibody to detect Vifs, and anti-HA antibody to detect PumaA3Z3. Tubulin was used as a loading control for the input samples.

(B) DN-CUL5-Flag and PumaA3Z3-HA were co-transfected with either PLVB Vif-V5, PLVB Vif Y201H-V5, PLV1695 Vif-V5 or PLV1695 Vif H201Y-V5. Cell lysates were immunoprecipitated using anti-Flag magnetic beads and analyzed by immunoblotting with anti-Flag antibody to detect DN-CUL5, anti-V5 antibody to detect Vifs, and anti-HA antibody to detect PumaA3Z3. Tubulin was used as a loading control for the input samples. (C) Structure of the PLVB Vif-PumaA3Z3 complex (PLVB Vif in blue; PumaA3Z3 in green), predicted using the AlphaFold server. A detailed view of the interaction interface between PLVB Vif and PumaA3Z3 is provided, highlighting the residues involved in the interaction. Yellow dashed lines denote hydrogen bonds. (D) Structure of the PLV1695 Vif-PumaA3Z3 complex (PLV1695 Vif in yellow; PumaA3Z3 in green), predicted using the AlphaFold server. A detailed view of the interface between PLV1695 Vif and PumaA3Z3 is provided, highlighting the residues of H201, R202 in PLV1695 Vif and K175, D182 in PumaA3Z3.

3.1.11 Identification of the 201YRF203 motif in PLVB Vif as the PumaA3Z3 likely binding Region

To further verify the PumaA3Z3 binding sites within PLVB Vif, I introduced single or double alanine substitutions in the vicinity of residue 201, generating the following PLVB Vif mutants: K198A, P199A, P200A, R202A, Y201R202-AA, F203A, and F204A. I then assessed the impact of these mutations on the ability of PLVB Vif to degrade PumaA3Z3. The degradation assays revealed that, compared to wild-type PLVB Vif, the R202A and Y201R202-AA mutants were unable to degrade PumaA3Z3 (Fig. 3.10A). Furthermore, the Y201H and F203A mutants exhibited a partial loss of degradation ability (Fig. 3.10A).

Next, co-transfection experiments were performed using wild-type PLVB Vif, along with the P200A, Y201H, R202A, and F203A mutants, each co-expressed with PumaA3Z3. FLAG-IP assay results showed that, compared to the wild-type, the Y201H, R202A, and F203A mutants lost their capacity to precipitate PumaA3Z3 (Fig. 3.10B).

Subsequently, the PLVB Vif-PumaA3Z3 complex was predicted using the AlphaFold server. The resulting models were analyzed in PyMOL to visualize the

structures and identify key interaction residues. The analysis revealed that PLVB Vif residues Y201, R202, and F203 form the interface that binds to PumaA3Z3 residues K175 and D182 (Fig. 3.10C). These findings further corroborate the Co-IP results shown in Fig. 3.10B.

Taken together, these findings suggest that the 201YRF203 motif in PLVB Vif constitutes the PumaA3Z3 binding region.

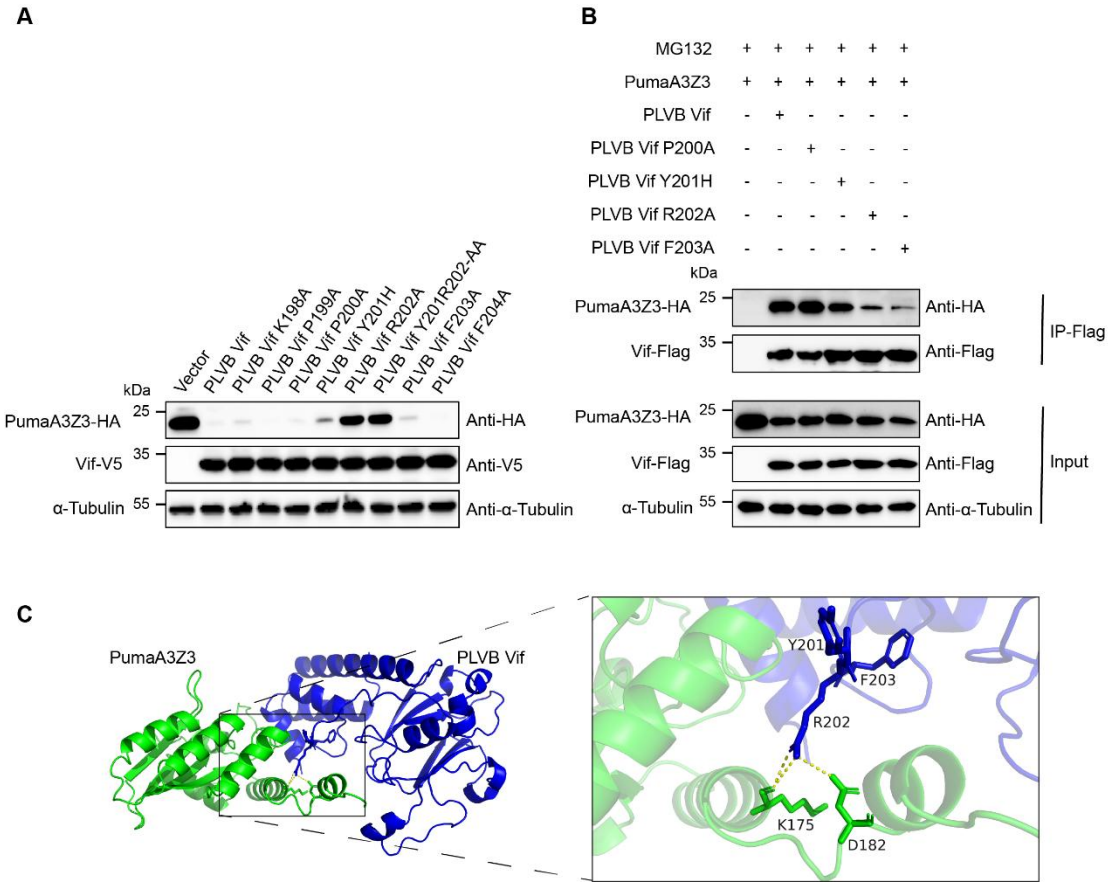

Fig. 3.10 The 201YRF203 motif in PLVB Vif constitutes the PumaA3Z3 interaction region. (A) 293T cells were transfected with expression plasmids for PumaA3Z3-HA, along with plasmids expressing either PLVB Vif-V5 or PLVB Vif mutants. pcDNA3.1(+) was used as a vector control. 48 hours post-transfection, cell lysates were analyzed by immunoblotting with anti-HA and anti-V5 antibodies. Tubulin was used as a loading control. (B) PLVB Vif-Flag or PLVB Vif mutant expression plasmids were co-transfected with the PumaA3Z3-HA expression plasmid, and MG132 was added to inhibit proteasomal degradation of PumaA3Z3. Cell lysates were immunoprecipitated using anti-Flag magnetic beads and analyzed by immunoblotting with an anti-Flag antibody to detect Vif

proteins and an anti-HA antibody to detect PumaA3Z3. Tubulin was used as a loading control for the input samples. (C) Structure of the PLVB Vif-PumaA3Z3 complex (PLVB Vif in blue; PumaA3Z3 in green), predicted using the AlphaFold server. A detailed view of the interaction interface between PLVB Vif and PumaA3Z3 is provided, highlighting the residues involved in the interaction. Yellow dashed lines denote hydrogen bonds.

3.1.12 The N-terminal region of PLVB Vif is not essential for PumaA3Z3 degradation and binding

Previous research has reported that FIV Vif selectively degrades Cat A3Z2 and A3Z3 through its N-terminal residues, specifically 24ML25 and 27I, which interact with Cat A3Z3[154]. These residues, 24ML25 and 27I in FIV Vif, correspond to 15YM16 and 18E in PLVB Vif. (Fig.3.11A). To investigate their role in PLVB Vif, I generated three single-alanine PLVB Vif mutants (Y15A, M16A, E18A) and three additional single-alanine mutants in adjacent residues (N20A, C21A, E23A). A3 degradation assays revealed that, compared to wild-type PLVB Vif, the M16A and E18A mutants showed a slight reduction in the ability to degrade PumaA3Z3, while the other N-terminal mutants degraded PumaA3Z3 similarly to the wild-type PLVB Vif (Fig. 3.11B).

Subsequently, the N-terminal mutants M16A and E18A were compared with the C-terminal mutant Y201H in DN-CUL5–Vif–A3 binding assays. 293T Cells were co-transfected with DN-CUL5 and PumaA3Z3, along with either wild-type PLVB Vif or one of the three mutants. Co-IP results revealed that DN-CUL5 complexed both wild-type and mutant forms of PLVB Vif. Compared to wild-type PLVB Vif, the Y201H mutant lost its ability to interact with PumaA3Z3, while the M16A and E18A mutations did not impair their interaction with PumaA3Z3 (Fig. 3.11C).

These findings suggest that, unlike FIV Vif, the N-terminal region of PLVB Vif is not critical for PumaA3Z3 degradation and binding.

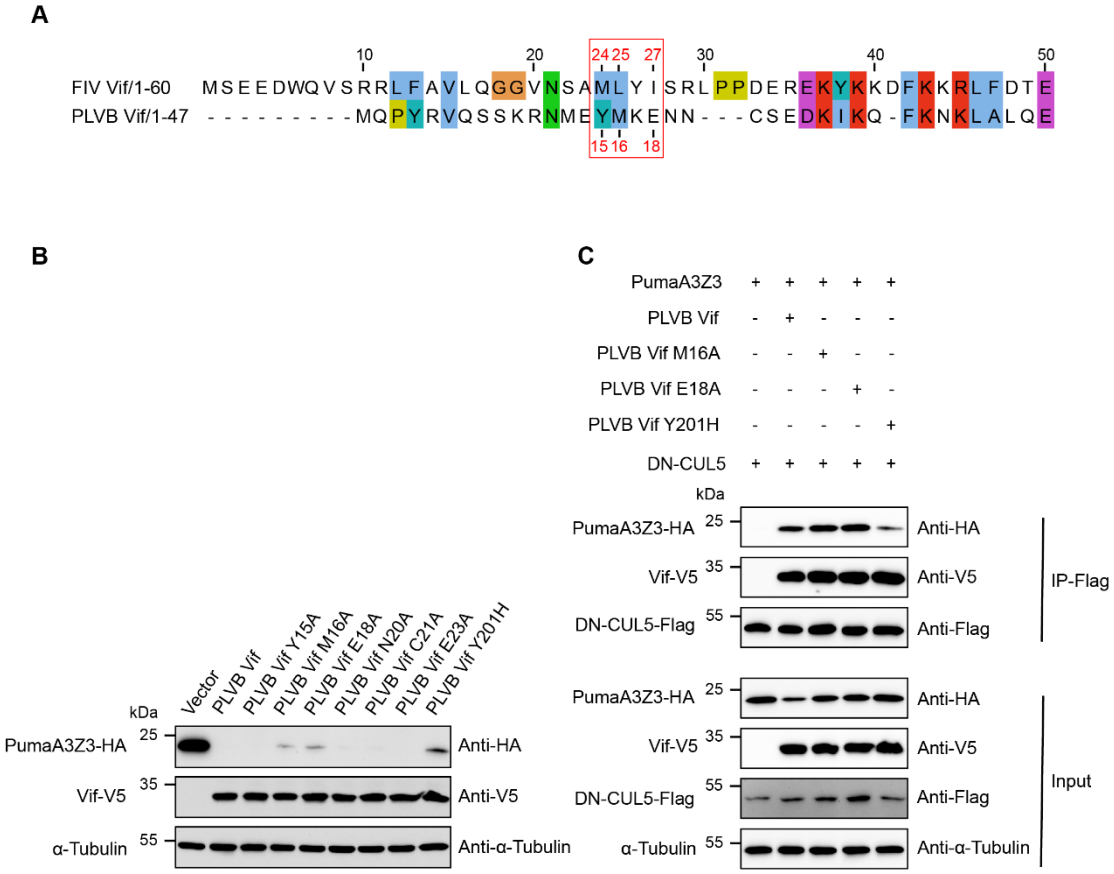

Fig. 3.11 The N-terminal region of PLVB Vif is not essential for PumaA3Z3 degradation and binding. (A) Sequence alignment of the FIV and PLVB Vif proteins. The alignment illustrates the N-terminal regions of FIV and PLVB Vif proteins, with conserved residues highlighted based on their physicochemical properties using the Clustal color scheme. For further details, refer to materials and methods section 2.3.4. Residues 24ML25 and 27I in FIV Vif correspond to 15YM16 and 18E in PLVB Vif and are specifically emphasized. (B) 293T cells were transfected with expression plasmids for PumaA3Z3-HA, along with plasmids expressing either PLVB Vif-V5 or PLVB Vif mutants. pcDNA3.1(+) was used as a vector control. 48 hours post-transfection, cell lysates were analyzed by immunoblotting with anti-HA and anti-V5 antibodies. Tubulin was used as a loading control. (C) DN-CUL5-Flag and PumaA3Z3-HA were co-transfected with either wild-type PLVB Vif-V5, PLVB Vif M16A, PLVB Vif E18A, or PLVB Vif Y201H. Cell lysates were immunoprecipitated using anti-Flag magnetic beads and analyzed by immunoblotting with anti-Flag antibody to detect DN-CUL5, anti-V5 antibody to detect Vif, and anti-HA antibody to detect PumaA3Z3. Tubulin was used as a loading control for the input samples.

3.1.13 The amino acid in the FIV Vif motif corresponding to the PLVB Vif 201YRF203 motif is responsible for CatA3Z3 interaction

The 201YRF203 motif of PLVB Vif corresponds to the 222QRF224 motif of FIV Vif (Fig. 3.12A). To investigate their roles, three single-alanine FIV Vif mutants (Q222A, R223A, F224A) and one additional single-alanine mutant in an adjacent residue (N221A) were generated. A3 degradation assays revealed that, compared to wild-type FIV Vif, the F224A mutant lost its ability to degrade CatA3Z3 and PumaA3Z3, while the other three mutants did not impair FIV Vif's ability to degrade these proteins (Fig. 3.12B). Previous research reported that FIV Vif's N-terminal residues, specifically 24ML25 and 27I, interact with CatA3Z3[154]. Therefore, I compared these N-terminal and C-terminal FIV Vif mutants in A3 degradation assays, and the results showed that both sets of mutants lost the ability to degrade CatA3Z3 (Fig. 3.12C). Furthermore, like the wild-type FIV Vif, the F224A mutant effectively degraded CatA3Z2 and CatA3Z2Z3 (Fig. 3.12D). Taken together, these findings suggest that the amino acid in the FIV Vif motif corresponding to the PLVB Vif 201YRF203 motif is responsible for CatA3Z3 degradation and interaction.

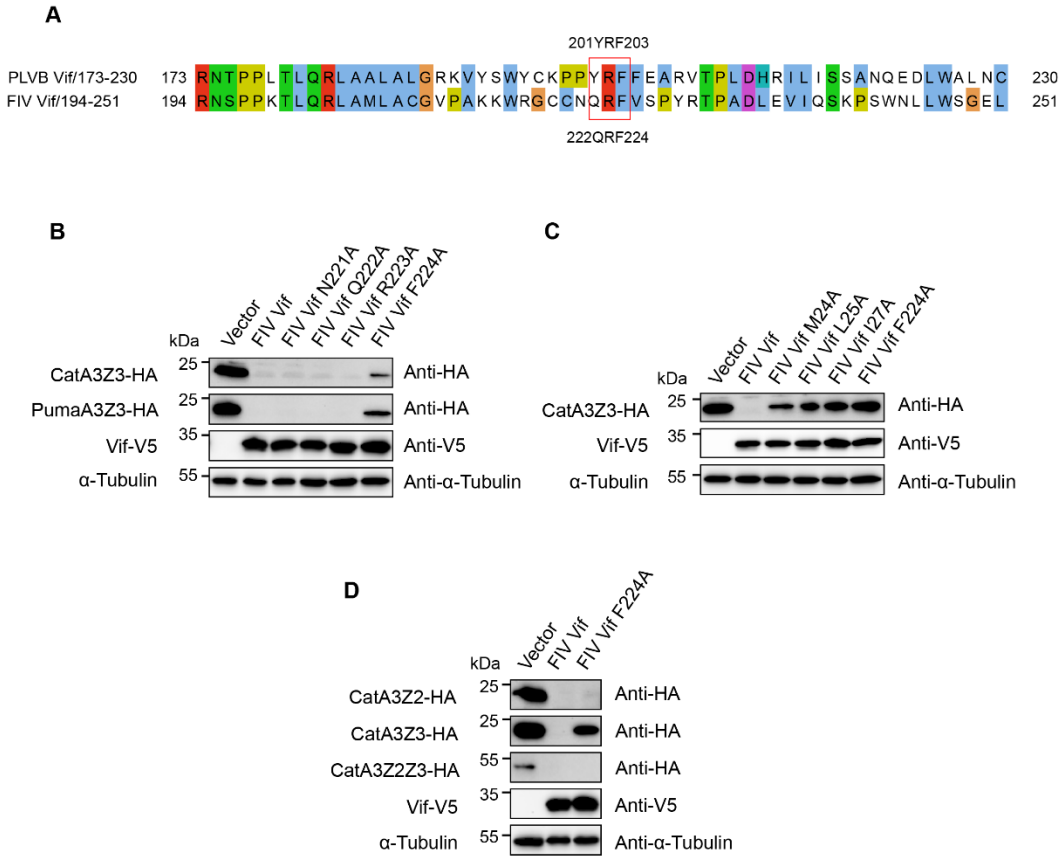

Fig. 3.12 The amino acid in the FIV Vif motif corresponding to the PLVB Vif 201YRF203 motif is responsible for CatA3Z3 interaction. (A) Sequence alignment of the PLVB and FIV Vif proteins. The alignment depicts the C-terminal regions of PLVB and FIV Vif proteins, with conserved residues highlighted based on their physicochemical properties using the Clustal color scheme. For further details, refer to materials and methods section 2.3.4. Residues 201YRF203 in PLVB Vif correspond to 222QRF224 in FIV Vif and are specifically emphasized. (B), (C), (D) 293T cells were transfected with expression plasmids for CatA3Z3-HA, PumaA3Z3-HA, CatA3Z2-HA, or CatA3Z2Z3-HA, along with plasmids expressing either wild-type FIV Vif-V5 or FIV Vif mutants. pcDNA3.1(+) was used as a vector control. 48 hours post-transfection, cell lysates were analyzed by immunoblotting with anti-HA and anti-V5 antibodies. Tubulin was used as a loading control.

3.1.14 The amino acids in PLVA Vif corresponding to the PLVB Vif 201YRF203 motif are responsible for interaction with BobcatA3Z3

The 201YRF203 motif of PLVB Vif corresponds to the 232CTF224 motif of PLVA Vif (Fig. 3.13A). To investigate their functional roles, three single-point mutants of

PLVA Vif (C232Y, T233A, F234A) were generated, along with an additional single-alanine mutant in an adjacent residue (Q231A). A3 degradation assays showed that, compared to wild-type PLVA Vif, all the four Vif mutants tested lost their ability to degrade BobcatA3Z3 (Fig. 3.13B).

Next, I employed DN-CUL5 as the bait protein to further explore the Vif-A3 interaction. I co-transfected DN-CUL5 and BobcatA3Z3 with either wild-type PLVA Vif or each of the four mutants. Co-IP results revealed that DN-CUL5 bound both wild-type and mutant forms of PLVA Vif. However, compared to the wild type, these four Vif mutants exhibited a loss of ability to bind BobcatA3Z3 (Fig. 3.13C).

Collectively, these findings indicate that the 231QCTF224 motif in PLVA Vif constitutes the BobcatA3Z3 interaction region.

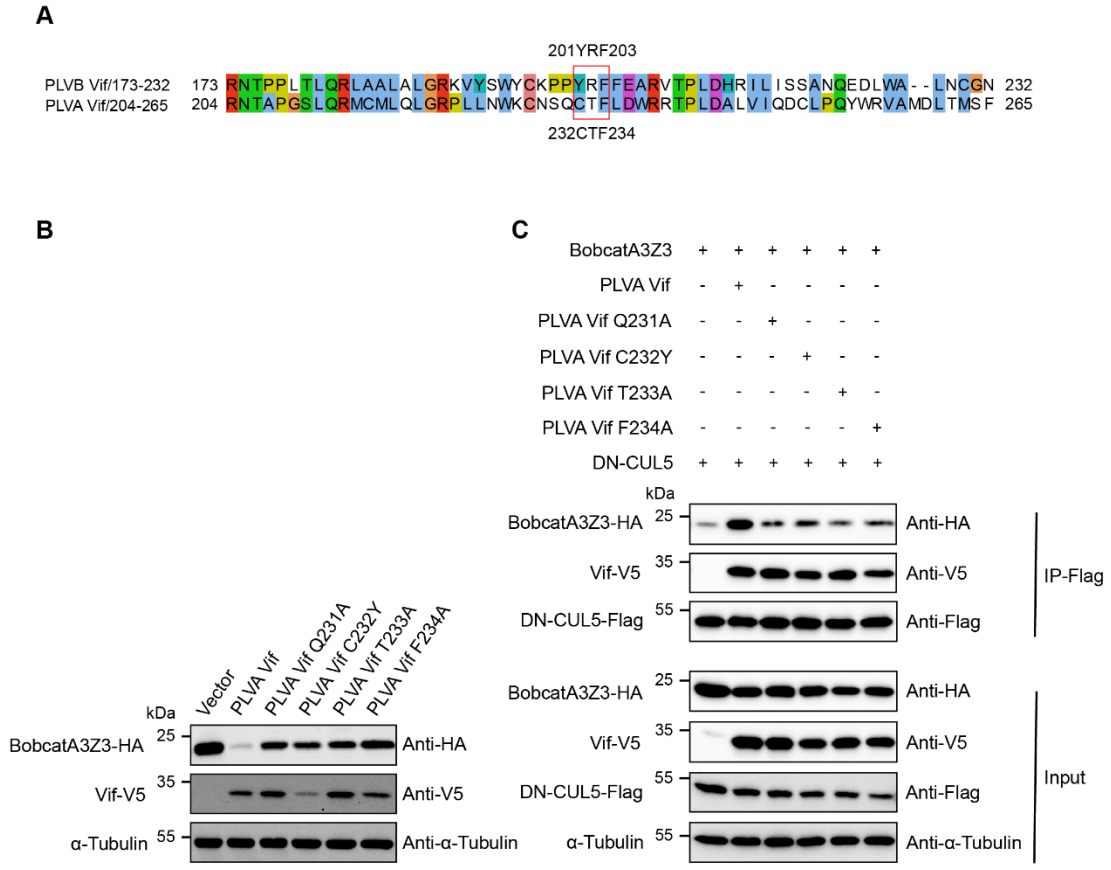

Fig. 3.13 The 231QCTF224 motif in PLVA Vif constitutes the BobcatA3Z3 interaction region.

(A) Sequence alignment of the PLVB and PLVA Vif proteins. The alignment depicts the C-terminal regions of PLVB and PLVA Vif proteins, with conserved residues highlighted based on their physicochemical properties using the Clustal color scheme. For further details, refer to materials and methods section 2.3.4. Residues 201YRF203 in PLVB Vif correspond to 232CTF234 in PLVA Vif and

are specifically emphasized. (B) 293T cells were transfected with expression plasmids for BobcatA3Z3-HA, along with plasmids expressing either wild-type PLVA Vif-V5, PLVA Vif Q231A, PLVA Vif C232Y, PLVA Vif T233A, or PLVA Vif F234A. pcDNA3.1(+) was used as a vector control. 48 hours post-transfection, cell lysates were analyzed by immunoblotting with anti-HA and anti-V5 antibodies. Tubulin was used as a loading control. (C) DN-CUL5-Flag and BobcatA3Z3-HA were co-transfected with either wild-type PLVA Vif-V5, PLVA Vif Q231A, PLVA Vif C232Y, PLVA Vif T233A, or PLVA Vif F234A. Cell lysates were immunoprecipitated using anti-Flag magnetic beads and analyzed by immunoblotting with anti-Flag antibody to detect DN-CUL5, anti-V5 antibody to detect Vif, and anti-HA antibody to detect BobcatA3Z3. Tubulin was used as a loading control for the input samples.

3.1.15 Both the N-terminal and C-terminal regions of PLVA Vif are critical for BobcatA3Z3 degradation and interaction

The 24M in FIV Vif, corresponds to 24Y in PLVA Vif (Fig. 3.14A). To investigate its role in PLVA Vif, I generated three single-alanine PLVA Vif mutants (Y24A). A3 degradation assays revealed that, compared to wild-type PLVA Vif, both Y24A and C232Y mutants lost the ability to degrade BobcatA3Z3 (Fig. 3.14B).

Next, the N-terminal mutant Y24A was compared with the C-terminal mutant C232Y in DN-CUL5–Vif–A3 binding assays. 293T cells were co-transfected with DN-CUL5 and BobcatA3Z3, along with either wild-type PLVA Vif or one of the two mutants. Co-IP results revealed that DN-CUL5 bound to both wild-type and mutant forms of PLVA Vif. Compared to wild-type PLVA Vif, both mutants lost the ability to bind BobcatA3Z3 (Fig. 3.14C).

Subsequently, the PLVA Vif-BobcatA3Z3 complex was predicted using the AlphaFold server. The resulting models were analyzed in PyMOL to visualize the structures and identify key interaction residues. The analysis revealed that the N-terminal PLVA Vif residue Y24 binds to BobcatA3Z3 residue H17, while the C-terminal PLVA Vif residues Q231, C232, T233, and F234 form the interface that interacts with BobcatA3Z3 residue R18 (Fig. 3.14D).

These findings further corroborate the Co-IP results shown in Fig. 3.13C and Fig.

3.14C, demonstrating that both the N-terminal and C-terminal regions of PLVA Vif are critical for BobcatA3Z3 degradation and interaction.

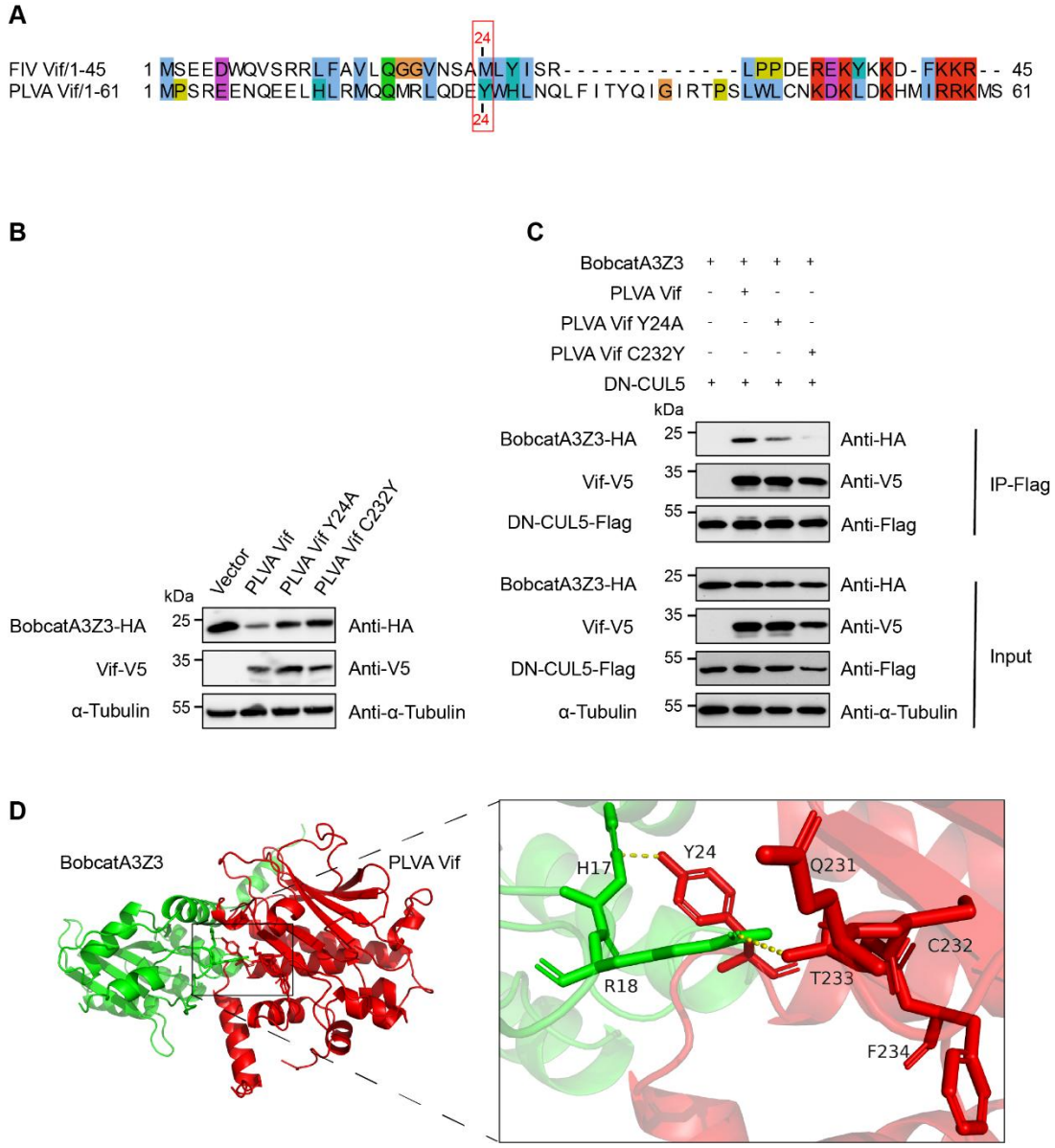

Fig. 3.14 Both the N-terminal and C-terminal regions of PLVA Vif are critical for BobcatA3Z3 degradation and interaction. (A) Sequence alignment of the FIV and PLVA Vif proteins. The alignment depicts the N-terminal regions of FIV and PLVA Vif proteins, with conserved residues highlighted based on their physicochemical properties using the Clustal color scheme. For further details, refer to materials and methods section 2.3.4. Residue 24M in FIV Vif corresponds to 24Y in PLVA Vif and is specifically emphasized. (B) 293T cells were transfected with expression plasmids for BobcatA3Z3-HA, along with plasmids expressing either wild-type PLVA Vif-V5, PLVA Vif Y24A, PLVA Vif C232Y. pcDNA3.1(+) was used as a vector control. 48 hours post-transfection, cell lysates

were analyzed by immunoblotting with anti-HA and anti-V5 antibodies. Tubulin was used as a loading control. (C) DN-CUL5-Flag and BobcatA3Z3-HA were co-transfected with either wild-type PLVA Vif-V5, PLVA Vif Y24A, PLVA Vif C232Y. Cell lysates were immunoprecipitated using anti-Flag magnetic beads and analyzed by immunoblotting with anti-Flag antibody to detect DN-CUL5, anti-V5 antibody to detect Vif, and anti-HA antibody to detect BobcatA3Z3. Tubulin was used as a loading control for the input samples. (D) Structure of the PLVA Vif-BobcatA3Z3 complex (PLVA Vif red; BobcatA3Z3 in green), predicted using the AlphaFold server. A detailed view of the interaction interface between PLVA Vif and BobcatA3Z3 is provided, highlighting the residues involved in the interaction. Yellow dashed lines indicate amino acid interactions.

3.1.16 The residues corresponding to 201YRF203 of PLVB Vif in HIV-1 Vif are responsible for the degradation of human A3s, but not for HIV-2 Vif

The 201YRF203 motif of PLVB Vif corresponds to 172DRW174 in HIV-1 Vif and 175DYR177 in HIV-2 Vif (Fig. 3.15A). Previous studies have reported that the 171EDRW174 region of HIV-1 Vif forms the A3F binding site and is crucial for HIV-1 Vif-induced A3F degradation[152]. To further investigate this, I generated four single-alanine mutants in the 171EDRW174 region of HIV-1 Vif. Similarly, single-point mutants were created in the 174RDYR177 region of HIV-2 Vif. A3 degradation assays revealed that, compared to wild-type HIV-1 Vif, the HIV-1 Vif D172A, R173A, and W174A mutants partially lost their ability to degrade human A3C and A3G, while the E171A mutation did not affect HIV-1 Vif's capacity to degrade these A3 proteins (Fig. 3.15B, C). In contrast, for HIV-2 Vif, none of the four mutants tested impaired its ability to degrade human A3C and A3G (Fig. 3.15D, E).

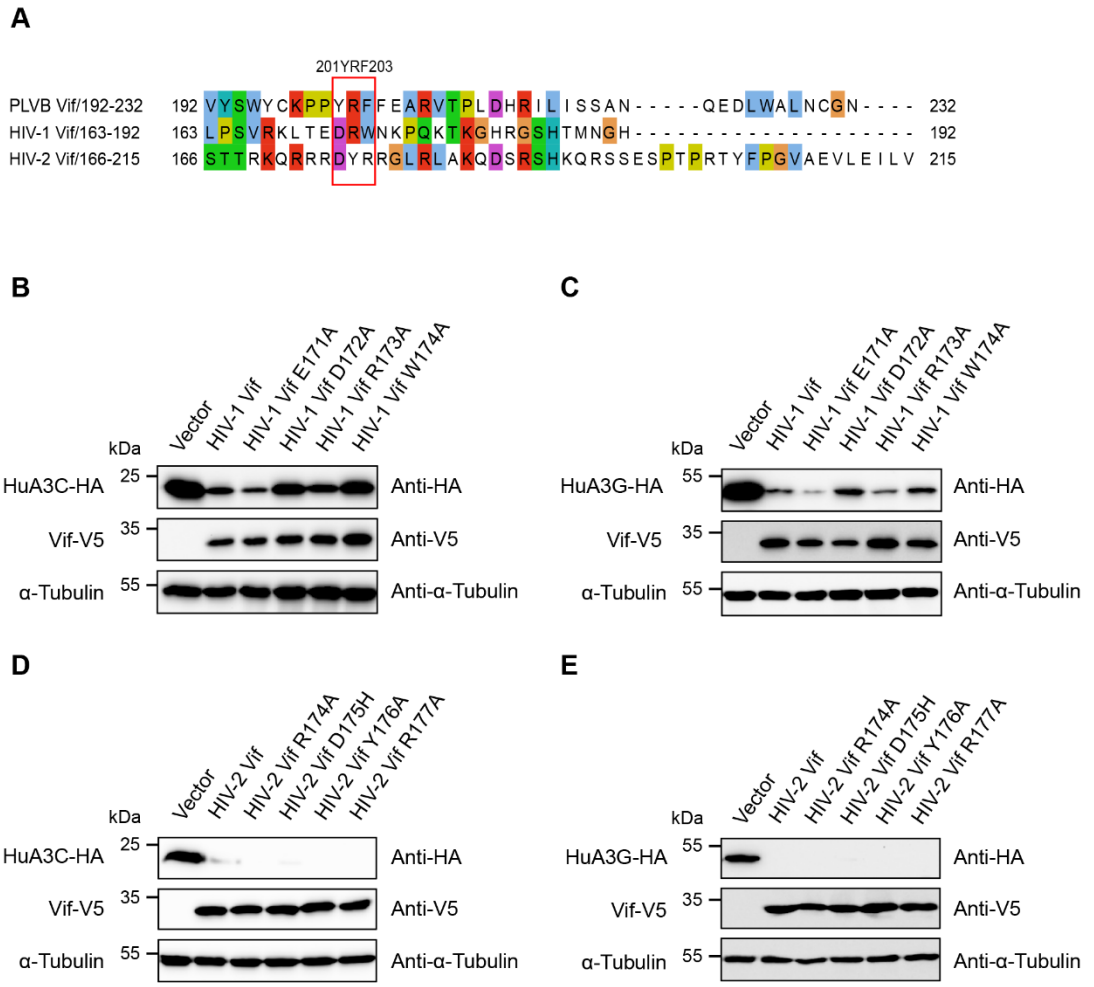

Fig. 3.15 The residues corresponding to 201YRF203 of PLVB Vif in HIV-1 Vif are responsible for the degradation of human A3s, but not for HIV-2 Vif. (A) Sequence alignment of the PLVB, HIV-1 and HIV-2 Vif proteins. The alignment illustrates the C-terminal regions of PLVB, HIV-1 and HIV-2 Vif proteins, with conserved residues highlighted based on their physicochemical properties using the Clustal color scheme. For further details, refer to materials and methods section 2.3.4. Residues 201YRF203 in PLVB Vif, which correspond to 172DRW174 in HIV-1 Vif and 175DYR177 in HIV-2, are specifically emphasized. (B), (C), (D), (E) 293T cells were transfected with expression plasmids for HumanA3C-HA or HumanA3G-HA, along with plasmids expressing either wild-type HIV-1 Vif-V5, HIV-1 Vif E171A, HIV-1 Vif D172A, HIV-1 Vif R173A, HIV-1 Vif W174A, HIV-2 Vif-V5, HIV-2 Vif R174A, HIV-2 Vif D175H, HIV-2 Vif Y176A, or HIV-2 Vif R177A. pcDNA3.1(+) was used as a vector control. 48 hours post-transfection, cell lysates were analyzed by immunoblotting with anti-HA and anti-V5 antibodies. Tubulin was used as a loading control.

3.2 Investigation of the interaction between Vif and CUL proteins

3.2.1 Investigation of the binding interaction of Vif Proteins with CUL2 and CUL5

HIV-1 Vif forms a Vif–E3 ligase complex with CUL 5, Elongin B/C, CBF-β, and RING box 2 proteins, where the cofactor CBF-β stabilizes the complex assembly[138](Fig. 3.16A). Similarly, FIV Vif forms a Vif-E3 ligase complex with CUL 5, Elongin B/C, and RING box 2 proteins, but it does not require CBF-β for A3 degradation[139] (Fig. 3.16B). Both CUL2 and CUL5 proteins recruit Elongin B/C as adaptor proteins. Previous research indicated that HIV-1 Vif specifically prefers CUL5 over CUL2 as the scaffold protein for A3G degradation[132]. Likewise, FIV Vif binds to CUL5 but not CUL2[157]. However, it is unknown whether other Vif proteins, such as PLVA or PLVB Vif, interact with Cullin family proteins.

To address this, I investigated the binding interactions of these Vif proteins with CUL2 and CUL5. Co-IP assays were performed using lysates from 293T cells co-transfected with expression plasmids for Vif-Flag/V5 and either Myc-CUL2 or Myc-CUL5. Co-IP results confirmed previous findings that FIV Vif, HIV-1 Vif, and HIV-2 Vif bind to CUL5 but not CUL2 (Fig. 3.16C, G, H). Interestingly, PLVA Vif was found to bind CUL5 and exhibited slight binding interaction to CUL2 (Fig. 3.16D). Notably, both PLVB Vif and PLV1695 Vif were observed to bind to both CUL2 and CUL5 (Fig. 3.16E, F). These findings demonstrate that the tested Vif proteins exhibit distinct binding interactions with CUL2 and CUL5.

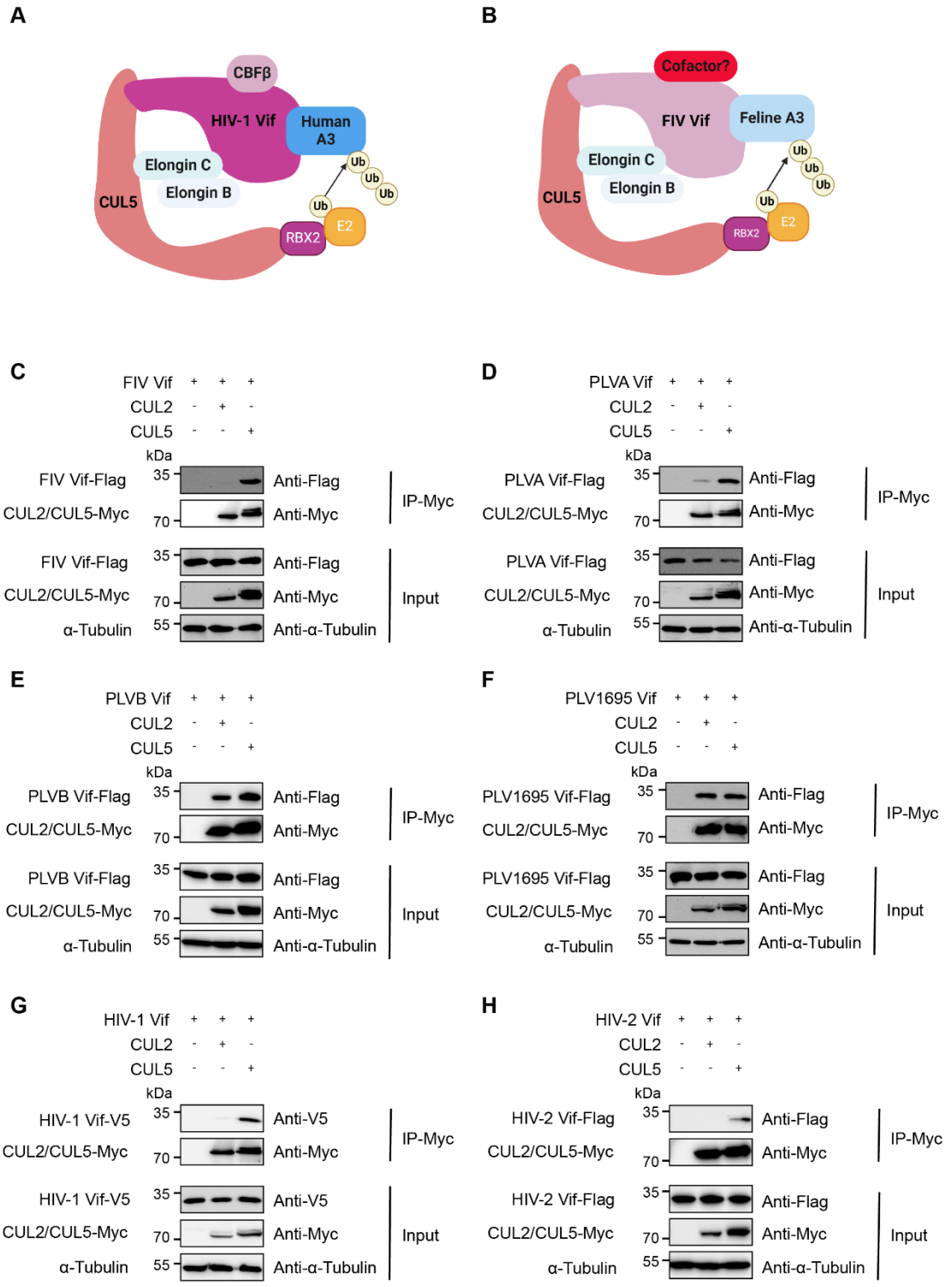

Fig. 3.16 Investigation of the interaction of Vif Proteins with CUL2 and CUL5. (A) Schematic representation of the HIV-1 Vif–E3 ligase complex. (B) Schematic representation of the FIV Vif–E3 ligase complex. (C)-(H) FIV Vif-Flag, PLVA Vif-Flag, PLVB Vif-Flag, PLV1695 Vif-Flag, HIV-1 Vif-V5, or HIV-2 Vif-Flag expression plasmids were co-transfected with either Myc-CUL2 or Myc-CUL5 in 293T cells. Cell lysates were immunoprecipitated using anti-Myc magnetic beads and analyzed by immunoblotting with anti-Flag/V5 antibodies to detect Vif proteins, and anti-Myc antibodies to detect

CUL2/CUL5. Tubulin was used as a loading control for input samples. Fig. 3.16A was adapted from: Collins DR, Collins KL. HIV-1 accessory proteins adapt cellular adaptors to facilitate immune evasion. PLoS Pathog 2014; 10(1):e1003851[141]. Licensed under CC BY 4.0 (https://creativecommons.org/licenses/by/4.0/). Reproduced with BioRender.com. Fig. 3.16B was created with BioRender.com.

3.2.2 DN-CUL2 and DN-CUL5 exhibit differential effects on the degradation of feline A3Z3 proteins by feline Vif proteins

CUL2 and CUL5 interact with RBX through their C-terminus, a region crucial for E3 ubiquitin ligase activity[130]. Dominant-negative CUL5 (DN-CUL5) or DN-CUL2 lacks the C-terminal domain, leading to the inhibition of substrate degradation mediated by SOCS box proteins[170]. Previous studies have shown that the expression of DN-CUL5 prevents the degradation of feline A3 proteins by FIV Vif, whereas DN-CUL2 has no effect on A3 degradation[157].

To further investigate this in other feline Vif proteins, I co-expressed feline Vifs and feline A3Z3s along with either DN-CUL2 or DN-CUL5. Immunoblot results revealed that only DN-CUL5, but not DN-CUL2, inhibited CatA3Z3 degradation mediated by FIV Vif (Fig. 3.17A), consistent with previous reports. Similarly, only DN-CUL5, but not DN-CUL2, inhibited BobcatA3Z3 degradation mediated by PLVA Vif (Fig. 3.17B). In contrast, both DN-CUL2 and DN-CUL5 inhibited PumaA3Z3 degradation mediated by PLVB Vif (Fig. 3.17C).

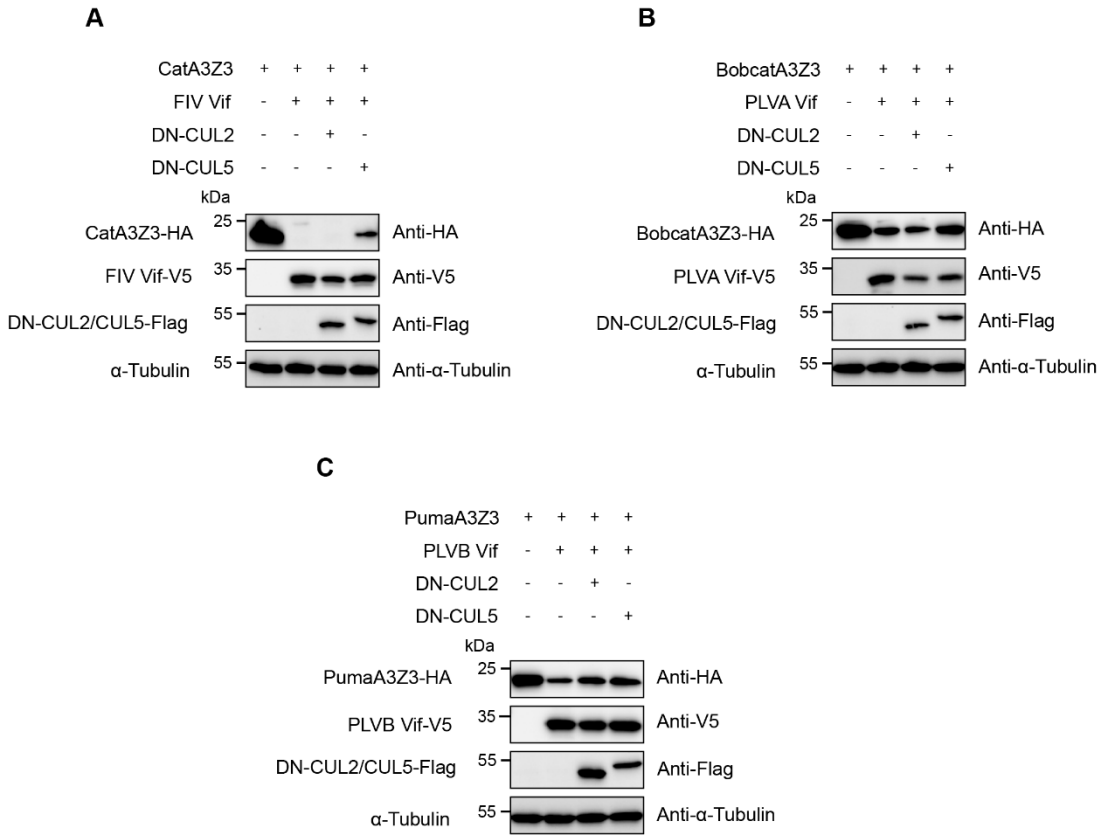

Fig. 3.17 DN-CUL2 and DN-CUL5 exhibit differential effects on the degradation of feline A3Z3 proteins by feline Vif proteins. (A), (B), (C) 293T cells were transfected with expression plasmids for CatA3Z3-HA, BobcatA3Z3-HA, or PumaA3Z3-HA, along with plasmids expressing either FIV Vif-V5, PLVA Vif-V5, or PLVB Vif-V5, and either DN-CUL2-Flag or DN-CUL5-Flag. pcDNA3.1 was used as a control plasmid in place of the feline Vif or DN-CUL2/5 expression plasmids. Forty-eight hours post-transfection, cell lysates were analyzed by immunoblotting with anti-HA, anti-V5, and anti-Flag antibodies. Tubulin was used as a loading control.

3.2.3 Identification of the 154IL155 region in PLVB Vif as critical for binding to both CUL2 and CUL5

The interaction interface of CUL5 is evolutionarily conserved across diverse HIV-1 and FIV Vif proteins[157]. In FIV Vif, a crucial hydrophobic region, 174IR175, is responsible for mediating CUL5 interaction, while in HIV-1 Vif, the corresponding region, 120IR121, facilitates this interaction[156, 157]. Mutation of the 174IR175 motif in FIV Vif disrupts its ability to induce degradation of feline A3 proteins[157]. By

comparing the PLVB Vif sequence to that of FIV Vif, I identified that the 154IL155 motif in PLVB Vif corresponds to the 174IR175 region in FIV Vif (Fig. 3.18A).

To investigate its functional significance, I generated a PLVB Vif mutant, 154IL155-AA, and assessed its activity in degrading PumaA3Z3. A3 degradation assays revealed that, in contrast to wild-type PLVB Vif, the 154IL155-AA mutant lost its ability to degrade PumaA3Z3 (Fig. 3.18B).

Next, to determine the role of the 154IL155 motif in CUL binding, I evaluated the interaction of the 154IL155-AA mutant with CUL2 and CUL5 via Co-IP assays. The results demonstrated that, compared to wild-type PLVB Vif, the 154IL155-AA mutant lost its capacity to bind both CUL2 and CUL5 (Fig. 3.18C). Collectively, these findings indicate that the conserved 154IL155 region in PLVB Vif is essential for binding to both CUL2 and CUL5.

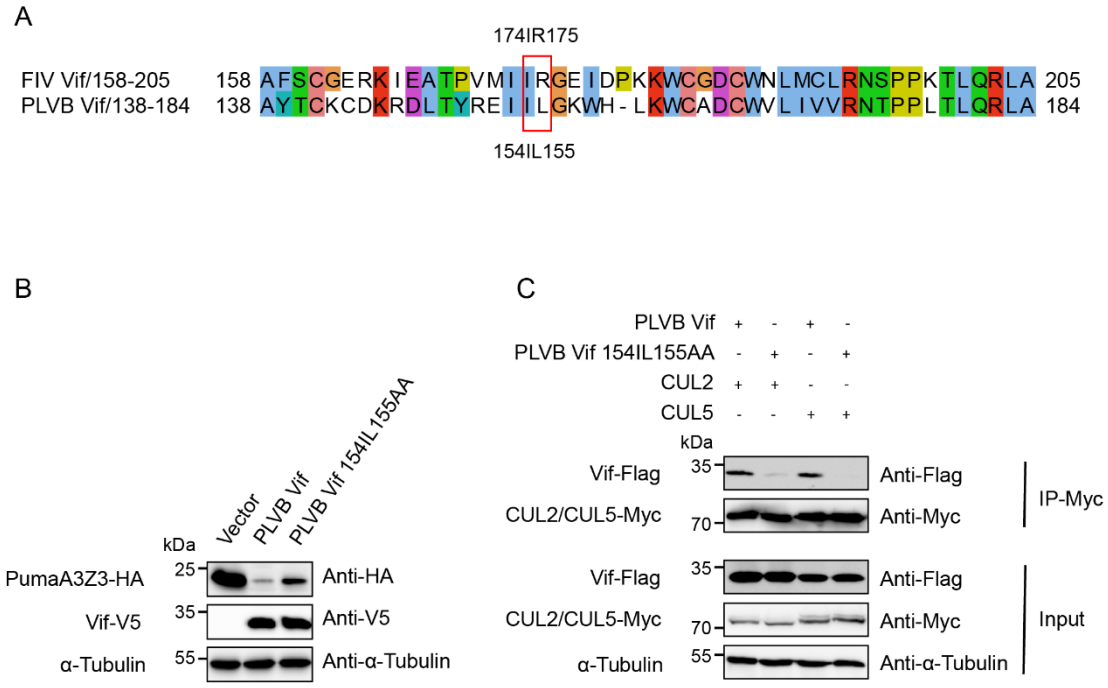

Fig. 3.18 The conserved 154IL155 region in PLVB Vif is essential for interaction to both CUL2 and CUL5. (A) Sequence alignment of the FIV and PLVB Vif proteins. The alignment illustrates the C-terminal regions of FIV and PLVB Vif proteins, with conserved residues highlighted based on their physicochemical properties using the Clustal color scheme. For further details, refer to materials and methods section 2.3.4. Residues 174IR175 in FIV Vif, corresponding to 154IL155 in PLVB Vif, are specifically emphasized. (B) 293T cells were transfected with expression plasmids for PumaA3Z3-

HA, along with plasmids expressing either wild-type PLVB Vif-V5 or the PLVB Vif 154IL155-AA mutant. pcDNA3.1(+) was used as a vector control. Forty-eight hours post-transfection, cell lysates were analyzed by immunoblotting using anti-HA and anti-V5 antibodies. Tubulin was used as a loading control. (C) 293T cells were co-transfected with expression plasmids for either wild-type PLVB Vif-Flag or the PLVB Vif 154IL155-AA mutant, together with either Myc-CUL2 or Myc-CUL5. Cell lysates were immunoprecipitated using anti-Myc magnetic beads and analyzed by immunoblotting with anti-Flag antibodies to detect Vif proteins and anti-Myc antibodies to detect CUL2/CUL5. Tubulin was used as a loading control for the input samples.

3.2.4 Identification of the 184IR185 region in PLVA Vif as critical for CUL5 interaction

The 174IR175 region in FIV Vif aligns with the 184IR185 region in PLVA Vif (Fig. 3.19A). To investigate its functional importance, I generated a PLVA Vif mutant (184IR185-AA) and assessed its ability to degrade BobcatA3Z3. Degradation assays revealed that, in contrast to wild-type PLVA Vif, the 184IR185-AA mutant lost the capacity to degrade BobcatA3Z3 (Fig. 3.19B).

To further elucidate the role of the 184IR185 motif in CUL5 binding, I conducted Co-IP assays to evaluate the binding activity of the 184IR185-AA mutant with CUL5. The results demonstrated that, compared to wild-type PLVA Vif, the 184IR185-AA mutant exhibited a loss of binding to CUL5 (Fig. 3.19C). These findings collectively underscore the importance of the conserved 184IR185 region in PLVA Vif for CUL5 binding.

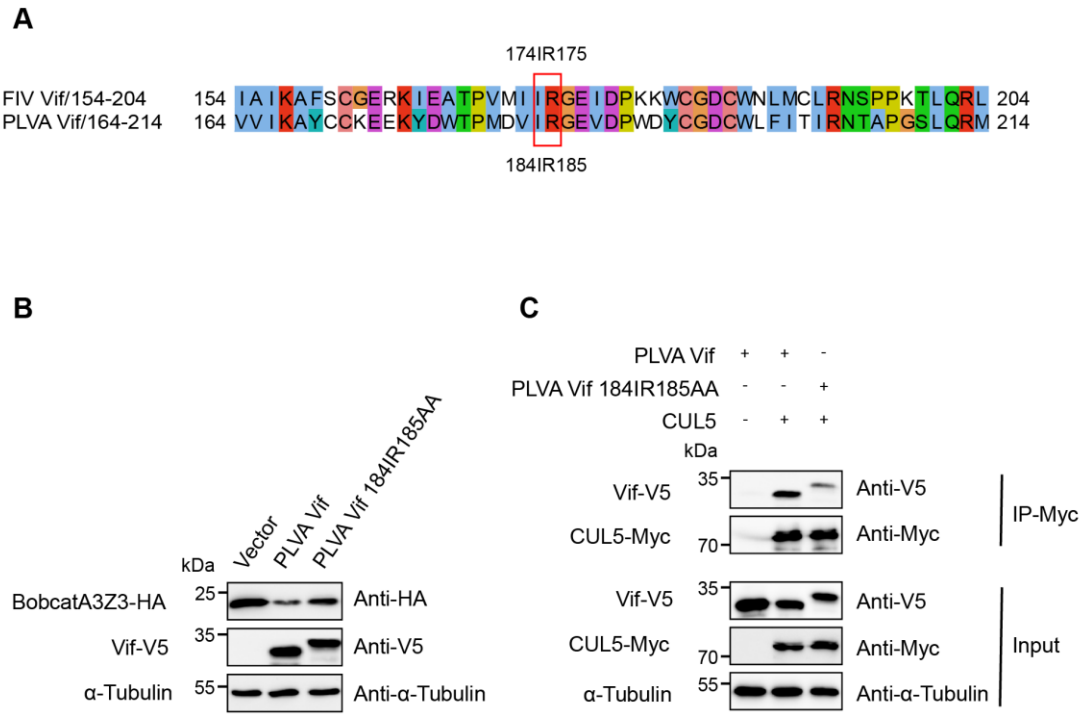

Figure 3.19 The conserved 184IR185 region in PLVA Vif is critical for CUL5 binding. (A) Sequence alignment of the FIV and PLVA Vif proteins. The alignment illustrates the C-terminal regions of FIV and PLVA Vif proteins, with conserved residues highlighted based on their physicochemical properties using the Clustal color scheme. For further details, refer to materials and methods section 2.3.4. Residues 174IR175 in FIV Vif, corresponding to 184IR185 in PLVA Vif, are specifically emphasized. (B) 293T cells were transfected with expression plasmids encoding BobcatA3Z3-HA, along with either wild-type PLVA Vif-V5 or the 184IR185-AA mutant. A pcDNA3.1(+) vector was used as a control. Forty-eight hours post-transfection, cell lysates were subjected to immunoblot analysis using anti-HA and anti-V5 antibodies, with tubulin serving as a loading control. (C) 293T cells were co-transfected with expression plasmids encoding either wild-type PLVA Vif-V5 or the 184IR185-AA mutant, along with Myc-tagged CUL5. Cell lysates were immunoprecipitated using anti-Myc magnetic beads, followed by immunoblot analysis with anti-V5 and anti-Myc antibodies to detect Vif and CUL5 proteins, respectively. Tubulin was used as a loading control in the input samples.

3.2.5 Investigation of the interaction of Vif proteins with CULs

PLVB Vif interacts with both CUL2 and CUL5; however, whether Vif proteins

interact with other CUL members is unknown. To investigate this, I tested the interactions of various Vif proteins with CUL1, -2, -3, -4A, -4B, and -5. Co-IP assays were performed using lysates from 293T cells co-transfected with expression plasmids encoding Vif-Flag and Myc-tagged CUL1, CUL2, CUL3, CUL4A, CUL4B, or CUL5.

The Co-IP results showed the following interactions between the Vif proteins and the six tested CUL proteins: FIV Vif interacts with CUL1 and CUL5, with very slight interaction with CUL4A and CUL4B (Fig. 3.20A). PLVA Vif complexes with CUL1 and CUL5 and shows slight precipitation of CUL2, CUL4A, and CUL4B (Fig. 3.20B). PLVB Vif interacts with CUL1, CUL2, and CUL5, with slightly with CUL4A and CUL4B (Fig. 3.16E, Fig. 3.20C). HIV-2 Vif complexes with CUL1 and CUL5, with slightly with CUL4A and CUL4B (Fig. 3.20D). For HIV-1 and SIV Vif, I focused on their binding interactions with CUL1, CUL2, and CUL5. Co-IP results indicated that HIV-1 Vif forms complexes with CUL1 and CUL5 (Fig. 3.20E), and similarly, $SIV_{gorilla}$ Vif also complexes with CUL1 and CUL5 (Fig. 3.20F). In summary, all Vif proteins tested likely bind to CUL1 and CUL5, with slight or very slight interaction to CUL4A and CUL4B. Among these, PLVB Vif is the only Vif protein confirmed to complex with CUL2.

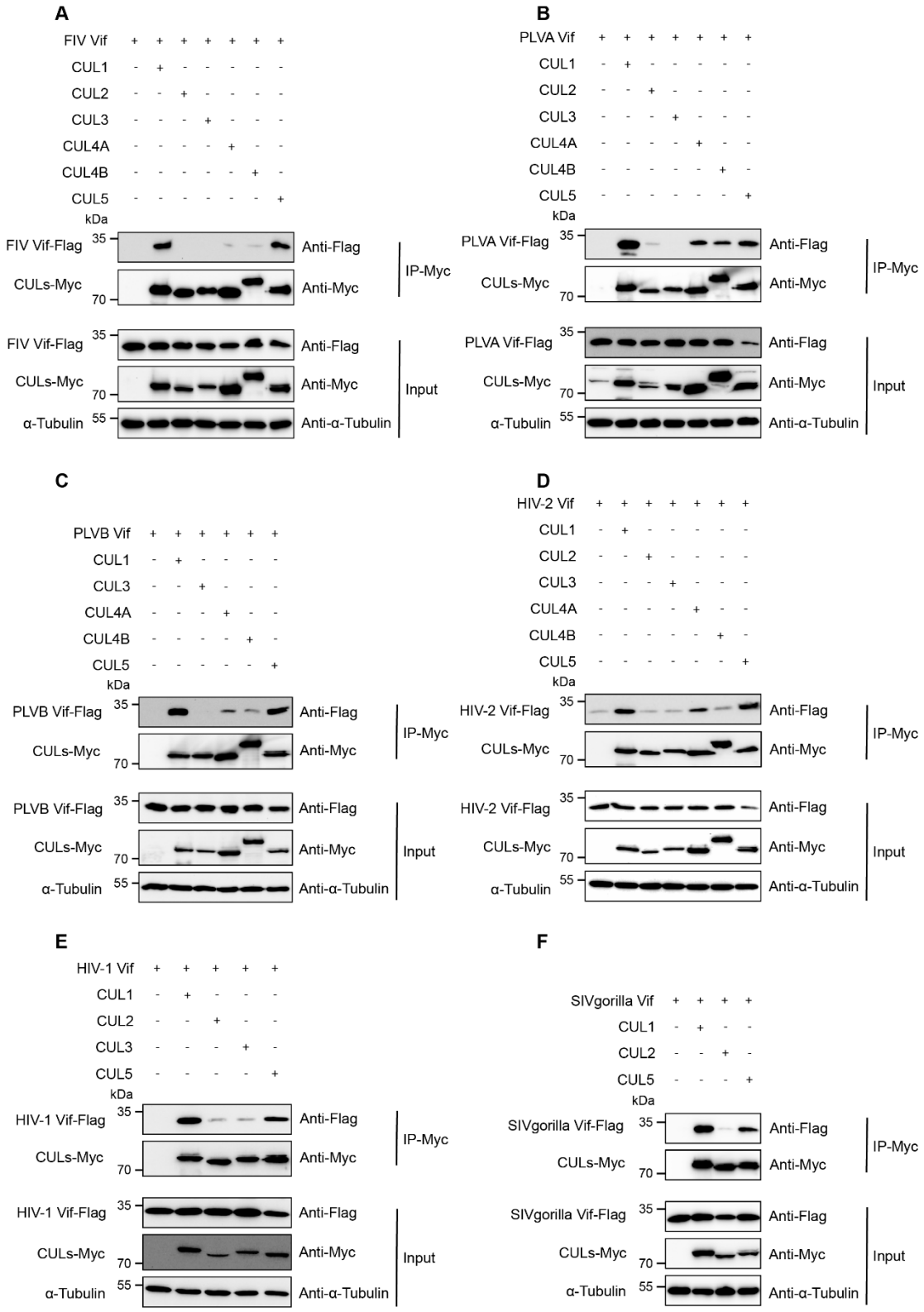

Fig. 3.20 Investigation of the interaction of Vif Proteins with CULs. (A)–(F) Expression plasmids for FIV Vif-Flag, PLVA Vif-Flag, PLVB Vif-Flag, HIV-2 Vif-Flag, HIV-1 Vif-Flag or SIVgorilla Vif-Flag were co-transfected with plasmids encoding Myc-tagged CUL1, CUL2, CUL3, CUL4A, CUL4B, or CUL5 in 293T cells. Cell lysates were immunoprecipitated using anti-Myc magnetic beads and

analyzed by immunoblotting with anti-Flag antibodies to detect Vif proteins, and anti-Myc antibodies to detect CUL proteins. Tubulin was used as a loading control for the input samples.

3.2.6 CUL1 binds to untagged Vif proteins derived from different HIV-1 strains

All tested Vif proteins complex CUL1 using the Flag tag (Fig. 3.20). To rule out the potential influence of the Flag tag on CUL1 binding, I used several untagged Vif proteins derived from HIV-1 strains to investigate the Vif–CUL1 interaction. Co-IP assays were performed using lysates from 293T cells co-transfected with expression plasmids encoding Myc-tagged CUL1 and untagged Vif from the NL4-3, LAI, F-1, or N-116 HIV-1 strains. The Co-IP results demonstrated that all untagged HIV-1 Vif strains tested interact with CUL1 (Fig. 3.21).

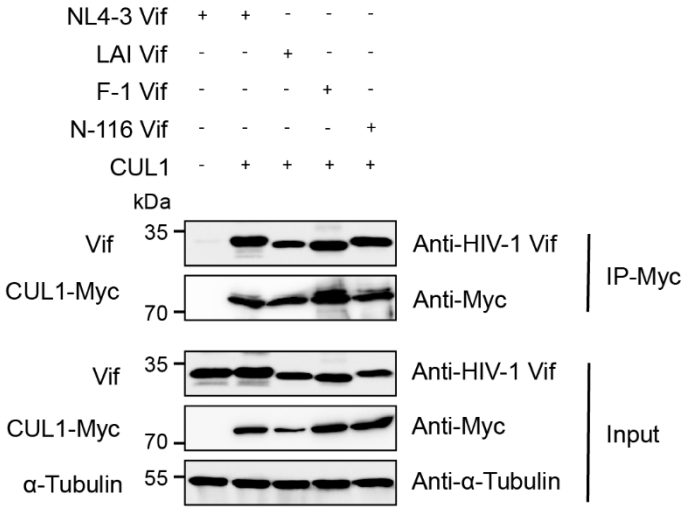

Fig. 3.21 CUL1 binds to untagged Vif proteins derived from different HIV-1 strains. 293T cells were co-transfected with expression plasmids encoding Myc-tagged CUL1 and untagged HIV-1 Vif expression plasmids derived from the NL4-3, LAI, F-1, or N-116 strains. Cell lysates were immunoprecipitated using anti-Myc magnetic beads and analyzed by immunoblotting with anti-HIV-1 Vif antibodies to detect Vif proteins, and anti-Myc antibodies to detect CUL1. Tubulin was used as a loading control for the input samples.

3.2.7 HIV-1 and PLVB Vif bind to small amounts of endogenous CUL1

CUL1 interacts with the adaptor protein SKP1, forming a core component of the SCF (SKP1–CUL1–F-box) complex, which subsequently targets substrates for

ubiquitination via an F-box protein substrate receptor[171]. To further investigate whether Vif proteins interact with endogenous CUL1, SKP1 was used as a positive control. First, Co-IP assays of CUL1, CUL2, and CUL5 with SKP1 confirmed that SKP1 binds specifically to CUL1, but not to CUL2 or CUL5 (Fig. 3.22A). Next, Co-IP assays were performed using lysates from 293T cells transfected with expression plasmids encoding Flag-tagged SKP1, HIV-1, or PLVB Vif. The Co-IP results demonstrated that SKP1 binds to endogenous CUL1 in 293T cells, and that HIV-1 and PLVB Vif bind to small amounts of endogenous CUL1 in these cells (Fig. 3.22B).

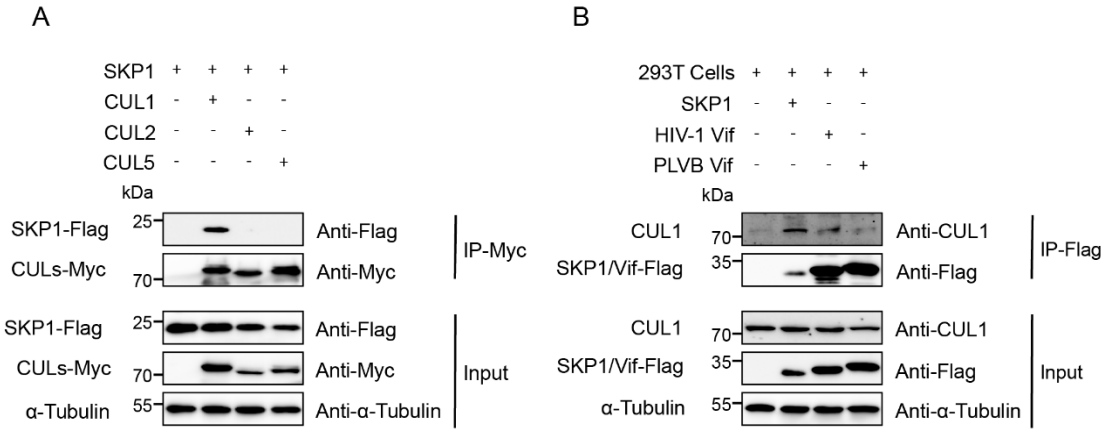

Fig. 3.22 HIV-1 and PLVB Vif interact with small amounts of endogenous CUL1. (A) Expression plasmids for SKP1-Flag were co-transfected with Myc-tagged CUL1, CUL2, or CUL5 plasmids in 293T cells. Cell lysates were immunoprecipitated using anti-Myc magnetic beads and analyzed by immunoblotting with anti-Flag antibodies to detect SKP1, and anti-Myc antibodies to detect the CUL proteins. Tubulin was used as a loading control for the input samples. (B) 293T cells were transfected with expression plasmids encoding Flag-tagged SKP1, HIV-1, or PLVB Vif. Cell lysates were immunoprecipitated using anti-Flag magnetic beads and analyzed by immunoblotting with anti-Flag antibodies to detect SKP1 and Vif proteins, and anti-Cullin 1 antibodies to detect endogenous CUL1. Tubulin was used as a loading control for the input samples.

3.2.8 DN-CUL1 has no effect on Vif-mediated degradation of A3 proteins

CUL1 interaction with Vif proteins has been found here, but it remains to be determined whether CUL1 plays a role in Vif-induced degradation of A3 proteins.

Dominant-negative CUL1 (DN-CUL1) carries a C-terminal truncation that disrupts its interaction with RBX and the E2 ubiquitin-conjugating enzyme. However, DN-CUL1 retains the ability to interact with substrates via SKP1 and F-box proteins[170](Fig. 2.23B). To investigate whether CUL1 is involved in Vif-mediated A3 degradation, Vif and A3 expression plasmids were co-transfected along with either DN-CUL1, DN-CUL5 or DN-CUL2. Immunoblotting results revealed that, in contrast to DN-CUL5, DN-CUL1 failed to inhibit the degradation of catA3Z3 by FIV Vif (Fig. 3.23C), pumaA3Z3 by PLVB Vif (Fig. 3.23D), humanA3C by HIV-1 Vif (Fig. 3.23E) and humanA3C by HIV-2 Vif (Fig. 3.23F). These results demonstrate that DN-CUL1 does not affect the degradation of A3 proteins by the tested Vif proteins.

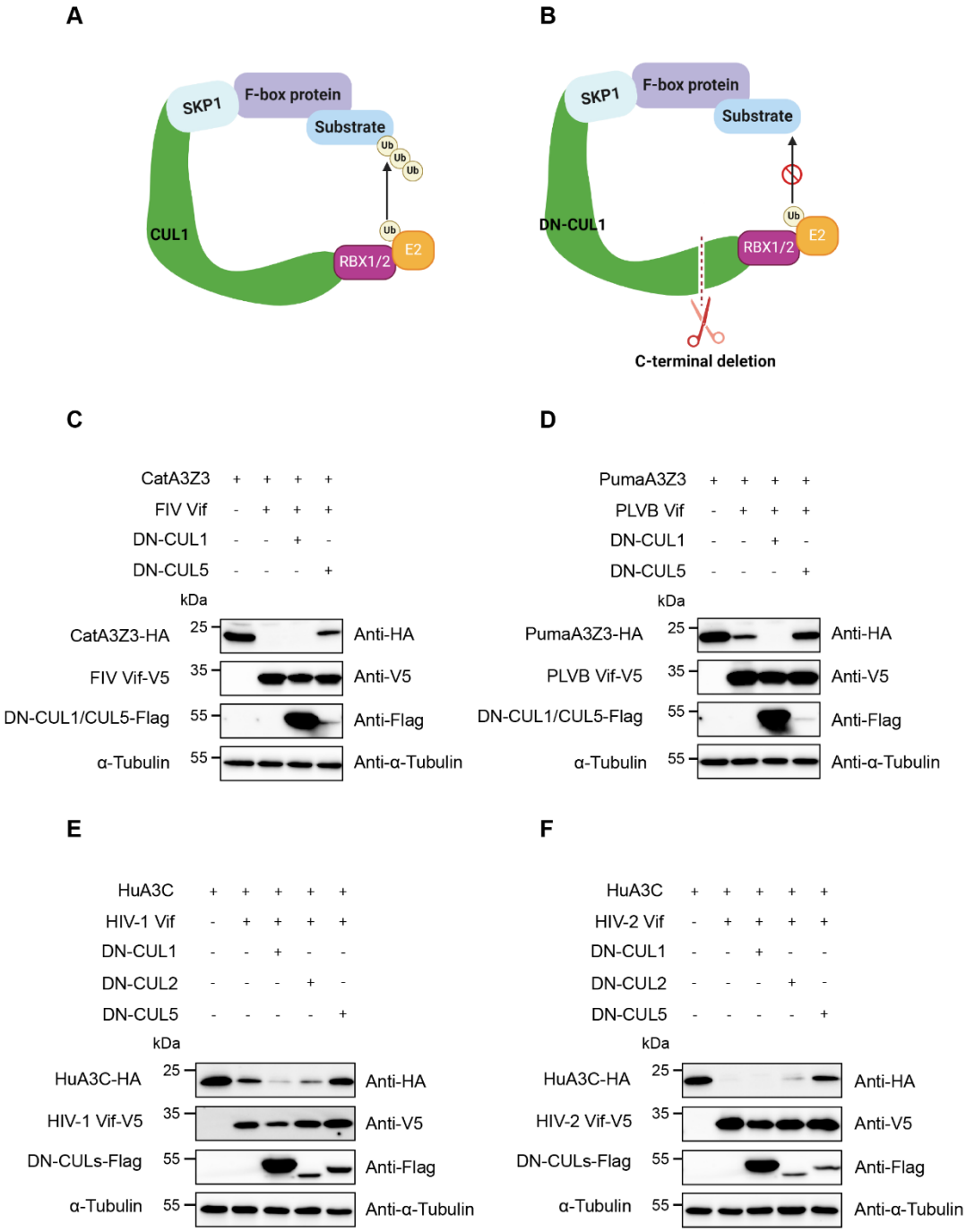

Fig. 3.23 DN-CUL1 has no effect on Vif-mediated degradation of A3 proteins. (A)Schematic representation of the CUL1–SKP1–F-box complex. (B) Schematic representation of the DN-CUL1–SKP1–F-box complex. (C)–(F) 293T cells were co-transfected with expression plasmids for CatA3Z3-HA, PumaA3Z3-HA, or HuA3C-HA along with plasmids expressing either FIV Vif-V5, PLVB Vif-V5, HIV-1 Vif-V5 or HIV-2 Vif-V5, and either DN-CUL1-Flag, DN-CUL5-Flag or DN-CUL2-Flag. pcDNA3.1 was used as a control plasmid in place of the Vif or DN-CULs expression plasmids. 48 hours post-transfection, cell lysates were analyzed by immunoblotting with anti-HA, anti-V5, and anti-Flag antibodies. Tubulin was used as a loading control. Fig. 3.23A was adapted from: Chen, Z.

Sui, J. Zhang, F. Zhang, C. (2015). Cullin family proteins and tumorigenesis: Genetic association and molecular mechanisms. Journal of Cancer, 6(3), 233–242[133]. Licensed under CC BY-NC 4.0 (https://creativecommons.org/licenses/by/4.0/). Reproduced with BioRender.com. Fig. 3.23B was created with BioRender.com.

3.2.9 PLVB Vif recruits both CUL2 and CUL5 to form E3 complexes for A3 degradation

Using DN-CUL5 as the bait protein for Co-IP has been demonstrated as an effective method for studying the Vif–A3 interaction, as shown in Fig. 3.5D, 3.9B, 3.11C, 3.13C and 3.14C. To investigate whether DN-CUL1 and DN-CUL2, like DN-CUL5, can capture the Vif–A3 complex and confirm their involvement in Vif-induced A3 degradation, Co-IP assays were performed. PumaA3Z3 was co-transfected with PLVB Vif, along with either DN-CUL1, DN-CUL2, or DN-CUL5. The Co-IP results showed that both DN-CUL2 and DN-CUL5 interact with PLVB Vif, whereas DN-CUL1 captured only a small amount of PLVB Vif (Fig. 3.24). Furthermore, PumaA3Z3 was detected in both the DN-CUL2–PLVB Vif and DN-CUL5–PLVB Vif immunoprecipitated complexes, but not in the DN-CUL1–PLVB Vif complex (Fig. 3.24). These findings, along with the results from Fig. 3.17C and Fig. 3.18B, C, indicate that PLVB Vif recruits both CUL2 and CUL5 to form E3 complexes responsible for A3 degradation. Regarding CUL1, the current results suggest that, compared to DN-CUL2 and DN-CUL5, DN-CUL1 captured only a small amount of PLVB Vif. Combined with the data from Fig. 3.23D, this implies that either CUL1 needs other proteins that bind the deleted domain to form a stable complex with Vif, or that the deleted C-terminal region in DN-CUL1 may serve as a binding site for PLVB Vif. To clarify whether CUL1 is involved in PLVB Vif-induced A3 degradation, future experiments should focus on identifying the binding sites between PLVB Vif and CUL1 before conducting further investigations.

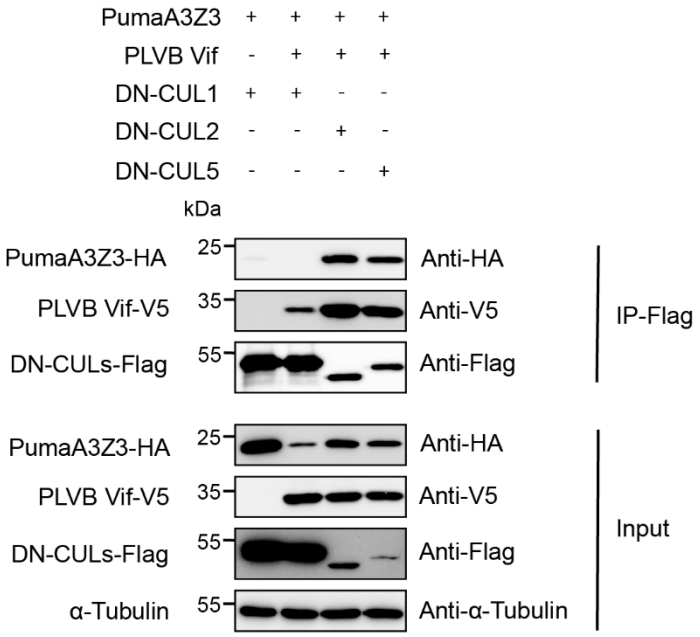

Fig. 3.24 PumaA3Z3 was detected in both the DN-CUL2-PLVB Vif and DN-CUL5-PLVB Vif immunoprecipitated complexes, but not in the DN-CUL1-PLVB Vif complex. 293T cells were co-transfected with plasmids expressing PumaA3Z3-HA and PLVB Vif-V5, along with either DN-CUL1-Flag, DN-CUL2-Flag, or DN-CUL5-Flag. Cell lysates were immunoprecipitated using anti-Flag magnetic beads and analyzed by immunoblotting with anti-Flag antibodies to detect DN-CULs, anti-V5 antibodies to detect PLVB Vif, and anti-HA antibodies to detect PumaA3Z3. Tubulin was used as a loading control for the input samples.

3.2.10 154IL155 region in PLVB Vif is not critical for CUL1 interaction

The 154IL155 region in PLVB Vif has been shown to be critical for interaction to both CUL2 and CUL5 (Fig. 3.18C). To determine whether this region is also essential for CUL1 interaction, Co-IP assays were performed using wild-type PLVB Vif or the 154IL155-AA mutant, with either CUL1 or CUL5. The results revealed that, compared to wild-type PLVB Vif, the 154IL155-AA mutant lost its ability to interact with CUL5 but retained this capacity with CUL1 (Fig. 3.25). These findings indicate that the 154IL155 region in PLVB Vif is not critical for CUL1 binding.

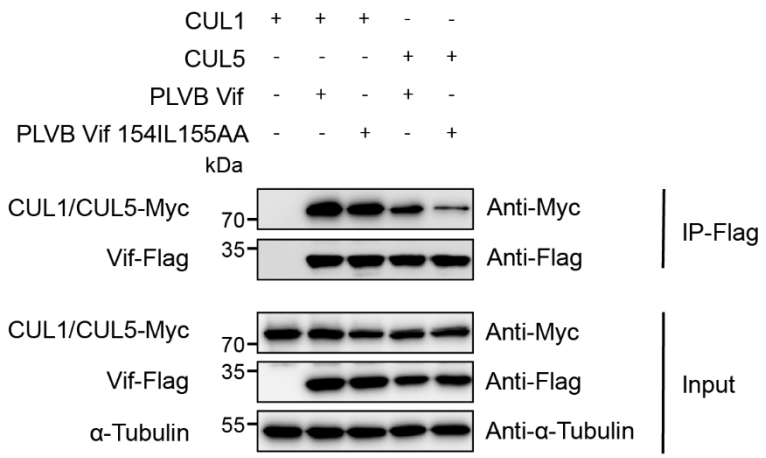

Fig. 3.25 154IL155 region in PLVB Vif is not critical for CUL1 interaction. 293T cells were co-transfected with expression plasmids for either wild-type PLVB Vif-Flag or the PLVB Vif 154IL155-AA mutant, together with either Myc-CUL1 or Myc-CUL5. Cell lysates were immunoprecipitated using anti-Flag magnetic beads and analyzed by immunoblotting with anti-Flag antibodies to detect Vif proteins and anti-Myc antibodies to detect CUL1/CUL5. Tubulin was used as a loading control for the input samples.

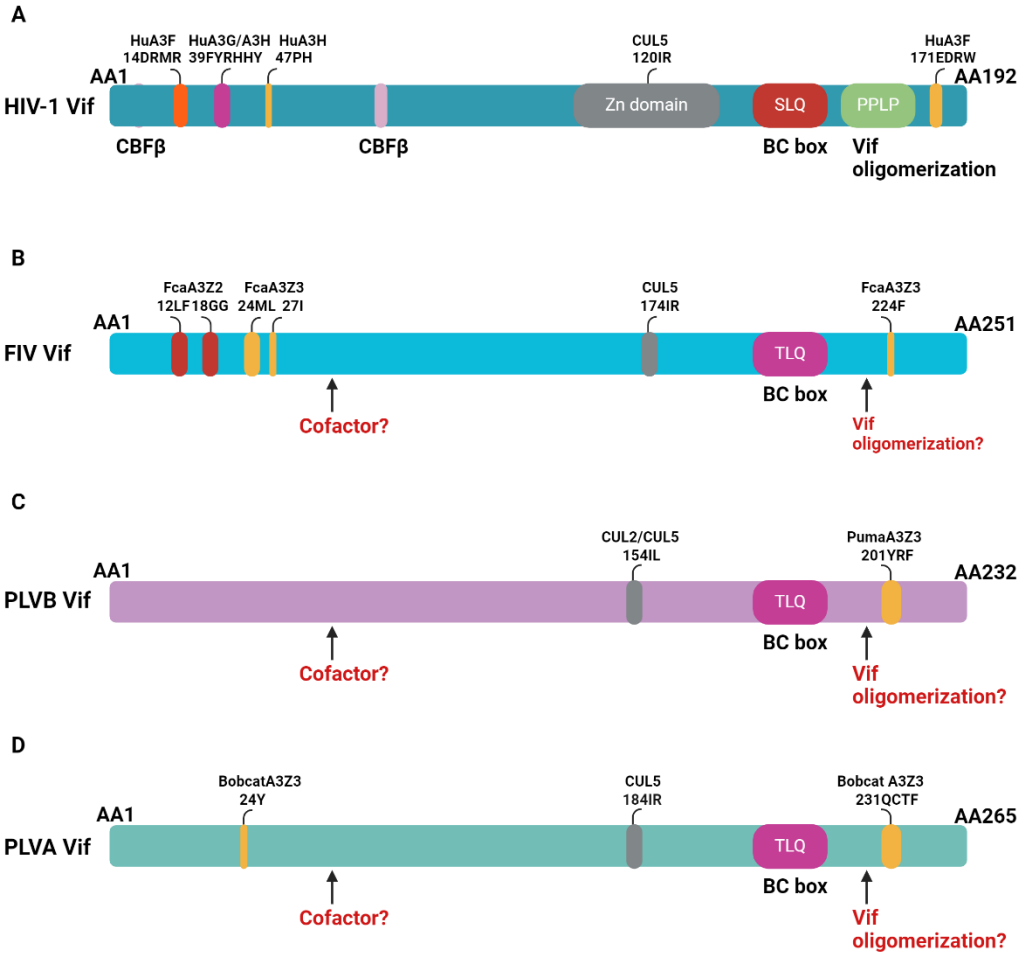

Fig. 3.26 Summary of Vif-A3 and Vif-CUL Interactions. Panels (A), (B), (C), and (D) illustrate the interactions of HIV-1, FIV, PLVB, and PLVA Vif proteins, respectively, with A3 and CUL proteins. Fig. 3.26A, B were adapted from: Zhang ZL, Gu QY, Marino D, Lee KL, Kong IK, Häussinger D, et al. Feline APOBEC3s, Barriers to Cross-Species Transmission of FIV? Viruses. 2018; 10(4)[65]. Published under the Creative Commons Attribution 4.0 International License (https://creativecommons.org/licenses/by/4.0/). Reproduced with BioRender.com. Fig. 3.26C, D were created with BioRender.com.

4. Discussion

4.1 The interaction between feline lentiviral Vif and feline A3 proteins

4.1.1 Feline lentiviral Vif proteins degrade their respective A3 proteins and can also cross species barriers to degrade A3 proteins from other feline species

Previous research has shown that primate lentiviral Vif proteins similarly degrade their own A3 proteins and are capable of cross-species degradation of some A3 proteins from some other primate species. In general, Vif can only degrade the A3 proteins of it viral host species, with some rare exceptions. For example, HIV-2 Vif efficiently degrades both huA3G and A3G proteins from African green monkeys (agmA3G) and sooty mangabey monkeys (smmA3G). SIVsmm Vif effectively degrades smmA3G, and demonstrates efficient degradation of huA3G and agmA3G[172]. One study further reported that HIV-2, SIVsmm, and SIVmac Vif proteins can even cross species to degrade feline CatA3Z3Z3[136]. In this study, I performed A3 degradation assays using Vif proteins and A3 proteins from both domestic cats and wild felids. The results showed that FIV Vif is capable of degrading domestic cat A3Z2, A3Z3, and A3Z2Z3, as well as the corresponding A3 proteins (A3Z2, A3Z3, and A3Z2Z3) from wild felids (bobcat and puma) (Fig. 3.1B, C, D). Additionally, Vif proteins from wild felids FIVs (PLVA and PLVB) were able to degrade both their own A3 proteins and those of domestic cats, specifically A3Z2, A3Z3, and A3Z2Z3 (Fig. 3.1B, C, D). These results demonstrated that Vif proteins

from lentiviruses of both domestic cats and wild felids degrade not only their own A3 proteins but also those of other feline species, like primate lentiviral Vif proteins. This finding provides a potential explanation for the rare cross-species transmission of feline lentiviruses among different feline species.

4.1.2 Identification of PLV1695 Vif specifically unable to degrade feline A3Z3

In this study, I identified a strain of PLVB Vif, named PLV1695 Vif, which is unable to degrade feline A3Z3 proteins but can degrade feline A3Z2 and A3Z2Z3 proteins (Fig. 3.1B, C, D). This finding aligns with a previous study that demonstrated the inability of PLV1695 Vif to counteract puma A3Z3[167]. PLV1695 is a prototypic infectious molecular clone of PLVB, which resulted from several passages in domestic cat[168]. It would be significant to assess the counteraction activity of the PLVB Vif variants that are currently circulating in wild pumas towards Feline A3Z3s. The differential ability of the PLVB Vif to degrade the restriction factor felineA3Z3 compared to the PLV1695 Vif holds significant implications for virus research. This finding suggests that the specific subtype of the PLVB virus, such as PLV1695, may have acquired a mutation or modification that affects its capacity to target and degrade felineA3Z3. Investigating the underlying mechanisms behind this difference could shed light on the interplay between viral proteins and host factors, providing valuable insights into viral evasion strategies and host-virus interactions. Additionally, investigating the underlying mechanisms may contribute to the development of targeted antiviral therapies or strategies to enhance host defense mechanisms against viral infections.

4.1.3 The antiviral activity of feline A3Z3 proteins against wild felid FIV

Previous research has primarily focused on the antiviral activity of feline A3 proteins against FIV in domestic cats[134, 136, 154]. In this study, I extended the analysis to include luciferase reporter viruses for FIV from wild felids. The *gag* gene from PLVA and the *gag* and *pol* genes from PLVB were cloned into packaging

constructs. The resulting luciferase activity confirmed that these viruses were suitable for the experiments (Fig. 3.2).

Infection assays showed that all tested feline A3Z3 proteins effectively inhibited ΔVif FIV, ΔVif PLVA, and ΔVif PLVB (Fig. 3.3 A, C, E). In contrast, the Vif proteins from FIV, PLVA, and PLVB were able to counteract the restriction mediated by feline A3Z3 (Fig. 3.3 B, D, F). Notably, infection assays confirmed that PLV1695 Vif failed to counteract the restriction mediated by these feline A3Z3 proteins (Fig. 3.4). These findings suggest that feline A3Z3 proteins serve as a barrier to cross-species transmission of FIV, likely contributing to the long-term co-evolution between FIVs and their host species. Furthermore, the arms race between feline A3 proteins and Vif proteins remains ongoing.

4.1.4 Established a novel experimental approach to investigate Vif-A3 interaction

To assess Vif-A3 binding, previous research employed Co-IP assays using the Vif SLQ/AAA mutant with A3 proteins[144]. The Vif SLQ/AAA mutant binds A3s without inducing their degradation; however, this method is primarily suited for testing the binding of Vif to A3 mutants, as wild-type Vif may degrade the A3 proteins being tested. Another approach involves using Vif-GST fusion proteins in GST pull-down assays to examine Vif-A3 binding[154]. However, the large molecular weight of GST may alter the conformation and function of Vif, potentially affecting the accuracy of the binding assay.

To address these limitations, this study established a novel experimental approach for testing Vif-A3 binding by using DN-CUL5 as a bait protein. DN-CUL5 contains a C-terminal deletion that prevents its binding to RBX2, thus inhibiting ubiquitination and proteasomal degradation of substrates. However, it retains the capacity to bind Vif, making it suitable as a bait protein to investigate the Vif-A3 binding complex without the need for proteasome inhibitors to block Vif-mediated degradation of A3. Co-IP results demonstrate that this method is effective for

investigating Vif-A3 binding (Fig. 3.5D, 3.9B, 3.11C, 3.13C and 3.14C), and it offers a valuable tool for future studies on Vif-A3 interactions.

4.1.5 Identification of residue 201 in PLV1695 Vif as responsible for its inability to counteract A3Z3 restriction

To counteract A3 restriction, Vif proteins bind to A3 proteins and recruit them to an E3 ubiquitin ligase complex, leading to the polyubiquitination and subsequent proteasomal degradation of A3 proteins[132, 169]. The binding of Vif to A3 proteins is therefore critical for the virus to evade host restriction. PLV1695 Vif was specifically identified as being unable to bind to A3Z3 (Fig. 3.5A, D), while retaining its ability to degrade both feline A3Z2 and A3Z2Z3 proteins (Fig. 3.1B, D). Chimeric experiments demonstrated that the C-terminal residues of Vif (positions 193-207) are crucial for PLVB Vif-mediated degradation of PumaA3Z3 (Fig. 3.6A, B, C). Mutation studies further identified residue 201 in Vif as a key determinant of the differential antagonism exerted by PLVB and PLV1695 Vif against PumaA3Z3 (Fig. 3.7A-E). Co-IP results confirmed that a single amino acid substitution, H201Y, confers PLV1695 Vif the ability to bind to A3Z3 (Fig. 3.9A, B). Conversely, the corresponding Y201H mutation in PLVB Vif abolishes its capacity to bind A3Z3 (Fig. 3.9A, B). The PLVB Vif-PumaA3Z3 and PLV1695 Vif-PumaA3Z3 complexes, predicted using the AlphaFold server, highlight residue 201 in PLVB and PLV1695 Vif as a key interaction site. These findings further corroborate the Co-IP results shown in Fig. 3.9A and Fig. 3.9B. Given that PLV1695 is a prototypic infectious molecular clone of PLVB, resulting from multiple passages in domestic cats[168], it is possible that cross-species restriction factors drove this mutation. This further supports the notion that the arms race between feline A3 proteins and Vif proteins is ongoing. The identification of this Vif residue (201) has significant implications for understanding the interaction between lentiviruses and host restriction factors.

4.1.6 The PLVB Vif 201YRF203 motif and its corresponding motifs in FIV,

PLVA, and HIV-1 Vif are responsible for A3 degradation and interaction

The 201YRF203 motif in PLVB Vif was identified as responsible for PumaA3Z3 degradation (Fig. 3.10A), with Co-IP results further confirming the 201YRF203 motif as the binding region for PumaA3Z3 (Fig. 3.10B). Similarly, analogous motifs or residues in FIV Vif (residue 224F) (Fig. 3.12A-D) and PLVA Vif (231QCTF224) (Fig. 3.13A-C) were found to be critical for the degradation and interaction with feline A3Z3. The corresponding motif in HIV-1 Vif, 171EDRW174, has been identified as the A3F binding region and is crucial for HIV-1 Vif-induced A3F degradation[152]. Furthermore, 171EDRW174 in HIV-1 Vif also plays a role in the degradation of A3C and A3G (Fig. 3.15A-C).

These findings suggest that despite the long evolutionary arms race between lentiviruses and their hosts, the 201YRF203 motif in different lentiviral Vifs has retained its function in A3 degradation and interaction. Given the conservation of this motif across various Vif proteins, it represents a potential target for the development of novel anti-HIV or anti-lentiviral therapeutics.

4.1.7 Differential degradation and interaction of A3Z3 by the N- and C-terminal regions of PLVB Vif compared to other feline Vif proteins

Previous research has established that the N-terminal residues of FIV Vif, specifically 24ML25 and 27I, interact with CatA3Z3[154]. In this study, the C-terminal residue F224 of FIV Vif was also identified as responsible for CatA3Z3 degradation and interaction (Fig. 3.12A-D). Similarly, the C-terminal motif of PLVA Vif, 231QCTF224 (Fig. 3.13A-C), along with the N-terminal residue 24Y (Fig. 3.14A-C), were found to be critical for degradation and interaction with Bobcat A3Z3. In contrast, for PLVB Vif, the C-terminal motif 201YRF203 was shown to be responsible for PumaA3Z3 degradation (Fig. 3.10A) and interaction (Fig. 3.10B), whereas the N-terminal residues corresponding to and adjacent to FIV Vif 24ML25 and 27I did not bind PumaA3Z3 (Fig. 3.11A-C). Notably, residues 24M, 25L, and 27I of Vif are conserved across several FIV lineages, including those from both

domestic and nondomestic cats, except for PLVB Vif[154] (Fig. 4.1). PLVB Vif differs markedly from Vifs of other FIV strains[154]. Studies have reported that PLVB exhibits high genetic diversity, with multiple strains circulating within puma populations[47, 58, 173]. Specifically, the N-terminal region of PLVB Vif contains two deletions[154]. While PLVB can infect domestic cats, these infections are frequently abortive[174-176], indicating an immune defense mechanism in domestic cats, possibly involving A3 proteins. Increased A3-mediated G-to-A hypermutations were observed in the viral genomes of PLVB during infections in domestic cats[168]. Taken together, these findings indicate that the divergent roles of the N- and C-terminal regions in feline lentiviral Vif proteins reflect an adaptation to the unique A3 proteins of each feline host. This differential targeting of Vif regions underscores the evolutionary pressure exerted by host-specific restriction factors, shaping the structure and function of Vif in a host-adapted manner. Additionally, the absence of N-terminal binding ability in PLVB Vif, likely due to N-terminal deletions, may limit its capacity for cross-species transmission by restricting its interaction with A3 proteins beyond its primary host species.

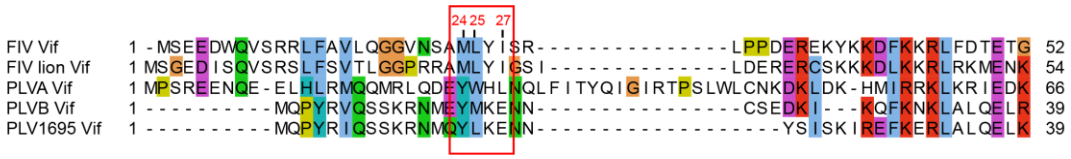

Fig. 4.1 Sequence alignment of feline Vif proteins. The alignment presents the N-terminal regions of feline Vif proteins, with conserved residues highlighted according to their physicochemical properties using the Clustal color scheme. For further details, refer to materials and methods section 2.3.4. Residues 24ML25 and 27I in FIV Vif, as well as their corresponding positions in FIV lion, PLVA, PLVB, and PLV1695 Vif, are emphasized.

4.1.8 Modeling of feline lentiviral Vif-feline A3Z3 complexes

In this study, the structures of the feline lentiviral Vif-feline A3Z3 complexes were predicted using the AlphaFold server. The resulting models were analyzed in PyMOL to visualize the structures and identify key interaction residues. These structural models align well with the observed A3 degradation patterns and Vif-A3

Co-IP results, as shown in Fig. 3.9A-D, Fig. 3.10A-C, and Fig. 3.14B-D.

The experiments for A3 degradation assays, Vif-A3 Co-IP, and prediction of Vif-A3 complexes were conducted independently. The consistency and mutual validation of the results across these methods further enhance the reliability of this study and demonstrate the robustness of the research approach.

Moreover, this integrated methodology highlights the scientific validity of combining structural prediction with experimental validation, offering a valuable tool for future investigations into Vif-A3 interactions. This approach provides new insights into the mechanisms of Vif-A3 interactions and lays a foundation for developing targeted therapeutic strategies.

4.2 The interaction between Vif and CUL proteins

To ensure efficient replication, lentiviruses counteract specific cellular restriction factors by hijacking the CUL-E3 ubiquitin ligase complex, thereby targeting these factors for proteasomal degradation. CUL proteins act as scaffolding components for modular, multi-subunit E3 ubiquitin ligase complexes. In HIV-1, three accessory proteins — Vif, Vpu, and Vpr — adapt CUL-E3 ubiquitin ligase complexes to counteract host antiviral responses. Specifically, Vif recruits the CUL5 E3 ligase complex and binds to A3 proteins to induce their polyubiquitination and degradation. Vpu interacts with the CUL1 ubiquitin ligase complex via β-TrCP and targets BST-2 or CD4 for ubiquitination and mis-localization. Vpr, in turn, engages with the CUL4A/DCAF1/DDB1/Rbx1 E3 ubiquitin ligase complex and binds to UNG2, leading to its polyubiquitination and degradation[141] (Fig. 4.2). Like HIV-1 Vif, FIV Vif forms a CUL5 E3 ligase complex that targets feline A3 proteins for degradation[137, 139]. Previous research has confirmed that FIV Vif specifically binds to CUL5, but not CUL2, and that a conserved interface for CUL5 interaction exists between HIV-1 and FIV Vif proteins[157]. However, it remains unclear whether other wild feline Vif proteins, such as PLVA or PLVB Vif, recruit the CUL5 E3 ligase or interact with other CUL proteins, necessitating further investigation.

The CUL family of proteins is evolutionarily conserved across mammals[129]. A comparison of the amino acid sequences of CUL proteins between humans and felines reveals a high degree of conservation (Table 4.1). Human and domestic cat CUL5 differ by only a single amino acid, and this variation does not appear to impact the protein's interaction with FIV Vif[137]. Additionally, it has been demonstrated that FIV Vif can induce the degradation of CatA3s in both feline kidney CRFK and human HEK293T cells, further confirming the ability of FIV Vif to interact with both human and feline CUL5 proteins[137, 154]. Consequently, in this study, human CUL proteins were employed to investigate the interaction between feline lentiviral Vif and CULs.

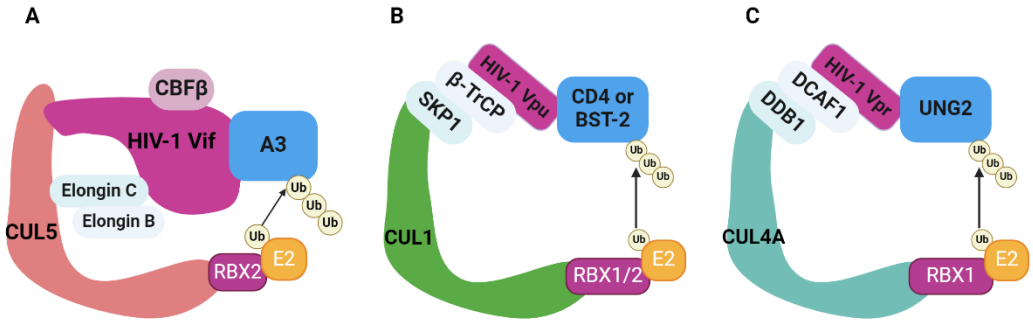

Fig. 4.2 Models of HIV-1 Vif, Vpu, and Vpr E3 Ligase Complexes. (A) Vif associates with the cellular cofactor CBF-β, which stabilizes its binding to the EloBC/RBX2/CUL5 E3 ubiquitin ligase complex. This complex also binds A3, facilitating its polyubiquitination and subsequent degradation. (B) Vpu recruits the SKP1/CUL1/F-Box (SCF) ubiquitin ligase complex via β-TrCP, targeting proteins such as BST-2 and CD4 for ubiquitination, leading to their mislocalization. (C) Vpr engages the DCAF1/DDB1/Rbx1/CUL4A E3 ubiquitin ligase complex and targets UNG2, promoting its polyubiquitination and degradation. Figure adapted from: Collins DR, Collins KL. HIV-1 accessory proteins adapt cellular adaptors to facilitate immune evasion. PLoS Pathog 2014; 10(1):e1003851[141]. Licensed under CC BY 4.0 (https://creativecommons.org/licenses/by/4.0/). Reproduced with BioRender.com.

Human CUL	Feline species	Number of amino acid differences	Percent identity (%)
CUL1	Domestic cat	2	99.7

	Bobcat	2	99.7
	Puma	2	95.1 (Puma CUL1 contains a truncation compared to human CUL1)
CUL2	Domestic cat	2	99.7
	Bobcat	1	99.9
	Puma	2	99.7
CUL3	Domestic cat	2	99.7
	Bobcat	2	91.1 (Bobcat CUL3 contains an insertion compared to human CUL3)
	Puma	23	96.9 (Puma CUL3 contains an insertion compared to human CUL3)
CUL4A	Domestic cat	45	94
	Bobcat	Data unavailable	-
	Puma	Data unavailable	-
CUL4B	Domestic cat	1	99.8
	Bobcat	Data unavailable	-
	Puma	Data unavailable	-
CUL5	Domestic cat	1	99.9
	Bobcat	1	99.9
	Puma	2	99.7

Table 4.1 Differences in amino acid sequences between feline and human CUL proteins. The nucleotide sequences of CULs were obtained from GenBank, and the respective accession numbers are as follows: CUL1: NM_001370660 for human, XM_023250691 for domestic cat, XM_047097018 for bobcat, and XM_025929384 for puma. CUL 2: NM_001198777 for human, XM_006933355 for domestic cat, XM_047065424 for bobcat, and XM_025930223 for puma. CUL 3: NM_001257197 for human, XM_023259738 for domestic cat, XM_047085986 for bobcat, and XM_025925517 for puma. CUL 4A: NM_001008895 for human, XM_023253394 for domestic cat. CUL 4B: NM_001079872 for human, NM_001048152 for domestic cat. CUL 5: NM_003478 for human, NM_001246321 for domestic cat, XM_047070776 for bobcat, and XM_025927963 for puma.

4.2.1 Differential binding of wild feline and domestic cat lentiviral Vif proteins to CUL2 and CUL5

Both CUL2 and CUL5 proteins recruit Elongin B/C as adaptor proteins, and both HIV-1 and FIV Vif contain a BC-box that directly binds to Elongin C[157, 177]. Previous research has shown that HIV-1 Vif specifically prefers CUL5 over CUL2 as the scaffold protein for A3G degradation[132]. Similarly, FIV Vif binds to CUL5 but not to CUL2[157].

In this study, results confirmed earlier findings that FIV Vif, HIV-1 Vif, and HIV-2 Vif bind to CUL5, but not to CUL2 (Fig. 3.16C, G, H). Notably, wild feline lentiviral Vif proteins — PLVB and PLV1695 Vif — were observed to bind both CUL2 and CUL5 (Fig. 3.16E, F), while PLVA Vif predominantly bound to CUL5, with slight binding to CUL2 (Fig. 3.16D).

Furthermore, both DN-CUL2 and DN-CUL5 inhibited PLVB Vif-mediated degradation of PumaA3Z3 (Fig. 3.17C), confirming that both CUL2 and CUL5 are functionally involved in the E3 ligase complex recruited by PLVB Vif.

Structural analysis indicates that residues L52 and W53 in CUL5 play a crucial role in the selection of CUL5 by HIV-1 Vif. These HIV-1 Vif-interacting amino acids in CUL5 are highly variable compared to their counterparts in CUL2 (Fig. 4.3). Substituting these residues in CUL5 with their equivalents in CUL2 significantly impairs CUL5's ability to interact with the HIV-1 Vif-organized complex[156]. Previous study reports that the 52LW53 region in CUL5 is also critical for binding to FIV Vif[157]. In this study, PLVB and PLV1695 Vif were found to interact with both CUL5 and CUL2. Given that L52 and W53 are conserved in CUL5 across human, domestic cat, and puma, and their counterparts in CUL2 (V47 and A48) are similarly conserved in these species (Fig. 4.3), this suggests that the ability of PLVB and PLV1695 Vif to bind both CUL5 and CUL2 may have evolved as an adaptive mechanism. This evolutionary adaptation likely enhances their capacity to interact with the host’s ubiquitin-proteasome machinery, thereby promoting viral replication and survival.

Taken together, these findings provide new insights into the adaptability of lentiviral Vif proteins in selecting CUL proteins for forming the E3 ubiquitin ligase complex, a critical step in A3 protein degradation. Unlike HIV-1 and FIV Vif, which exhibit selective binding to CUL5, the results demonstrate that wild feline lentiviral Vif proteins, such as PLVB and PLV1695, can bind to both CUL2 and CUL5. This broader binding spectrum may confer an evolutionary advantage, enabling these Vif proteins to function effectively across diverse cellular environments, thereby

increasing their adaptability and pathogenic potential.

Fig. 4.3 Sequence alignment of the N-terminal regions of human, domestic cat, and puma CUL5 proteins compared with CUL2. Sequence alignment visualized using the Clustal color scheme, which highlights conserved residues based on their physicochemical properties. For further details, refer to materials and methods section 2.3.4. Residues L52 and W53 in CUL5, along with their corresponding positions in CUL2, are specifically marked to emphasize their variability and potential functional significance.

4.2.2 Identification of a conserved interface of HIV-1, FIV, PLVA and PLVB Vifs with CUL 5

The interaction interface between CUL5 and Vif proteins is evolutionarily conserved across HIV-1 and FIV strains[157]. In FIV Vif, the hydrophobic region 174IR175 plays a critical role in mediating CUL5 binding, while in HIV-1 Vif, the corresponding region, 120IR121, facilitates this interaction[156, 157]. In this study, I identified the corresponding motif in PLVB Vif, 154IL155, which binds to both CUL2 and CUL5 (Fig. 3.18C). A3 degradation assays further demonstrated that, unlike the wild-type PLVB Vif, the 154IL155-AA mutant lost its ability to degrade PumaA3Z3 (Fig. 3.18B). Similarly, the equivalent motif in PLVA Vif, 184IR185, was shown to be critical for CUL5 binding (Fig. 3.19C), and A3 degradation assays confirmed that 184IR185 is essential for BobcatA3Z3 degradation (Fig. 3.19B). Interestingly, immunoblotting revealed that the PLVA Vif 184IR185-AA mutant migrated more slowly than the wild-type protein, despite both proteins having the same amino acid count and minimal molecular weight difference, which typically would not cause a shift in migration on a Western blot (Fig. 3.19B, C). This difference in migration could be attributed to altered charge distribution, conformation, or post-translational modifications resulting from the mutation.

Together, these findings indicate that the CUL5-binding interface in Vif is conserved across HIV-1, FIV, PLVA, and PLVB proteins, underscoring the evolutionary

conservation of Vif-CUL5 interactions among lentiviruses. This conserved interface may suggest a shared mechanism by which various lentiviral Vif proteins hijack the CUL5 E3 ligase complex for A3 protein degradation. Furthermore, this interface offers a promising target for developing novel anti-HIV and anti-lentiviral therapeutics.

4.2.3 PLVB Vif recruits both CUL2 and CUL5 E3 ligase complexes to mediate A3 protein degradation

Previous studies have reported that Vif proteins from various lentiviral clades, including primate lentiviruses (HIV-1 and SIVmac), BIV, FIV, and MVV, can hijack the CUL5 E3 ligase complex in human cells[139]. It has also been reported that BIV and Jembrana disease virus (JDV) utilize CUL2, Elongin B/C, and RBX1, but not CUL5 or CBF-β, to form a CRL2 E3 ubiquitin ligase, which mediates the degradation of restrictive bovine A3 proteins[178, 179].

In this study, PLVB Vif was found to bind both CUL2 and CUL5 (Fig. 3.16E), and inhibition assays demonstrated that both DN-CUL2 and DN-CUL5 suppressed PLVB Vif-mediated degradation of PumaA3Z3 (Fig. 3.17C). Furthermore, PumaA3Z3 was detected in immunoprecipitated complexes of both DN-CUL2-PLVB Vif and DN-CUL5-PLVB Vif, but not in the DN-CUL1-PLVB Vif complex (Fig. 3.24). Collectively, these results indicate that PLVB Vif recruits both CUL2 and CUL5 to form E3 ligase complexes that mediate A3 protein degradation (Fig. 4.4). To the best of my knowledge, this is the first report of a lentiviral Vif protein recruiting both CUL2 and CUL5 for the degradation of A3 proteins.

This novel finding highlights an unexpected level of flexibility and complexity in Vif-mediated immune evasion strategies. It also raises important questions about whether other lentiviral Vif proteins might possess similar capabilities, which could have significant implications for the development of broad-spectrum antiviral therapies targeting Vif-Cullin interactions.

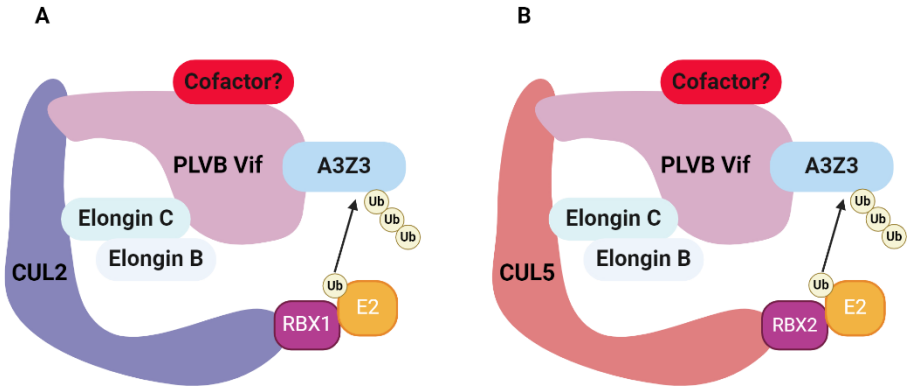

Fig. 4.4 Models of PLVB Vif-E3 Ligase Complexes. (A) PLVB Vif assembles an E3 ligase complex with CUL2, Elongin B/C, and RING box 2 proteins. This complex binds A3Z3, promoting its polyubiquitination and subsequent degradation. (B) PLVB Vif also forms an E3 ligase complex with CUL5, Elongin B/C, and RING box 2 proteins, which similarly targets A3Z3 for polyubiquitination and degradation. Created with BioRender.com.

4.2.4 Differential binding of FIV, PLVA, PLVB, HIV and SIV Vif proteins to CUL family members

PLVB Vif was identified as binding to both CUL2 and CUL5. To further investigate whether Vif proteins interact with other CUL family members, Co-IP assays were performed. The results showed the following interactions between the Vif proteins and the six tested CUL proteins: FIV Vif interacts with CUL1 and CUL5, with very slight interaction with CUL4A and CUL4B (Fig. 3.20A). PLVA Vif complexes with CUL1 and CUL5 and shows slight precipitation of CUL2, CUL4A, and CUL4B (Fig. 3.20B). PLVB Vif interacts with CUL1, CUL2, and CUL5, with slightly with CUL4A and CUL4B (Fig. 3.16E, Fig. 3.20C). HIV-2 Vif complexes with CUL1 and CUL5, with slightly with CUL4A and CUL4B (Fig. 3.20D). For HIV-1 and SIV Vif, I focused on their binding interactions with CUL1, CUL2, and CUL5. Co-IP results indicated that HIV-1 Vif forms complexes with CUL1 and CUL5 (Fig. 3.20E), and similarly, $SIV_{gorilla}$ Vif also complexes with CUL1 and CUL5 (Fig. 3.20F). In summary, all Vif proteins tested likely bind to CUL1 and CUL5, with slight or very slight interaction to CUL4A and CUL4B. Among these, PLVB Vif is the only Vif protein confirmed to

complex with CUL2 (Table 4.2).

All tested Vif proteins (FIV, PLVA, PLVB, HIV-1, HIV-2 and $SIV_{gorilla}$) consistently bind to both CUL1 and CUL5. This suggests that the interaction between Vif proteins and these specific CULs is highly conserved across lentiviruses. CUL5 has been well-documented as the primary scaffold protein recruited by HIV-1 and FIV Vif to assemble the E3 ubiquitin ligase complex that facilitates the degradation of A3 proteins[132, 157]. The consistent binding to CUL1 is also notable, as CUL1 is typically associated with the SCF (SKP1-Cullin-F-box) ubiquitin ligase complex, which is involved in various cellular processes, including protein degradation[180]. However, the specific role of Vif-CUL1 interaction requires further investigation.

Slight or very slight binding to CUL4A and CUL4B was observed across all Vif proteins tested. CUL4A/B typically form complexes with DDB1 to mediate DNA damage responses and regulate cell cycle progression[181]. Although these interactions are weak, they may still have functional significance. It is possible that under certain conditions, Vif proteins can partially engage CUL4A/B to modulate host immune responses or cellular pathways. Further studies are needed to determine whether these weak interactions contribute to alternative Vif-mediated degradation pathways.

Vif Proteins	CUL1	CUL 2	CUL 3	CUL 4A	CUL 4B	CUL 5	Figures
FIV Vif	+	−	−	+/−	+/−	+	Fig. 3.20A
PLVA Vif	+	+/−	−	+/−	+/−	+	Fig. 3.20B
PLVB Vif	+	+	−	+/−	+/−	+	Fig. 3.16E, 3.20C
HIV-1 Vif	+	−	−	N.T.	N.T.	+	Fig. 3.20E
HIV-2 Vif	+	−	−	+/−	+/−	+	Fig. 3.20D
SIVgorilla Vif	+	−	N.T.	N.T.	N.T.	+	Fig. 3.20F

Table 4.2. Interaction of Vif proteins with CUL family proteins. + indicates an interaction, +/− denotes a slight interaction, − means no interaction, and N.T. indicates not tested.

4.2.5 Novel insights into the interaction of Vif proteins with CUL1: functional role remains unclear

Previous research confirmed that HIV-1 Vpu interacts with the CUL1 E3 complex

via β-TrCP, targeting BST-2 or CD4 for ubiquitination and mis-localization[141]. Whether other viral proteins interact with CUL1 remains unknown. In this study, all tested Vif proteins (FIV, PLVA, PLVB, HIV-1, HIV-2 and $SIV_{gorilla}$) consistently bind to CUL1 (Fig. 3.20A-F), marking this as a novel finding. CUL1 also binds to untagged HIV-1 Vif strains (NL4-3, LAI, F-1, and N-116) (Fig. 3.21). Furthermore, both HIV-1 and PLVB Vif bind to small amounts of endogenous CUL1 in 293T cells (Fig. 3.22B).

The current model suggests that CUL1 interacts with the adaptor protein SKP1, forming a core component of the SCF (SKP1-CUL1-F-box) complex, which subsequently targets substrates for ubiquitination via an F-box protein substrate receptor[171]. Inhibition assays revealed that, unlike DN-CUL5, DN-CUL1 failed to inhibit the degradation of CatA3Z3 by FIV Vif (Fig. 3.23C), PumaA3Z3 by PLVB Vif (Fig. 3.23D), huA3C by HIV-1 Vif (Fig. 3.23E) and huA3C by HIV-2 Vif (Fig. 3.23F), demonstrating that DN-CUL1 does not affect A3 protein degradation by the tested Vif proteins. Additionally, DN-CUL1 does not capture PumaA3Z3 in the PLVB Vif immunoprecipitated complexes, unlike DN-CUL2 or DN-CUL5 (Fig. 3.24).

These findings suggest that the specific function of Vif proteins binding to CUL1 remains unclear. This interaction might be nonspecific, or it may have a specific functional role that requires further investigation in future experiments.

Although this study provides new insights into the interaction between lentiviral Vif proteins and host restriction factor A3, as well as host CUL proteins, the identification of conserved interfaces for A3 and CUL5 binding in Vif proteins presents promising targets for the development of novel anti-HIV and anti-lentiviral therapeutics. However, further in vivo investigations are needed to analyze these interactions more comprehensively. In summary, we propose a novel perspective on the interactions between lentiviral Vif proteins and host restriction factors A3, as well as host CUL proteins. These findings offer new avenues for uncovering the complex dynamics of lentiviral protein-host protein interactions.

5. References

1. UNAIDS. **Global HIV & AIDS statistics — Fact sheet**. In; 2023.

2. WHO. **HIV/AIDS**. In; 2023.

3. Services USDoHaH. **Global Statistics**. In; 2023.

4. John M. Coffin SHH, Harold Varmus. **Retroviruses**. Cold Spring Harbor Laboratory Press; 1997.

5. Weiss RA. **How Does Hiv Cause Aids**. *Science* 1993; 260(5112):1273-1279.

6. Mahieux R, Gessain A. **Adult T-cell leukemia/lymphoma and HTLV-1**. *Curr Hematol Malig Rep* 2007; 2(4):257-264.

7. Payne LN, Nair V. **The long view: 40 years of avian leukosis research**. *Avian Pathology* 2012; 41(1):11-19.

8. Hartmann K. **Clinical aspects of feline immunodeficiency and feline leukemia virus infection**. *Vet Immunol Immunop* 2011; 143(3-4):190-201.

9. Dull T, Zufferey R, Kelly M, Mandel RJ, Nguyen M, Trono D, et al. **A third-generation lentivirus vector with a conditional packaging system**. *Journal of Virology* 1998; 72(11):8463-8471.

10. Kustikova O, Fehse B, Modlich U, Yang M, Düllmann J, Kamino K, et al. **Clonal dominance of hematopoietic stem cells triggered by retroviral gene marking**. *Science* 2005; 308(5725):1171-1174.

11. Coffin J, Blomberg J, Fan H, Gifford R, Hatziioannou T, Lindemann D, et al. **ICTV Virus Taxonomy Profile: Retroviridae 2021**. *Journal of General Virology* 2021; 102(12).

12. Jane Flint VRR, Glenn F. Rall, Theodora Hatziioannou, Anna Marie Skalka. **Principles of Virology**. 5th ed: ASM Press; 2020.

13. Sharp PM, Hahn BH. **Origins of HIV and the AIDS Pandemic**. *Csh Perspect Med* 2011; 1(1).

14. Ayouba A, Akoua-Koffi C, Calvignac-Spencer S, Esteban A, Locatelli S, Li H, et al. **Evidence for continuing cross-species transmission of SIVsmm to humans: characterization of a new HIV-2 lineage in rural Cote d'Ivoire**. *AIDS*

2013; 27(15):2488-2491.

15. Olmsted RA, Barnes AK, Yamamoto JK, Hirsch VM, Purcell RH, Johnson PR. **Molecular-Cloning of Feline Immunodeficiency Virus**. *P Natl Acad Sci USA* 1989; 86(7):2448-2452.

16. Pedersen NC, Yamamoto JK, Ishida T, Hansen H. **Feline Immunodeficiency Virus-Infection**. *Vet Immunol Immunop* 1989; 21(1):111-129.

17. North TW, Lacasse RA. **Testing Anti-Hiv Drugs in the Fiv Model**. *Nature Medicine* 1995; 1(5):410-411.

18. van Regenmortel MHV FC, Bishop DHL, Carstens EB, Estes MK, Lemon SM, Maniloff J, Mayo MA, McGeoch DJ, Pringle CR. **Seventh Report of the International Commitee on Taxonomy of Viruses**. Academic Press; 2000.

19. Keckesova Z, Ylinen LM, Towers GJ, Gifford RJ, Katzourakis A. **Identification of a RELIK orthologue in the European hare (Lepus europaeus) reveals a minimum age of 12 million years for the lagomorph lentiviruses**. *Virology* 2009; 384(1):7-11.

20. Katzourakis A, Tristem M, Pybus OG, Gifford RJ. **Discovery and analysis of the first endogenous lentivirus**. *P Natl Acad Sci USA* 2007; 104(15):6261-6265.

21. Gifford RJ, Katzourakis A, Tristem M, Pybus OG, Winters M, Shafer RW. **A transitional endogenous lentivirus from the genome of a basal primate and implications for lentivirus evolution**. *Proc Natl Acad Sci U S A* 2008; 105(51):20362-20367.

22. Gilbert C, Maxfield DG, Goodman SM, Feschotte C. **Parallel Germline Infiltration of a Lentivirus in Two Malagasy Lemurs**. *Plos Genetics* 2009; 5(3).

23. Han GZ, Worobey M. **Endogenous Lentiviral Elements in the Weasel Family (**

). *Molecular Biology and Evolution* 2012; 29(10):2905-2908.

24. Cui J, Holmes EC. **Endogenous Lentiviruses in the Ferret Genome**. *Journal of Virology* 2012; 86(6):3383-3385.

25. Hron T, Fábryová H, Paces J, Elleder D. **Endogenous lentivirus in Malayan**

colugo (Galeopterus variegatus), a close relative of primates. *Retrovirology* 2014; 11.

26. Hron T, Farkasová H, Padhi A, Paces J, Elleder D. **Life History of the Oldest Lentivirus: Characterization of ELVgv Integrations in the Dermopteran Genome**. *Molecular Biology and Evolution* 2016; 33(10):2659-2669.

27. Platt EJ, Wehrly K, Kuhmann SE, Chesebro B, Kabat D. **Effects of CCR5 and CD4 cell surface concentrations on infections by macrophagetropic isolates of human immunodeficiency virus type 1**. *Journal of Virology* 1998; 72(4):2855-2864.

28. Shimojima M, Miyazawa T, Ikeda Y, McMonagle EL, Haining H, Akashi H, et al. **Use of CD134 as a primary receptor by the feline immunodeficiency virus**. *Science* 2004; 303(5661):1192-1195.

29. de Parseval A, Chatterji U, Sun PQ, Elder JH. **Feline immunodeficiency virus targets activated CD4+ T cells by using CD134 as a binding receptor**. *P Natl Acad Sci USA* 2004; 101(35):13044-13049.

30. Willett BJ, McMonagle EL, Ridha S, Hosie MJ. **Differential utilization of CD134 as a functional receptor by diverse strains of feline immunodeficiency virus**. *Journal of Virology* 2006; 80(7):3386-3394.

31. Dharan A, Bachmann N, Talley S, Zwikelmaier V, Campbell EM. **Nuclear pore blockade reveals that HIV-1 completes reverse transcription and uncoating in the nucleus**. *Nat Microbiol* 2020; 5(9):1088-1095.

32. Briggs JAG, Simon MN, Gross I, Kräusslich HG, Fuller SD, Vogt VM, et al. **The stoichiometry of Gag protein in HIV-1**. *Nat Struct Mol Biol* 2004; 11(7):672-675.

33. Bieniasz PD. **Late budding domains and host proteins in enveloped virus release**. *Virology* 2006; 344(1):55-63.

34. Okoye AA, Picker LJ. **CD4+T-cell depletion in HIV infection: mechanisms of immunological failure**. *Immunol Rev* 2013; 254:54-64.

35. Février M, Dorgham K, Rebollo A. **CD4+ T Cell Depletion in Human Immunodeficiency Virus (HIV) Infection: Role of Apoptosis**. *Viruses-Basel*

2011; 3(5):586-612.

36. Bruxelle JF, Trattnig N, Mureithi MW, Landais E, Pantophlet R. **HIV-1 Entry and Prospects for Protecting against Infection**. *Microorganisms* 2021; 9(2).

37. Jewanraj J, Ngcapu S, Liebenberg LJP. **Semen: A modulator of female genital tract inflammation and a vector for HIV-1 transmission**. *Am J Reprod Immunol* 2021; 86(5).

38. Cavarelli M, Le Grand R. **The importance of semen leukocytes in HIV-1 transmission and the development of prevention strategies**. *Hum Vacc Immunother* 2020; 16(9):2018-2032.

39. Campo J, Perea MA, del Romero J, Cano J, Hernando V, Bascones A. **Oral transmission of HIV, reality or fiction? An update**. *Oral Dis* 2006; 12(3):219-228.

40. Kaul R, Liu CM, Park DE, Galiwango RM, Tobian AAR, Prodger JL. **The Penis, the Vagina and HIV Risk: Key Differences (Aside from the Obvious)**. *Viruses-Basel* 2022; 14(6).

41. Cohn LB, Chomont N, Deeks SG. **The Biology of the HIV-1 Latent Reservoir and Implications for Cure Strategies**. *Cell Host Microbe* 2020; 27(4):519-530.

42. Wensing AM, Calvez V, Ceccherini-Silberstein F, Charpentier C, Gunthard HF, Paredes R, et al. **2022 update of the drug resistance mutations in HIV-1**. *Top Antivir Med* 2022; 30(4):559-574.

43. Frankel AD, Young JAT. **HIV-1: Fifteen proteins and an RNA**. *Annu Rev Biochem* 1998; 67:1-25.

44. VandeWoude S, Apetrei C. **Going wild: Lessons from naturally occurring T-lymphotropic lentiviruses**. *Clin Microbiol Rev* 2006; 19(4):728-762.

45. de Rozières S, Mathiason CK, Rolston MR, Chatterji U, Hoover EA, Elder JH. **Characterization of a highly pathogenic molecular clone of feline immunodeficiency virus clade C**. *Journal of Virology* 2004; 78(17):8971-8982.

46. Diehl LJ, Mathiasondubard CK, Oneil LL, Obert LA, Hoover EA. **Induction of Accelerated Feline Immunodeficiency Virus-Disease by Acute-Phase Virus Passage**. *Journal of Virology* 1995; 69(10):6149-6157.

47. Troyer JL, Pecon-Slattery J, Roelke ME, Johnson W, VandeWoude S, Vazquez-Salat N, et al. **Seroprevalence and genomic divergence of circulating strains of Feline immunodeficiency virus among Felidae and Hyaenidae species**. *Journal of Virology* 2005; 79(13):8282-8294.

48. O'Brien SJ, Troyer JL, Brown MA, Johnson WE, Antunes A, Roelke ME, et al. **Emerging Viruses in the Felidae: Shifting Paradigms**. *Viruses-Basel* 2012; 4(2):236-257.

49. Carpenter MA, Brown EW, MacDonald DW, O'Brien S J. **Phylogeographic patterns of feline immunodeficiency virus genetic diversity in the domestic cat**. *Virology* 1998; 251(2):234-243.

50. Olmsted RA, Hirsch VM, Purcell RH, Johnson PR. **Nucleotide-Sequence Analysis of Feline Immunodeficiency Virus - Genome Organization and Relationship to Other Lentiviruses**. *P Natl Acad Sci USA* 1989; 86(20):8088-8092.

51. Troyer JL, VandeWoude S, Pecon-Slattery J, McIntosh C, Franklin S, Antunes A, et al. **FIV cross-species transmission: An evolutionary prospective**. *Vet Immunol Immunop* 2008; 123(1-2):159-166.

52. VandeWoude S, Troyer J, Poss M. **Restrictions to cross-species transmission of lentiviral infection gleaned from studies of FIV**. *Vet Immunol Immunop* 2010; 134(1-2):25-32.

53. Pecon-Slattery J, Troyer JL, Johnson WE, O'Brien SJ. **Evolution of feline immunodeficiency virus in Felidae: Implications for human health and wildlife ecology**. *Vet Immunol Immunop* 2008; 123(1-2):32-44.

54. Lee J, Malmberg JL, Wood BA, Hladky S, Troyer R, Roelke M, et al. **Feline Immunodeficiency Virus Cross-Species Transmission: Implications for Emergence of New Lentiviral Infections**. *Journal of Virology* 2017; 91(5).

55. Lee JS, Bevins SN, Serieys LEK, Vickers W, Logan KA, Aldredge M, et al. **Evolution of Puma Lentivirus in Bobcats (Lynx rufus) and Mountain Lions (Puma concolor) in North America**. *Journal of Virology* 2014; 88(14):7727-7737.

56. Troyer JL, Roelke ME, Jespersen JM, Baggett N, Buckley-Beason V, MacNulty D, et al. **FIV diversity: FIV Ple subtype composition may influence disease outcome in African lions**. *Vet Immunol Immunopathol* 2011; 143(3-4):338-346.

57. Franklin SP, Troyer JL, Terwee JA, Lyren LM, Boyce WM, Riley SPD, et al. **Frequent transmission of immunodeficiency viruses among bobcats and pumas**. *Journal of Virology* 2007; 81(20):10961-10969.

58. Carpenter MA, Brown EW, Culver M, Johnson WE, PeconSlattery J, Brousset D, et al. **Genetic and phylogenetic divergence of feline immunodeficiency virus in the puma (Puma concolor)**. *Journal of Virology* 1996; 70(10):6682-6693.

59. Nishimura Y, Goto Y, Yoneda K, Endo Y, Mizuno T, Hamachi M, et al. **Interspecies transmission of feline immunodeficiency virus from the domestic cat to the Tsushima cat (Felis bengalensis euptilura) in the wild**. *Journal of Virology* 1999; 73(9):7916-7921.

60. Zielonka J, Münk C. **Cellular Restriction Factors of Feline Immunodeficiency Virus**. *Viruses-Basel* 2011; 3(10):1986-2005.

61. Münk C, Beck T, Zielonka J, Hotz-Wagenblatt A, Chareza S, Battenberg M, et al. **Functions, structure, and read-through alternative splicing of feline APOBEC3 genes**. *Genome Biol* 2008; 9(3):R48.

62. Hong Y, Fink E, Hu QY, Kiosses WB, Elder JH. **OrfA Downregulates Feline Immunodeficiency Virus Primary Receptor CD134 on the Host Cell Surface and Is Important in Viral Infection**. *Journal of Virology* 2010; 84(14):7225-7232.

63. Troyer RM, Thompson J, Elder JH, VandeWoude S. **Accessory Genes Confer a High Replication Rate to Virulent Feline Immunodeficiency Virus**. *Journal of Virology* 2013; 87(14):7940-7951.

64. Sundstrom M, Chatterji U, Schaffer L, de Rozières S, Elder JH. **Feline immunodeficiency virus OrfA alters gene expression of splicing factors and proteasome-ubiquitination proteins**. *Virology* 2008; 371(2):394-404.

65. Zhang ZL, Gu QY, Marino D, Lee KL, Kong IK, Häussinger D, et al. **Feline APOBEC3s, Barriers to Cross-Species Transmission of FIV?** *Viruses-Basel*

2018; 10(4).

66. Wolf D, Goff SP. **Host Restriction Factors Blocking Retroviral Replication**. *Annual Review of Genetics* 2008; 42:143-163.

67. Jimenez-Guardeno JM, Apolonia L, Betancor G, Malim MH. **Immunoproteasome activation enables human TRIM5alpha restriction of HIV-1**. *Nat Microbiol* 2019; 4(6):933-940.

68. Kim K, Dauphin A, Komurlu S, McCauley SM, Yurkovetskiy L, Carbone C, et al. **Cyclophilin A protects HIV-1 from restriction by human TRIM5alpha**. *Nat Microbiol* 2019; 4(12):2044-2051.

69. Selyutina A, Persaud M, Simons LM, Bulnes-Ramos A, Buffone C, Martinez-Lopez A, et al. **Cyclophilin A Prevents HIV-1 Restriction in Lymphocytes by Blocking Human TRIM5alpha Binding to the Viral Core**. *Cell Rep* 2020; 30(11):3766-3777 e3766.

70. Saenz DT, Teo WL, Olsen JC, Poeschla EM. **Restriction of feline immunodeficiency virus by Ref1, Lv1, and primate TRIM5α proteins**. *Journal of Virology* 2005; 79(24):15175-15188.

71. Mandell MA, Kimura T, Jain A, Johansen T, Deretic V. **TRIM proteins regulate autophagy: TRIM5 is a selective autophagy receptor mediating HIV-1 restriction**. *Autophagy* 2014; 10(12):2387-2388.

72. Reymond A, Meroni G, Fantozzi A, Merla G, Cairo S, Luzi L, et al. **The tripartite motif family identifies cell compartments**. *Embo J* 2001; 20(9):2140-2151.

73. Takeda E, Kono K, Hulme AE, Hope TJ, Nakayama EE, Shioda T. **Fluorescent Image Analysis of HIV-1 and HIV-2 Uncoating Kinetics in the Presence of Old World Monkey TRIM5a**. *Plos One* 2015; 10(3).

74. Nisole S, Stoye JP, Saïb A. **Trim family proteins: Retroviral restriction and antiviral defence**. *Nat Rev Microbiol* 2005; 3(10):799-808.

75. Stremlau M, Song BW, Javanbakht H, Perron M, Sodroski J. **Cyclophilin A: An auxiliary but not necessary cofactor for TRIM5α restriction of HIV-1**. *Virology* 2006; 351(1):112-120.

76. McEwan WA, Schaller T, Ylinen LM, Hosie MJ, Towers GJ, Willett BJ. **Truncation of TRIM5 in the Feliformia explains the absence of retroviral restriction in cells of the domestic cat**. *Journal of Virology* 2009; 83(16):8270-8275.

77. Dietrich I, Macintyre A, McMonagle E, Price AJ, James LC, McEwan WA, et al. **Potent Lentiviral Restriction by a Synthetic Feline TRIM5 Cyclophilin A Fusion**. *Journal of Virology* 2010; 84(17):8980-8985.

78. Münk C, Willemsen A, Bravo IG. **An ancient history of gene duplications, fusions and losses in the evolution of APOBEC3 mutators in mammals**. *BMC Evol Biol* 2012; 12:71.

79. LaRue RS, Andresdottir V, Blanchard Y, Conticello SG, Derse D, Emerman M, et al. **Guidelines for naming nonprimate APOBEC3 genes and proteins**. *J Virol* 2009; 83(2):494-497.

80. Zhang H, Yang B, Pomerantz RJ, Zhang CM, Arunachalam SC, Gao L. **The cytidine deaminase CEM15 induces hypermutation in newly synthesized HIV-1 DNA**. *Nature* 2003; 424(6944):94-98.

81. Mangeat B, Turelli P, Caron G, Friedli M, Perrin L, Trono D. **Broad antiretroviral defence by human APOBEC3G through lethal editing of nascent reverse transcripts**. *Nature* 2003; 424(6944):99-103.

82. Jarmuz A, Chester A, Bayliss J, Gisbourne J, Dunham I, Scott J, et al. **An anthropoid-specific locus of orphan C to U RNA-editing enzymes on chromosome 22**. *Genomics* 2002; 79(3):285-296.

83. Münk C, Jensen BE, Zielonka J, Häussinger D, Kamp C. **Running loose or getting lost: how HIV-1 counters and capitalizes on APOBEC3-induced mutagenesis through its Vif protein**. *Viruses* 2012; 4(11):3132-3161.

84. Hrecka K, Hao CL, Gierszewska M, Swanson SK, Kesik-Brodacka M, Srivastava S, et al. **Vpx relieves inhibition of HIV-1 infection of macrophages mediated by the SAMHD1 protein**. *Nature* 2011; 474(7353):658-661.

85. Laguette N, Sobhian B, Casartelli N, Ringeard M, Chable-Bessia C, Ségéral E,

et al. **SAMHD1 is the dendritic- and myeloid-cell-specific HIV-1 restriction factor counteracted by Vpx**. *Nature* 2011; 474(7353):654-657.

86. Descours B, Cribier A, Chable-Bessia C, Ayinde D, Rice G, Crow Y, et al. **SAMHD1 restricts HIV-1 reverse transcription in quiescent CD4(+) T-cells**. *Retrovirology* 2012; 9:87.

87. Li MM, Zhang D, Zhu MY, Shen YX, Wei W, Ying SC, et al. **Roles of SAMHD1 in antiviral defense, autoimmunity and cancer**. *Rev Med Virol* 2017; 27(4).

88. Mlcochova P, Sutherland KA, Watters SA, Bertoli C, de Bruin RAM, Rehwinkel J, et al. **A G1-like state allows HIV-1 to bypass SAMHD1 restriction in macrophages**. *Embo J* 2017; 36(5):604-616.

89. Yang S, Zhan Y, Zhou YJ, Jiang YF, Zheng XC, Yu LX, et al. **Interferon regulatory factor 3 is a key regulation factor for inducing the expression of SAMHD1 in antiviral innate immunity**. *Sci Rep-Uk* 2016; 6.

90. Jang S, Zhou XH, Ahn J. **Substrate Specificity of SAMHD1 Triphosphohydrolase Activity Is Controlled by Deoxyribonucleoside Triphosphates and Phosphorylation at Thr592**. *Biochemistry* 2016; 55(39):5635-5646.

91. White TE, Brandariz-Nuñez A, Valle-Casuso JC, Amie S, Nguyen L, Kim B, et al. **Contribution of SAM and HD domains to retroviral restriction mediated by human SAMHD1**. *Virology* 2013; 436(1):81-90.

92. Mereby SA, Maehigashi T, Holler JM, Kim DH, Schinazi RF, Kim B. **Interplay of ancestral non-primate lentiviruses with the virus-restricting SAMHD1 proteins of their hosts**. *J Biol Chem* 2018; 293(42):16402-16412.

93. Wang C, Meng L, Wang J, Zhang K, Duan S, Ren P, et al. **Role of Intracellular Distribution of Feline and Bovine SAMHD1 Proteins in Lentiviral Restriction**. *Virol Sin* 2021; 36(5):981-996.

94. Neil SJ, Zang T, Bieniasz PD. **Tetherin inhibits retrovirus release and is antagonized by HIV-1 Vpu**. *Nature* 2008; 451(7177):425-430.

95. Van Damme N, Goff D, Katsura C, Jorgenson RL, Mitchell R, Johnson MC, et

al. **The interferon-induced protein BST-2 restricts HIV-1 release and is downregulated from the cell surface by the viral Vpu protein**. *Cell Host Microbe* 2008; 3(4):245-252.

96. Miyakawa K, Ryo A, Murakami T, Ohba K, Yamaoka S, Fukuda M, et al. **BCA2/Rabring7 promotes tetherin-dependent HIV-1 restriction**. *PLoS Pathog* 2009; 5(12):e1000700.

97. Cocka LJ, Bates P. **Identification of alternatively translated Tetherin isoforms with differing antiviral and signaling activities**. *PLoS Pathog* 2012; 8(9):e1002931.

98. Galao RP, Le Tortorec A, Pickering S, Kueck T, Neil SJ. **Innate sensing of HIV-1 assembly by Tetherin induces NFkappaB-dependent proinflammatory responses**. *Cell Host Microbe* 2012; 12(5):633-644.

99. Sauter D. **Counteraction of the multifunctional restriction factor tetherin**. *Frontiers in Microbiology* 2014; 5.

100. Hotter D, Sauter D, Kirchhoff F. **Emerging Role of the Host Restriction Factor Tetherin in Viral Immune Sensing**. *Journal of Molecular Biology* 2013; 425(24):4956-4964.

101. Yin X, Hu Z, Gu QY, Wu XL, Zheng YH, Wei P, et al. **Equine Tetherin Blocks Retrovirus Release and Its Activity Is Antagonized by Equine Infectious Anemia Virus Envelope Protein**. *Journal of Virology* 2014; 88(2):1259-1270.

102. Neil SJD. **The Antiviral Activities of Tetherin**. *Intrinsic Immunity* 2013; 371:67-104.

103. Morrison JH, Guevara RB, Marcano AC, Saenz DT, Fadel HJ, Rogstad DK, et al. **Feline Immunodeficiency Virus Envelope Glycoproteins Antagonize Tetherin through a Distinctive Mechanism That Requires Virion Incorporation**. *Journal of Virology* 2014; 88(6):3255-3272.

104. Dietrich I, McMonagle EL, Petit SJ, Vijayakrishnan S, Logan N, Chan CN, et al. **Feline tetherin efficiently restricts release of feline immunodeficiency virus but not spreading of infection**. *J Virol* 2011; 85(12):5840-5852.

105. Celestino M, Calistri A, Del Vecchio C, Salata C, Chiuppesi F, Pistello M, et al. **Feline Tetherin Is Characterized by a Short N-Terminal Region and Is Counteracted by the Feline Immunodeficiency Virus Envelope Glycoprotein**. *Journal of Virology* 2012; 86(12):6688-6700.

106. Morrison JH, Poeschla EM. **The Feline Immunodeficiency Virus Envelope Signal Peptide Is a Tetherin Antagonizing Protein**. *mBio* 2023; 14(2):e0016123.

107. Haller O. **Dynamins Are Forever: MxB Inhibits HIV-1**. *Cell Host Microbe* 2013; 14(4):371-373.

108. Mänz B, Dornfeld D, Götz V, Zell R, Zimmermann P, Haller O, et al. **Pandemic Influenza A Viruses Escape from Restriction by Human MxA through Adaptive Mutations in the Nucleoprotein**. *Plos Pathogens* 2013; 9(3).

109. Goujon C, Moncorgé O, Bauby H, Doyle T, Ward CC, Schaller T, et al. **Human MX2 is an interferon-induced post-entry inhibitor of HIV-1 infection**. *Nature* 2013; 502(7472):559-562.

110. Crameri M, Bauer M, Caduff N, Walker R, Steiner F, Franzoso FD, et al. **MxB is an interferon-induced restriction factor of human herpesviruses**. *Nat Commun* 2018; 9.

111. Yi DR, An N, Liu ZL, Xu FW, Raniga K, Li QJ, et al. **Human MxB Inhibits the Replication of Hepatitis C Virus**. *Journal of Virology* 2019; 93(1).

112. Meier K, Jaguva Vasudevan AA, Zhang Z, Bahr A, Kochs G, Haussinger D, et al. **Equine MX2 is a restriction factor of equine infectious anemia virus (EIAV)**. *Virology* 2018; 523:52-63.

113. Busnadiego I, Kane M, Rihn SJ, Preugschas HF, Hughes J, Blanco-Melo D, et al. **Host and Viral Determinants of Mx2 Antiretroviral Activity**. *Journal of Virology* 2014; 88(14):7738-7752.

114. Mitchell PS, Young JM, Emerman M, Malik HS. **Evolutionary Analyses Suggest a Function of MxB Immunity Proteins Beyond Lentivirus Restriction**. *Plos Pathogens* 2015; 11(12).

115. Inuzuka M, Hayakawa M, Ingi T. **Serinc, an activity-regulated protein family,**

incorporates serine into membrane lipid synthesis. *J Biol Chem* 2005; 280(42):35776-35783.

116. Usami Y, Wu YF, Göttlinger HG. **SERINC3 and SERINC5 restrict HIV-1 infectivity and are counteracted by Nef**. *Nature* 2015; 526(7572):218-223.

117. Pye VE, Rosa A, Bertelli C, Struwe WB, Maslen SL, Corey R, et al. **A bipartite structural organization defines the SERINC family of HIV-1 restriction factors**. *Nat Struct Mol Biol* 2020; 27(1):78-83.

118. Rosa A, Chande A, Ziglio S, De Sanctis V, Bertorelli R, Goh SL, et al. **HIV-1 Nef promotes infection by excluding SERINC5 from virion incorporation**. *Nature* 2015; 526(7572):212-217.

119. Sood C, Marin M, Chande A, Pizzato M, Melikyan GB. **SERINC5 protein inhibits HIV-1 fusion pore formation by promoting functional inactivation of envelope glycoproteins**. *J Biol Chem* 2017; 292(14):6014-6026.

120. Zeng C, Waheed AA, Li T, Yu J, Zheng YM, Yount JS, et al. **SERINC proteins potentiate antiviral type I IFN production and proinflammatory signaling pathways**. *Sci Signal* 2021; 14(700):eabc7611.

121. Heigele A, Kmiec D, Regensburger K, Langer S, Peiffer L, Stürzel CM, et al. **The Potency of Nef-Mediated SERINC5 Antagonism Correlates with the Prevalence of Primate Lentiviruses in the Wild**. *Cell Host Microbe* 2016; 20(3):381-391.

122. Beitari S, Ding SL, Pan QH, Finzi A, Liang C. **Effect of HIV-1 Env on SERINC5 Antagonism**. *Journal of Virology* 2017; 91(4).

123. Cano-Ortiz L, Gu QY, de Sousa-Pereira P, Zhang ZL, Chiapella C, Twizerimana AP, et al. **Feline Leukemia Virus-B Envelope Together With its GlycoGag and Human Immunodeficiency Virus-1 Nef Mediate Resistance to Feline SERINC5**. *Journal of Molecular Biology* 2022; 434(6).

124. Barry M, Fruh K. **Viral modulators of cullin RING ubiquitin ligases: culling the host defense**. *Sci STKE* 2006; 2006(335):pe21.

125. Goldberg AL. **Protein degradation and protection against misfolded or**

damaged proteins. *Nature* 2003; 426(6968):895-899.

126. Kimura Y, Tanaka K. **Regulatory mechanisms involved in the control of ubiquitin homeostasis**. *J Biochem* 2010; 147(6):793-798.

127. Metzger MB, Hristova VA, Weissman AM. **HECT and RING finger families of E3 ubiquitin ligases at a glance**. *Journal of Cell Science* 2012; 125(3):531-537.

128. Yang Q, Zhao J, Chen D, Wang Y. **E3 ubiquitin ligases: styles, structures and functions**. *Mol Biomed* 2021; 2(1):23.

129. Sarikas A, Hartmann T, Pan ZQ. **The cullin protein family**. *Genome Biology* 2011; 12(4).

130. Okumura F, Joo-Okumura A, Nakatsukasa K, Kamura T. **The role of cullin 5-containing ubiquitin ligases**. *Cell Division* 2016; 11.

131. Guo YY, Dong LY, Qiu XL, Wang YS, Zhang BL, Liu HN, et al. **Structural basis for hijacking CBF-β and CUL5 E3 ligase complex by HIV-1 Vif**. *Nature* 2014; 505(7482):229-233.

132. Yu XH, Yu YK, Liu BD, Luo K, Kong W, Mao PY, et al. **Induction of APOBEC3G ubiquitination and degradation by an HIV-1 Vif-Cul5-SCF complex**. *Science* 2003; 302(5647):1056-1060.

133. Chen Z, Sui J, Zhang F, Zhang C. **Cullin family proteins and tumorigenesis: genetic association and molecular mechanisms**. *J Cancer* 2015; 6(3):233-242.

134. Zielonka J, Marino D, Hofmann H, Yuhki N, Löchelt M, Münk C. **Vif of feline immunodeficiency virus from domestic cats protects against APOBEC3 restriction factors from many felids**. *J Virol* 2010; 84(14):7312-7324.

135. Löchelt M, Romen F, Bastone P, Muckenfuss H, Kirchner N, Kim YB, et al. **The antiretroviral activity of APOBEC3 is inhibited by the foamy virus accessory Bet protein**. *P Natl Acad Sci USA* 2005; 102(22):7982-7987.

136. Zhang ZL, Gu QY, Vasudevan AAJ, Hain A, Kloke BP, Hasheminasab S, et al. **Determinants of FIV and HIV Vif sensitivity of feline APOBEC3 restriction factors**. *Retrovirology* 2016; 13.

137. Wang JW, Zhang WY, Lv MY, Zuo T, Kong W, Yu XH. **Identification of a Cullin5-ElonginB-ElonginC E3 Complex in Degradation of Feline Immunodeficiency Virus Vif-Mediated Feline APOBEC3 Proteins**. *Journal of Virology* 2011; 85(23):12482-12491.

138. Jager S, Kim DY, Hultquist JF, Shindo K, LaRue RS, Kwon E, et al. **Vif hijacks CBF-beta to degrade APOBEC3G and promote HIV-1 infection**. *Nature* 2012; 481(7381):371-375.

139. Kane JR, Stanley DJ, Hultquist JF, Johnson JR, Mietrach N, Binning JM, et al. **Lineage-Specific Viral Hijacking of Non-canonical E3 Ubiquitin Ligase Cofactors in the Evolution of Vif Anti-APOBEC3 Activity**. *Cell Rep* 2015; 11(8):1236-1250.

140. Ai YW, Zhu DT, Wang CH, Su C, Ma J, Ma JZ, et al. **Core-Binding Factor Subunit Beta Is Not Required for Non-Primate Lentiviral Vif-Mediated APOBEC3 Degradation**. *Journal of Virology* 2014; 88(20):12112-12122.

141. Collins DR, Collins KL. **HIV-1 accessory proteins adapt cellular adaptors to facilitate immune evasion**. *PLoS Pathog* 2014; 10(1):e1003851.

142. Letko M, Booiman T, Kootstra N, Simon V, Ooms M. **Identification of the HIV-1 Vif and Human APOBEC3G Protein Interface**. *Cell Rep* 2015; 13(9):1789-1799.

143. Kitamura S, Ode H, Nakashima M, Imahashi M, Naganawa Y, Kurosawa T, et al. **The APOBEC3C crystal structure and the interface for HIV-1 Vif binding**. *Nat Struct Mol Biol* 2012; 19(10):1005-U1053.

144. Zhang ZL, Gu QY, Vasudevan AAJ, Jeyaraj M, Schmidt S, Zielonka J, et al. **Vif Proteins from Diverse Human Immunodeficiency Virus/Simian Immunodeficiency Virus Lineages Have Distinct Binding Sites in A3C**. *Journal of Virology* 2016; 90(22):10193-10208.

145. Nakashima M, Ode H, Kawamura T, Kitamura S, Naganawa Y, Awazu H, et al. **Structural Insights into HIV-1 Vif-APOBEC3F Interaction**. *Journal of Virology* 2016; 90(2):1034-1047.

146. Huthoff H, Malim MH. **Identification of amino acid residues in APOBEC3G required for regulation by human immunodeficiency virus type 1 Vif and virion encapsidation**. *Journal of Virology* 2007; 81(8):3807-3815.

147. Zhen AJ, Wang T, Zhao K, Xiong Y, Yu XF. **A Single Amino Acid Difference in Human APOBEC3H Variants Determines HIV-1 Vif Sensitivity**. *Journal of Virology* 2010; 84(4):1902-1911.

148. Zhang WY, Chen GY, Niewiadomska AM, Xu RZ, Yu XF. **Distinct Determinants in HIV-1 Vif and Human APOBEC3 Proteins Are Required for the Suppression of Diverse Host Anti-Viral Proteins**. *Plos One* 2008; 3(12).

149. Russell RA, Pathak VK. **Identification of two distinct human immunodeficiency virus type 1 Vif determinants critical for interactions with human APOBEC3G and APOBEC3F**. *Journal of Virology* 2007; 81(15):8201-8210.

150. Binka M, Ooms M, Steward M, Simon V. **The activity spectrum of Vif from multiple HIV-1 subtypes against APOBEC3G, APOBEC3F, and APOBEC3H**. *J Virol* 2012; 86(1):49-59.

151. Refsland EW, Hultquist JF, Luengas EM, Ikeda T, Shaban NM, Law EK, et al. **Natural polymorphisms in human APOBEC3H and HIV-1 Vif combine in primary T lymphocytes to affect viral G-to-A mutation levels and infectivity**. *PLoS Genet* 2014; 10(11):e1004761.

152. Dang Y, Davis RW, York IA, Zheng YH. **Identification of 81LGxGxxIxW89 and 171EDRW174 domains from human immunodeficiency virus type 1 Vif that regulate APOBEC3G and APOBEC3F neutralizing activity**. *J Virol* 2010; 84(11):5741-5750.

153. Donahue JP, Vetter ML, Mukhtar NA, D'Aquila RT. **The HIV-1 Vif PPLP motif is necessary for human APOBEC3G binding and degradation**. *Virology* 2008; 377(1):49-53.

154. Gu Q, Zhang Z, Cano Ortiz L, Franco AC, Häussinger D, Münk C. **Feline Immunodeficiency Virus Vif N-Terminal Residues Selectively Counteract**

Feline APOBEC3s. *J Virol* 2016; 90(23):10545-10557.

155. Zimmerman ES, Schulman BA, Zheng N. **Structural assembly of cullin-RING ubiquitin ligase complexes**. *Curr Opin Struc Biol* 2010; 20(6):714-721.

156. Guo Y, Dong L, Qiu X, Wang Y, Zhang B, Liu H, et al. **Structural basis for hijacking CBF-beta and CUL5 E3 ligase complex by HIV-1 Vif**. *Nature* 2014; 505(7482):229-233.

157. Gu Q, Zhang Z, Gertzen CGW, Häussinger D, Gohlke H, Münk C. **Identification of a Conserved Interface of Human Immunodeficiency Virus Type 1 and Feline Immunodeficiency Virus Vifs with Cullin 5**. *J Virol* 2018; 92(6).

158. Luo K, Xiao ZX, Ehrlich E, Yu YK, Liu BD, Zheng S, et al. **Primate lentiviral virion infectivity factors are substrate receptors that assemble with cullin 5-E3 ligase through a HCCH motif to suppress APOBEOG**. *P Natl Acad Sci USA* 2005; 102(32):11444-11449.

159. Wang J, Zhang W, Lv M, Zuo T, Kong W, Yu X. **Identification of a Cullin5-ElonginB-ElonginC E3 complex in degradation of feline immunodeficiency virus Vif-mediated feline APOBEC3 proteins**. *J Virol* 2011; 85(23):12482-12491.

160. Loewen N, Barraza R, Whitwam T, Saenz DT, Kemler I, Poeschla EM. **FIV Vectors**. *Methods Mol Biol* 2003; 229:251-271.

161. Pizzato M, Erlwein O, Bonsall D, Kaye S, Muir D, McClure MO. **A one-step SYBR Green I-based product-enhanced reverse transcriptase assay for the quantitation of retroviruses in cell culture supernatants**. *J Virol Methods* 2009; 156(1-2):1-7.

162. Saenz DT, Barraza R, Loewen N, Teo W, Poeschla EM. **Feline immunodeficiency virus-based lentiviral vectors**. *Cold Spring Harb Protoc* 2012; 2012(1):71-76.

163. Fouchier RAM, Meyer BE, Simon JHM, Fischer U, Malim MH. **HIV-1 infection of non-dividing cells: evidence that the amino-terminal basic region of the viral matrix protein is important for Gag processing but not for post-entry**

nuclear import. *Embo J* 1997; 16(15):4531-4539.

164. Fouchier RAM, Simon JHM, Jaffe AB, Malim MH. **Human immunodeficiency virus type 1 Vif does not influence expression or virion incorporation of gag-, pol-, and env-encoded proteins**. *Journal of Virology* 1996; 70(12):8263-8269.

165. Edgar RC. **MUSCLE: multiple sequence alignment with high accuracy and high throughput**. *Nucleic Acids Res* 2004; 32(5):1792-1797.

166. Jalview. **The Clustal Color Scheme**. In: Jalview; 2024.

167. Yoshikawa R, Nakano Y, Yamada E, Izumi T, Misawa N, Koyanagi Y, et al. **Species-specific differences in the ability of feline lentiviral Vif to degrade feline APOBEC3 proteins**. *Microbiol Immunol* 2016; 60(4):272-279.

168. Poss M, Ross HA, Painter SL, Holley DC, Terwee JA, Vandewoude S, et al. **Feline lentivirus evolution in cross-species infection reveals extensive G-to-A mutation and selection on key residues in the viral polymerase**. *J Virol* 2006; 80(6):2728-2737.

169. Mehle A, Goncalves J, Santa-Marta M, McPike M, Gabuzda D. **Phosphorylation of a novel SOCS-box regulates assembly of the HIV-1 Vif-Cul5 complex that promotes APOBEC3G degradation**. *Gene Dev* 2004; 18(23):2861-2866.

170. Jin J, Ang XL, Shirogane T, Wade Harper J. **Identification of substrates for F-box proteins**. *Methods Enzymol* 2005; 399:287-309.

171. Petroski MD, Deshaies RJ. **Function and regulation of cullin-RING ubiquitin ligases**. *Nat Rev Mol Cell Biol* 2005; 6(1):9-20.

172. Letko M, Silvestri G, Hahn BH, Bibollet-Ruche F, Gokcumen O, Simon V, et al. **Vif proteins from diverse primate lentiviral lineages use the same binding site in APOBEC3G**. *J Virol* 2013; 87(21):11861-11871.

173. Carpenter MA, O'Brien SJ. **Coadaptation and immunodeficiency virus: lessons from the Felidae**. *Curr Opin Genet Dev* 1995; 5(6):739-745.

174. VandeWoude S, OBrien SJ, Langelier K, Hardy WD, Slattery JP, Zuckerman EE, et al. **Growth of lion and puma lentiviruses in domestic cat cells and**

comparisons with FIV. *Virology* 1997; 233(1):185-192.

175. VandeWoude S, O'Brien SJ, Hoover EA. **Infectivity of lion and puma lentiviruses for domestic cats**. *J Gen Virol* 1997; 78 (Pt 4):795-800.

176. VandeWoude S, Hageman CL, Hoover EA. **Domestic cats infected with lion or puma lentivirus develop anti-feline immunodeficiency virus immune responses**. *J Acquir Immune Defic Syndr* 2003; 34(1):20-31.

177. Salter JD, Morales GA, Smith HC. **Structural insights for HIV-1 therapeutic strategies targeting Vif**. *Trends Biochem Sci* 2014; 39(9):373-380.

178. Su X, Wang H, Zhou X, Li Z, Zheng B, Zhang W. **Jembrana disease virus Vif antagonizes the inhibition of bovine APOBEC3 proteins through ubiquitin-mediate protein degradation**. *Virology* 2018; 519:53-63.

179. Zhang W, Wang H, Li Z, Liu X, Liu G, Harris RS, et al. **Cellular requirements for bovine immunodeficiency virus Vif-mediated inactivation of bovine APOBEC3 proteins**. *J Virol* 2014; 88(21):12528-12540.

180. Nguyen KM, Busino L. **The Biology of F-box Proteins: The SCF Family of E3 Ubiquitin Ligases**. *Adv Exp Med Biol* 2020; 1217:111-122.

181. Zhou P, Yan F. **CRL4 Ubiquitin Pathway and DNA Damage Response**. *Adv Exp Med Biol* 2020; 1217:225-239.

Acknowledgements

First and foremost, I would like to express my deepest gratitude to my supervisor, Prof. Dr. Carsten Münk, for his outstanding mentorship and unwavering support throughout my PhD journey. I am profoundly grateful for the opportunity to work in his laboratory and for his trust, encouragement, and patience. His enthusiasm, insightful guidance, and genuine commitment to this project have been invaluable fand instrumental in shaping my research experience.

I also extend my heartfelt thanks to my second supervisor, Prof. Dr. Philipp Lang, for his insightful contributions, constructive suggestions, and steadfast support during my research.

I am deeply appreciative of the invaluable help and collaboration of several distinguished scientists: Prof. Dr. Sue VandeWoude, Dr. Kei Sato, Dr. Viviana Simon, Dr. Zeli Zhang, and Dr. Qinyong Gu. Their generous contributions of reagents, technical expertise, and valuable time have significantly advanced the success of this project.

I am immensely grateful to all the members of Prof. Dr. Carsten Münk's lab for fostering a collaborative and stimulating working environment. A special note of thanks goes to Wioletta Hörschken for her exceptional technical assistance and steadfast support.

I also wish to thank the Department of Gastroenterology, Hepatology, and Infectious Diseases at Universitätsklinikum Düsseldorf for providing the resources and infrastructure essential for my research. I am sincerely grateful to the staff of the department for their considerate assistance and support throughout my studies.

Finally, my heartfelt gratitude goes to my family. To my daughter, Yishu Li, my wife, and my parents: thank you for your understanding, encouragement, and unconditional support throughout this journey. Your unwavering belief in me has been my greatest source of strength and inspiration.